Toxicometabolomics of Cathinone Derivatives

Dissertation
zur Erlangung des Grades
des Doktors der Naturwissenschaften
der Naturwissenschaftlich-Technischen Fakultät
der Universität des Saarlandes

von

Sascha Kevin Manier

Saarbrücken
2020

Tag des Kolloquiums: 20.11.2020

Dekan: Prof. Dr. Jörn Eric Walter

Berichterstatter: Prof. Dr. Markus R. Meyer

    Prof. Dr. Christian Ducho

Vorsitz: Prof. Dr. Veit Flockerzi

Akad. Mitarbeiter: Dr. Stefan Boettcher

Vorwort

Die nachfolgende Arbeit entstand unter der Anleitung von Herrn Univ.-Prof. Dr. Markus R. Meyer in der Abteilung für Experimentelle und Klinische Toxikologie der Fachrichtung Experimentelle und Klinische Pharmakologie und Toxikologie der Universität des Saarlandes in Homburg (Saar) von November 2016 bis Mai 2020.

Danksagung

Ich möchte mich besonders bei meinem Doktorvater Herrn Univ.-Prof. Dr. Markus R. Meyer für die herzliche Aufnahme in seinen Arbeitskreis, der Vergabe dieses interessanten und herausfordernden Dissertationsthemas, seiner stets sachlichen und konstruktiven Kritik und der Möglichkeit zur aktiven Teilnahme an nationalen und internationalen Fachkongressen bedanken. Seine stetige Offenheit gegenüber neuen und oft auch unkonventionellen Gedanken und Methoden war eine wichtige Voraussetzung, ohne die diese Arbeit nicht möglich gewesen wäre. Gleichzeitig hat mich seine freundliche, stets bestimmte und immer lösungsorientierte Art und Weise diesen Arbeitskreis zu leiten sehr geprägt.

Ich danke Herrn Univ.-Prof. Dr. Christian Ducho für die Übernahme des Koreferats, sowie Herrn Univ.-Prof. Dr. Dr. h. c. Hans H. Maurer für seine Teilnahme an Diskussionen, seiner fachliche Unterstützung und der frühen Förderung in diesem Arbeitskreis. Zunächst durch die Möglichkeit mein Wahlpflichtpraktikum, später mein Diplom in diesem Arbeitskreis anzufertigen und zuletzt durch die Vermittlung an meinen Doktorvater konnte ich lange Zeit von seinem beinahe unendlichen Erfahrungsschatz und seiner zielstrebigen Art lernen.

"Every sane society allows a certain number of people to deviate. You don't have to join, you don't have to play the game. A society which is insane and unsure of itself cannot allow that to happen. It says everybody must join, everybody must work, everybody must belong. And then freedom disappears."

Alan Wilson Watts (1915 - 1973)

IV

Zusammenfassung

Die vorliegende Arbeit untersuchte den Metabolismus der synthetischen Cathinone alpha-PBP, alpha-PVT, alpha-PHP, alpha-PEP, and alpha-POP mit und ohne Metabolomik. Der Metabolismus wurde konventionell untersucht, sowie die Kinetikparameter der beteiligten Cytochrom P450 (CYP) Enzyme bestimmt. Ein ungerichtetes Metabolomik (UM)-Arbeitsschema wurde entwickelt, optimiert und auf Inkubationen mit gepoolten humanen Lebermikrosomen (pHLM), sowie HepaRG Zellen angewandt. Alle untersuchten Cathinone wurden reduziert, bildeten Laktame und wurden an ihren Pyrrolidinringen hydroxyliert. Hauptsächlich am Metabolismus beteiligt waren die polymorph exprimierten CYP2D6, CYP2C9 und CYP2C19. Die Entwicklung des UM Arbeitsschema zeigte, dass die Parameter der Präprozessierung und die Auflösung des Massenspektrometers wichtig für die Wiederfindung von Analyten sind. Angewandt auf pHLM stellte sich UM als effektiver im Vergleich zu konventionellen Methoden heraus, wobei die Ergebnisse vergleichbar mit primären humanen Hepatozyten waren. Die Untersuchung verschiedener Rekonstitutionsmittelmischungen zeigte, dass eine Zusammensetzung von 30% Methanol und 70% Acetonitril gut geeignet ist, um hohe Feature-Flächen und Gesamtfeaturezahlen zu erhalten. Die Anwendung von UM auf Inkubationen mit HepaRG Zellen führte zur Detektion von unerwarteten Aminosäure-Addukten. Diese Addukte wurden bisher noch nicht in der Literatur beschrieben und können wahrscheinlich auch im Menschen detektiert werden.

VI

Summary

The presented work investigated the metabolism of the synthetic cathinones alpha-PBP, alpha-PVT, alpha-PHP, alpha-PEP, and alpha-POP with and without metabolomics techniques. The metabolism was elucidated using conventional methods and the kinetic parameters of the involved cytochrome P450 (CYP) enzymes were determined. An untargeted metabolomics (UM) workflow was developed, optimized, and applied to incubations using pooled human liver microsomes (pHLM) and HepaRG cells. All investigated cathinones underwent reduction of the cathinone oxo group, lactam formation and hydroxylation of the pyrrolidine ring. The CYP enzymes involved in the metabolism were polymorphically expressed including CYP2D6, CYP2C9, and CYP2C19. Development of the UM workflow revealed the preprocessing parameters and the resolution of the mass spectrometer as vital parameters effecting the recovery of analytes. The metabolomics approach using pHLM appeared to be more effective than the conventional approach, detecting almost as much metabolites as primary human hepatocytes. The investigation of different reconstitution solvent mixtures showed that a composition of 30% methanol and 70% acetonitrile was well suited to obtain high feature areas and total feature counts. Applying UM to incubations using HepaRG cells led to the detection of unexpected amino acid adducts with the investigated cathinones. These adducts were not described in previous publications and are likely detectable in humans, as well.

VIII

Abbreviations

alpha-PBP alpha-pyrrolidinobutyrophenone

alpha-PEP alpha-pyrrolidinoenanthophenone

alpha-PHP alpha-pyrrolidinohexanophenone

alpha-POP alpha-pyrrolidinooctanophenone

alpha-PVT alpha-pyrrolidinopentiothiophenone

CV   coefficient of variation

CYP   cytochrome P540

DA   dopamine

DOA   drugs of abuse

EMCDDA European Monitoring Centre for Drugs and Drug Addiction

FMO   flavin-containing monooxygenases

GC   gas chromatography

HRMS   high resolution mass spectrometry

i.e.   id est, that is

LC   liquid chromatography

LSD   lysergic acid diethylamide

MDMA   3,4-methylendioxy-N-methylamphetamine

MS   mass spectrometry

NA   noradrenaline

NMR nuclear magnetic resonance

NPS   new psychoactive substances

PCA   principal component analysis

PHH   primary human hepatocytes

pHLM pooled human liver microsomes

pHS9 pooled human liver S9 fraction

PLS-DA partial least squares discriminant analysis

RAF   relative activity factor

SER   serotonin

TM   targeted metabolomics

UGT   uridine 5'-diphospho-glucuronosyltransferases

UM   untargeted metabolomics

UNODC United Nations Office on Drugs and Crimes

X

Contents

1 General Part

1.1 New Psychoactive Substances

1.1.1 Origin, Development, and Legal Encounter

The origin of drugs of abuse (DOA) in general can be found in defense mechanisms of plants. It is very likely that substances such as nicotine, morphine, and cocaine were initially produced by plants for protection against insect herbivores[1]. Although also potentially dangerous for mammals, humans started using them ages ago for mind expansion or treatment of diseases[2–4]. For a long time, their use and misuse occurred in their natural form such as coca leaves or dried juice of poppy, either raw or as alcoholic beverages[2,3]. Then in 1874, it was achieved to acetylate morphine using acetic anhydride[5]. The resulting substance heroin was later marketed to reduce the side effects of morphine and became one of the first synthetic drugs of abuse[6,7]. It was followed by amphetamine in 1887[8], methamphetamine in 1893[9,10], and 3,4-methylendioxy-N-methylamphetamine (MDMA) in 1912[11]. Together with naturally occurring drugs of abuse such as cannabis and cocaine, these substances are still shaping the modern consume of drugs of abuse[12,13].

While these and other substances started to be strictly controlled during the 20th century, a number of different substances with similar effects became more and more popular[14–18]. New Psychoactive Substances (NPS) began to increase their share on the modern drug market several years ago[19,20]. Due to many narcotics laws prohibiting accurately defined chemical structures, NPS circumvent these laws by introducing slight changes to them[21]. The result is a legal substance that inherits similar pharmacological effects from its original[21]. Due to these properties and additionally to avoid criminal prosecution they are often labeled as "legal highs", "research chemicals", or "bath salts"[22]. Other NPS such as synthetic cannabinoids did not originate from a prohibited structural predecessor, but were for example designed to study the structure–activity

relationship of Δ^9-tetrahydrocannabinol[23]. They often remained of academic interest until their published synthesis was reused for the production of NPS[24]. A similar history have former therapeutic drugs such as benzylpiperazine that was once used as an antihelminthic agent in veterinary medicine and later as an antidepressant, but was finally removed from the market due to its severe adverse effects and also reappeared as NPS[25]. Although not specifically new in a synthetic meaning, psychoactive substances of natural origin such as the herb of *Salvia divinorum* EPLING & JÁTIVA-M. or leaves of the Kratom tree *Mitragyna speciosa* KORTH. appeared as well on the drug market as NPS[26].

Between 2007 and 2017, 66 countries worldwide reported seizures of NPS to the United Nations Office on Drugs and Crimes (UNODC)[13]. It appears that most of them were seized on the American continent, followed by Asia and Europe. Currently NPS are classified in more than six different categories such as synthetic cannabinoids, aminoindanes, synthetic cathinones, or tryptamines, with cannabinoids dominating the quantities of synthetic NPS seizures ever since 2010[13]. By the end of December 2018 a total of 892 substances were reported to the UNODC early warning advisory, three times the number that is under international control by the Single Convention on Narcotic Drugs and its amendments[13]. Concerning Europe, a total of 730 NPS were monitored by the end of 2018 by the European Monitoring Centre for Drugs and Drug Addiction (EMCDDA)[12]. Regarding the period from 2005 to 2017, the amount of newly occurring substances that were reported to the EMCDDA reached a peak in 2014 with 101 NPS per year, it appears that recent years leveled at 50-60 substances per year, indicating a stabilization of the NPS market[12]. Although not dominating the quantities of seized material, synthetic cannabinoids appear to be at least the most often seized NPS category on the european scale. The impact of NPS on Germany can only be estimated by the results of consumer surveys. These indicate that the amount of adults (18-64 years) having used NPS in the past was at 2.8%, while the amount of young adults (18-25 years) remains stable at 2.2%[27,28]. However, projects monitoring the substance traffic in prisons indicate that a high number of NPS is used in prisons to avoid their detectability by rapid tests[27].

Nevertheless, Germany introduced a new law in 2016 to prohibit supply-related actions concerning NPS including acquisition, possession, and trade[29]. In contrast to the already existing German narcotics law with its first announcement in 1929 and its last revision in 1994, it did not contain clearly defined substances but basic structures and substitution boundaries to cover a high number of substances that are likely to be used as NPS[30,31]. With this procedure, Germany followed the analogue approach similar to

the United States Federal Analogue Act[21] to encounter the uprising of NPS in recent years. Other approaches to pursue legal containment of NPS include the neurochemical approach that controls substances without taking their chemical composition into account but their pharmacological effect on the brain or the general prohibition of every substance that is not explicitly permitted[21].

1.1.2 Cathinone-Derived New Psychoactive Substances

Cathinone-derived NPS are synthetic substances based on the chemical structure of cathinone ((S)-2-amino-1-phenyl-1-propanone), the main alkaloid of *Catha edulis* (VAHL) FORSSK. ex ENDL., colloquially named khat[26]. In comparison to cathinone, modifications were observed on the amino group including the addition of one or two alkyl groups, as well as its replacement with a pyrrolidine ring. Modifications on the phenyl ring include addition of one or two alkyl groups, a methoxy or methylenedioxy group, as well as the substitution of hydrogen with halogens or the replacement with a naphthalene ring. Additionally the 1-propanone backbone was found to be replaced with 1-alkanones of different length[32]. These modifications often occur in combination with each other, resulting in a highly diversified category of NPS. Next to synthetic cannabinoids, cathinone derivatives, being commonly named "bath salts", appear to be one of the most often seized susbtances, both on the international and the european scale[12,13,32].

The pharmacology of synthetic cathinones is mainly characterized by their inhibition of serotonin (SER), dopamine (DA), and noradrenaline (NA) reuptake transporters and their ability to release these monoamines[33]. Although all of them inhibit the reuptake of SER, DA, and NA to a certain extend, their selectivity varies allowing their pharmacological classification into three groups. The first group of cathinones is characterized by its pharmacological profile similar to a combination of cocaine and MDMA and are non selective reuptake inhibitors, as well as SER releasers. This group includes substances such as mephedrone, methylone, and naphyrone. The second group contains cathinones that act similar to methamphetamine by acting mainly as catecholamine inhibitors and DA releasers such as methcathinone and flephedrone. The last group includes cathinones that do only inhibit the reuptake of SER, DA, and NA but do not release any of them such as pyrovalerone and 3,4-methylenedioxypyrovalerone[33].

Recreational use of synthetic cathinones has been described by consumers to result in increased energy, empathy, and sociability[34,35]. These subjective effects often come along with dangerous adverse effects that can be summarized as a sympathomimetic

toxidrome[34]. Symptoms of that toxidrome include agitation, psychosis, tachycardia, hypertension, seizures, and hyperthermia[34–36]. Fatalities that were the result of an intake of synthetic cathinone include causes such as kidney injuries and liver failure, sometimes in combination with injuries that were the result of an agitated delirium[36,37]. Studies evaluating the chronic abuse of cathinones are limited. Due to data that is obtained from chronic khat users, long term abuse might lead to increased psychiatric symptoms such as psychosis as well as myocardial infarction[38]. The treatment of the sympathomimetic toxidrome is primarily symptomatic. The administration of benzodiazepines represents the method of choice to encounter agitation, psychosis, or seizures[34]. Antipsychotic drugs such as haloperidol may help with a persisting psychosis but must be used with care due to their possible aggravation of hyperthermia, dysrhythmia, and lowering the seizure threshold[34,36]. Anticonvulsive drugs such as phenytoin for the treatment of seizures should be generally avoided due to their sodium channel blocking properties that might as well aggravate dysrhythmias[34]. Due to the high diversity of synthetic cathinones, a distinguished diagnosis is only possible after analysis using gas chromatography (GC) or liquid chromatography (LC) coupled to mass spectrometry (MS)[34,35]. A differential diagnosis concerning the compound that was consumed is important not least because the sold preparations are often incorrectly labeled concerning their content but also since the consume of NPS is mostly found in combination with other drugs[36,37,39]. Determination of plasma concentrations is theoretically possible, although concentrations do not seem to correlate with their clinical effects and thus are not helpful concerning the treatment of adverse effects[34].

1.2 Toxicokinetics Studies

1.2.1 Metabolism

The detection of NPS in blood or urine often requires knowledge about the substance's toxicokinetic properties[40,41]. Many substances undergo extensive metabolism that results in many biomarkers allowing the distinct and reliable determination of the consumed drug[42–44]. Few substances such as amphetamine or aminoindane are mainly excreted unchanged or sparsely metabolized leading to a difficult confirmation of an intake by the detection of metabolites[45,46]. In special cases, the parent compound is not detectable any more in biological samples, making merely metabolites a suitable analytical target for their detection[44,47]. Additionally, substances such as synthetic cannabinoids

or derivatives of lysergic acid diethylamide (LSD) can merely differ in their precursor form and result in the same metabolites[48,49]. These circumstances make metabolism studies of NPS necessary to ensure their detection in human biosamples after an intake and support the physicians in their choice of an appropriate treatment. Due to obvious ethical reasons it is not justifiable to perform clinical studies by administering NPS to volunteers. Nevertheless in rare cases, authentic urine from drug consumers can be obtained from the emergency room enabling the investigation of their metabolism in humans[50].

Thus, several metabolism models were established to investigate the metabolic fate of NPS and other drugs[51,52]. These models can be divided into in vivo models such rats, pigs, or zebrafish larvae and in vitro models including cell fractions of pooled human liver, cell cultures, or organ slices[51–53]. In vivo models appear to be beneficial concerning the complexity of a metabolizing organism such as reuptake into liver cells or the concentration of metabolites after renal excretion but they often suffer from species differences[54,55]. Rats for example are known to be very efficient acetylators, whereas humans tend to be intermediate ones[54].

In vitro models facilitate the investigation of the human-specific metabolism without clinical studies, since they can be obtained from human donors[51]. Nevertheless, they also suffer from certain limitations. In vitro models are often closed systems that lack the interaction of multiple metabolic pathways compared to living systems[51]. Additionally, the metabolic reactions that can be observed are limited to the tissue or subcellular fraction they were obtained from[51,56]. Pooled human liver microsomes (pHLM) for example merely contain the endoplasmatic reticulum of liver cells and thus only enzymes that are located there[51,56]. Assuming that all necessary co-substrates were added, pHLM enable the investigation of reactions catalyzed by cytochrome P450 (CYP) enzymes, flavin-containing monooxygenases (FMO), and uridine 5'-diphospho-glucuronosyltransferases (UGT)[51,56]. Reactions catalyzed by those enzymes that are located in the cytosole including those catalyzed by glutathione *S*-transferases or sulfotransferases cannot be observed. However, most metabolic steps observed for DOA and NPS include those catalyzed by CYP enzymes, FMO, and UGT. If a more comprehensive study is necessary, the addition of pooled human liver cytosole to pHLM or the application of the unseparated pooled human liver S9 fraction (pHS9) is possible but usually results in lower enzyme activities[57,58].

The application of whole cells for metabolism studies is usually found in cell lines such as HepG2 and HepaRG or primary human hepatocytes[59]. These models are often ap-

plied since they are better suited to represent the physiology of liver cells[58,59]. Cell lines such as HepG2 or HepaRG originate from liver cancer cells of a single donor that were immortalized and thus can grow and divide indefinitely under optimal conditions[59]. The fact that they originate from a single donor makes them prone to interindividual variabilities concerning their metabolism. HepaRG cells for example significantly lack CYP2D6 activity due to the fact that their donor was a CYP2D6 poor metabolizer[60]. Primary human hepatocytes (PHH) are currently the gold standard concerning in vitro CYP induction and metabolism studies since they contain all relevant human enzymes, co-substrates, and drug transporters[58,61,62]. They are prepared from fresh tissue samples by enzymatic digestion or mechanical force and therefore difficult to obtain as well as expensive in their application[59]. Since they are not immortalized, they merely grow and divide to a limited extend which implies their regular need for fresh preparation[61]. These circumstances lead to a decreased stability in their phenotype and a higher susceptibility to variability[61,63].

1.2.2 In Vitro-In Vivo Correlation

The detection of certain metabolites in vitro does not necessary lead to their detection in vivo[51,64]. One reason for this are experimental conditions that are often adjusted to match the detectability of potential metabolites by the applied method[64]. Adjusting the substrate concentration to higher amounts can lead to the detection of metabolites formed by enzymes whose low substrate affinity does not lead to any relevant metabolite formation under physiological substrate concentrations[64]. Another reason is the high amount of different enzymes that are involved in the metabolite formation[51]. Several enzymes such as those from the CYP enzyme superfamily are polymorphically expressed leading to phenotypes with different enzyme activities, often qualitatively addressed as "poor metabolizer", "intermediate metabolizer", or "extensive metabolizer"[65]. If the amount of enzymes involved in the metabolism of a substance is limited to few enzymes, the involvement of polymorphically expressed enzymes bears the risk of high interindividual variability[46]. If several enzyme isoforms are involved, the determination of the contribution of each isoform to the total hepatic net clearance is necessary to interpret the results properly[64]. Since CYP enzymes are the most important enzymes for the metabolism of drugs, an initial screening using the most abundant CYP isoform of the human liver is usually performed in prior[66–68]. Although CYP enzymes are expressed in various types of tissues in the human body, the liver is accepted to be the quantitatively

most meaningful organ[64,66]. The calculation of the hepatic clearance in vivo is achieved by the determination of kinetic parameters for each of the involved isoforms and the subsequent scaling of these parameters to activities found in vivo[51,64,66]. Scaling is performed using the relative activity factor (RAF)-approach[69]. The RAF compares the turnover rate of a model substrate in the isolated enzyme system with that found in human liver microsomes and thus allows the correction of an enzyme's specific clearance and the determination of its "contribution" to the hepatic total net clearance[69]. A low contribution of a polymorphically expressed isoform to the total hepatic net clearance is therefore not expected to result in high interindividual variability.

1.3 Metabolomics

The metabolome summarizes all molecules with a molecular weight less than 1500 Da[70]. Concerning humans, this includes endogenous metabolites, metabolites from food and its additives, as well as those metabolites from the gut microbiome[70]. Since metabolites are the end product of all physiological processes, they reflect the phenotype of an organism the closest[71]. Metabolomics studies use small molecule profiling to assess significant changes in the metabolome of an organism for example after pathophysiological stimuli or genetic modifications[72–75]. These studies are usually performed using nuclear magnetic resonance (NMR) or high resolution mass spectrometry (HRMS) coupled with LC, as well as GC-MS and can be conducted either "targeted" or "untargered"[70,72].
The aim of targeted metabolomics (TM) experiments is to quantitatively assess well-selected metabolites within a network to allow deeper insights into a hypothesis[72]. Since the analytical targets need to be defined in prior, the success and value of TM depends on the significance of the investigated metabolites. Therefore, an objective approach is necessary that evaluates the relevance of as much metabolites as possible for a given question and facilitates the formation of the corresponding hypothesis. This can be achieved by untargeted metabolomics (UM) experiments. UM uses impartial sample preparations and analysis methods to enable the detection of as many analytes as possible. The obtained analytical runs are typically preprocessed using algorithms that perform an abstraction of the analytical data using "peak-picking" and summarize them in a table which can subsequently be evaluated using several statistical methods[76–79]. Concerning LC-HRMS/MS analyses, the abstraction of the analytical information includes the detection of chromatographical peaks and their integration for example by specific deviations in mass traces and continuous wavelet transformation[80], as well as

the alignment of chromatographical peaks across all samples and the correction of retention time deviations[76,81]. Although not always clearly distinguished in literature, the two-dimensional LC-MS signal, that was registered and integrated during peak-picking is commonly termed "feature" during statistical evaluation[76,80,82]. Several Software solutions exist to conduct preprocessing of analytical data obtained from LC-HRMS/MS analyses, such as MZmine 2[78], XCMS[76], and Metalign[77]. Studies that performed a comparison of those tools, revealed that XCMS appears to be the most suitable software solution for such tasks[83–85].

Statistical evaluation of UM experiments is a nontrivial step in a study that requires detailed knowledge of the applied statistical methods to avoid false positive features. Typical metabolomics experiments consist of few observations (i.e. analyses) that are characterized by a multitude of variables (i.e. metabolites)[70,71]. This results in an accumulation of type I errors, commonly referred to as the multiple testing issue[70]. For this reason, univariate statistics such as Student's t-test in case of a two-group comparison are not suited for the evaluation of metabolomics experiments, since the resulting p-value is prone to false positives[70]. However, the combination of Student's t-test and the fold-change of the features' abundances in form of a Volcano plot is a helpful tool to preliminarily evaluate features[86]. Due to the fact that metabolomics data are characterized by multiple observations of which each is characterized by multiple variables, dimensionality reduction methods such as principal component analysis (PCA) and partial least squares discriminant analysis (PLS-DA) are widely applied. PCA uses linear transformation of the multivariate data set to achieve a dimensionality reduction[87]. The essential goal is to preserve the variance, that allows the discrimination of the given observations in the lower dimensional result[87]. A PCA mainly results in two output tables, the scores that represent the observations reduced to a lower dimension and the loadings that represent the influence of each variable to the dimension reduction[71]. Both can be used to inspect the similarity of each observation by their arrangement in a plot, as well as the variable that caused it[71]. Since PCA is a non-supervised method that does not consider the affiliation of an analysis to a treatment group and is highly influenced by the variability within and between groups, it is well suited to assess the quality of the obtained data[71,88]. PLS-DA is another widely applied dimension reduction method that uses a regression model to fit the data matrix to a matrix representing the group membership. The results of PLS-DA correspond to that of a PCA, but since group membership of each observation is part of the regression analysis this method is referred to as a supervised method[71]. Although easy to interpret and widely implemented in

statistical software packages, PLS-DA is often misused due to its original purpose for calibration and not classification[89]. Supervised methods such as PLS-DA are known to over-fit models leading to an overly optimistic representation of the initial data[71,89,90]. This implies the necessity to perform a validation of the obtained model. Model validations are conducted either by leaving one or more observations out when creating the corresponding model and subsequently predict the group membership of the left-out observations. The accuracy of the prediction is one of the main aspects that determines the quality of the assessed model[71,91].

Toxicometabolomics, essentially applying metabolomics to toxicology of exogenous compounds such as drugs of abuse or NPS, may avoid several disadvantages of conventional metabolism studies[92]. Comparable to TM, conventional metabolism studies investigate the formation of expected biotransformation products that are the result of already known reactions[48,53,93]. This approach is depending on the knowledge of the investigator and does not reflect the investigation of unexpected metabolites which may bias the result.

2 Aims and scopes

The aims of this work were to evaluate conventional metabolism studies by comparing the metabolism of five synthetic cathinones alpha-pyrrolidinobutyrophenone (alpha-PBP), alpha-pyrrolidinopentiothiophenone (alpha-PVT), alpha-pyrrolidinohexanophenone (alpha-PHP), alpha-pyrrolidinoenanthophenone (alpha-PEP), and alpha-pyrrolidinooctanophenone (alpha-POP) using different in vivo and in vitro models. The chemical structures of the investigated synthetic cathinones are given in Figure 1. The results of conducted metabolism studies using pHLM should be compared to those published in literature and additionally fortified by the determination of kinetic parameters of the involved CYP enzymes. To improve these conventional metabolism studies, this work aimed to use UM techniques. This should be achieved by the development of a general UM workflow and the optimization of used algorithms and experimental conditions. The investigation using UM should be conducted using pHLM and HepaRG cells.
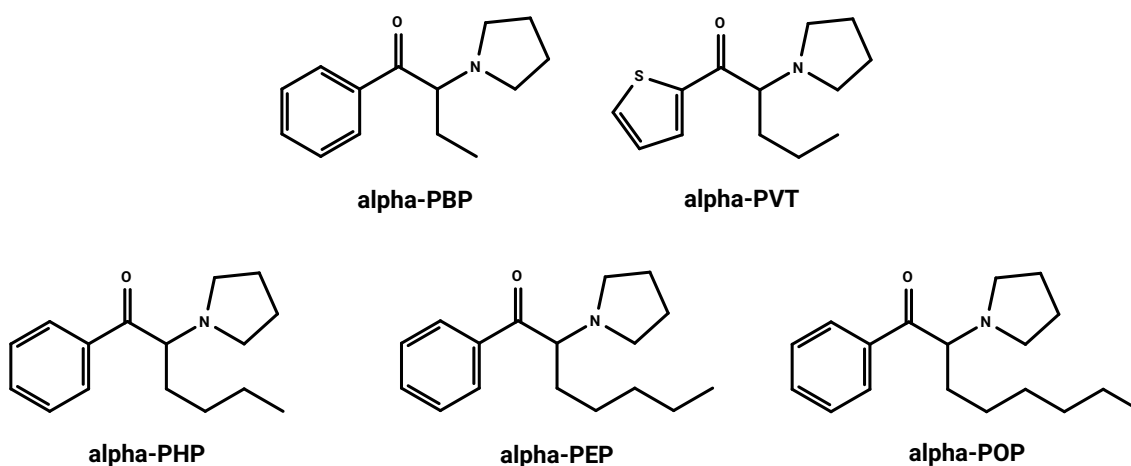
Figure 1: Chemical structures of alpha-PBP, alpha-PVT, alpha-PHP, alpha-PEP, and alpha-POP.

2 Aims and scopes

The following steps had to be conducted:

- Investigation of the metabolism of alpha-PBP, alpha-PVT, alpha-PHP, alpha-PEP, and alpha-POP using pHLM and LC-HRMS/MS and comparison of different metabolism models for investigation of their metabolism

- Determination of the kinetic parameters of CYP isoforms involved in the metabolism of the five synthetic cathinones

- Development of a LC-HRMS/MS method for UM with special focus on drugs and drugs of abuse

- Development of an algorithm for the dynamic optimization of peak-picking parameters using XCMS

- Investigation of the metabolism of synthetic cathinones using pHLM and UM techniques exemplified for alpha-PBP and alpha-PEP

- Development of a workflow to the analysis of HepaRG cells and their surrounding medium

- Investigation of the metabolism of synthetic cathinones using HepaRG cells and UM techniques exemplified for alpha-PBP and alpha-PEP

3 Publication of the results

The results of the studies were published in the following publications:

3.1 Different in vitro and in vivo tools for elucidating the human metabolism of alpha-cathinone-derived drugs of abuse (DOI: 10.1002/dta.2355)[94]

Author contributions   Sascha K. Manier conducted and evaluated the experiments and composed the manuscript, Lilian H. J. Richter developed and drafted the incubations using pooled human liver S9 fraction, Jan Schäper acquired and provided the investigated new psychoactive substances, Hans H. Maurer and Markus R. Meyer assisted with the interpretation of the analytical experiments and with scientific discussions.

WILEY

Different in vitro and in vivo tools for elucidating the human metabolism of alpha-cathinone-derived drugs of abuse

Sascha K. Manier[1] | Lilian H.J. Richter[1] | Jan Schäper[2] | Hans H. Maurer[1] | Markus R. Meyer[1]

[1] Department of Experimental and Clinical Toxicology, Institute of Experimental and Clinical Pharmacology and Toxicology, Saarland University, Center for Molecular Signaling (PZMS), Homburg, Germany

[2] State Bureau of Criminal Investigation Bavaria, München, Germany

Correspondence
Markus R. Meyer, Department of Experimental and Clinical Toxicology, Center for Molecular Signaling (PZMS), Saarland University, 66421 Homburg, Germany.
Email: markus.meyer@uks.eu

Abstract

In vitro and in vivo experiments are widely used for studying the metabolism of new psychoactive substances (NPS). The availability of such data is required for toxicological risk assessments and development of urine screening approaches. This study investigated the in vitro metabolism of the 5 pyrrolidinophenone-derived NPS alpha-pyrrolidinobutyrophenone (alpha-PBP), alpha-pyrrolidinopentiothiophenone (alpha-PVT), alpha-pyrrolidinohexanophenone (alpha-PHP), alpha-pyrrolidinoenanthophenone (alpha-PEP, PV8), and alpha-pyrrolidinooctanophenone (alpha-POP, PV9). First, they were incubated with pooled human liver microsomes (pHLM) or pooled human liver S9 fraction (pS9) for identification of the main phase I and II metabolites. All substances formed hydroxy metabolites and lactams. Longer alkyl chains resulted in keto group and carboxylic acid formation. Comparing these results with published data obtained using pHLM, primary human hepatocytes (PHH), and authentic human urine samples, PHH provided the most extensive metabolism. Second, enzyme kinetic studies showed that the initial metabolic steps were formed by cytochrome P450 isoforms (CYP) CYP1A2, CYP2B6, CYP2C9, CYP2C19, CYP2D6, and CYP3A4 resulting in pyrrolidine, thiophene or alkyl hydroxy metabolites depending on the length of the alkyl chain. The kinetic parameters indicated an increasing affinity of the CYP enzymes with increase of the length of the alkyl chain. These parameters were then used to calculate the contribution of a single CYP enzyme to the in vivo hepatic clearance. CYP2C19 and CYP2D6 were mainly involved in the case of alpha-PBP and CYP1A2, CYP2C9 and CYP2C19 in the case of alpha-PVT, alpha-PHP, alpha-PEP, and alpha-POP.

KEYWORDS

alpha-cathinones, CYP kinetics, in vitro, metabolism, NPS

1 | INTRODUCTION

Several approaches have been established for studying drug metabolism.[1-3] One option is the use of in vitro systems such as cDNA-expressed recombinant single human cytochrome P450 (CYP) enzymes, fractions of liver homogenate (all after addition of the corresponding co-substrates), or cell cultures.[4] Among liver fractions, pooled human liver microsomes (pHLM), pooled human liver cytosol (pHLC), and pooled human S9 fraction (pS9) are commonly employed. pHLM is the most frequently applied in vitro model for metabolite profiling.[1] pS9 combines both pHLM and pHLC, and allows simultaneous investigation of phase I and phase II metabolites.[5] Cell cultures can, for example, consist of immortalized cancer cells. Also primary

human hepatocytes (PHH) are used.[6] PHH are the most suitable cells for the investigation of drug metabolism while immortalized cell cultures allow high throughput assays.[6] Liver slices can also be applied containing the full range of enzymes and cofactors necessary for phase I and II metabolism.[4] A second option is to use in vivo samples resembling the high complexity of a whole organisms.[7]

In contrast to drug development, controlled human studies of drugs of abuse are usually not performed[3] and in vivo animal studies may suffer from species differences.[7] Therefore, a combination of in vitro assays and samples taken from clinical or forensic casework may provide a solid base for collecting this information. Animal samples taken after controlled drug application may round-out the panel.[2,3] In clinical and forensic toxicology, such metabolism studies

of particularly new psychoactive substances (NPS) are necessary for toxicological risk assessments and for development of urine screening approaches.[3]

In the following, comparative studies on the metabolism of 5 pyrrolidinophenone-derived NPS (structures given in Figure 1), namely alpha-pyrrolidinobutyrophenone (alpha-PBP), alpha-pyrrolidinopentiothiophenone (alpha-PVT), alpha-pyrrolidinohexanophenone (alpha-PHP), alpha-pyrrolidinoenanthophenone (alpha-PEP, PV8), and alpha-pyrrolidinooctanophenone (alpha-POP, PV9) are described. Pyrrolidinophenone-derived NPS are synthetic derivatives of the natural alkaloid cathinone. The primary amine moiety within the cathinone molecule is replaced by a pyrrolidine ring and the alpha-carbon is substituted with alkyl chains of different length. Consumption and seizure of these substances have been reported in Europe as well as Japan.[8-11] So far, pharmacological studies have only been published for alpha-PBP, showing that the substance is inhibiting the monoamine reuptake for dopamine and norepinephrine, with minor effects at the serotonin transporter.[12] Clinical features associated with acute intoxication include agitation and tachycardia as well as chest pain and tachycardia.[13] Kolanos et al[14] identified the pyrrolidine ring and the length of the alpha-chain as crucial structural properties for alpha-PVP, another alpha-cathinone, which determine the potency for dopamine reuptake.

To evaluate the different assays mentioned above, the 5 NPS were incubated with pHLM or pS9 for identification of the main phase I and II metabolites. The results were then compared with published results obtained from pHLM, PHH, and authentic human urine samples.[11,15-19] In addition, the kinetic parameters of CYP isoforms involved in the metabolism were determined for assessing hepatic clearances and to predict possible individual variations in drug elimination or the risk of drug-drug or drug-food interactions.

2 | EXPERIMENTAL

2.1 | Chemicals and reagents

alpha-PBP, alpha-PVT, alpha-PHP, alpha-PEP, and alpha-POP were provided by the Bavarian State Criminal Police Office (Munich, Germany). alpha-PVP was provided by the Hesse State Criminal Police Office (Wiesbaden, Germany). NADP-Na$_2$, acetonitrile (LC–MS grade), and methanol (LC–MS grade) were obtained from VWR (Darmstadt, Germany). 3'-phosphoadenosine-5'-phosphosulfate (PAPS), S-(5'-adenosyl)-l-methionine (SAM), dithiothreitol (DTT), reduced glutathione (GSH), acetylcarnitine transferase (AcT), acetylcarnitine, acetyl coenzyme A (AcCoA), MgCl$_2$, K$_2$HPO$_4$, KH$_2$PO$_4$, superoxide
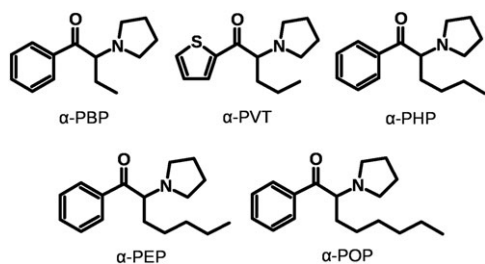
dismutase, isocitrate dehydrogenase, isocitrate, Tris, ammonium formate, and formic acid were obtained from Sigma (Taufkirchen, Germany). Water was purified with a Millipore filtration unit (18.2 Ω water resistance). Baculovirus-infected insect cell microsomes containing human cDNA-expressed CYP enzymes (ICM, Supersomes), CYP1A2, CYP2A6, CYP2B6, CYP2C8, CYP2C9, CYP2C19, CYP2D6, CYP2E1 (2 nmol/mL), CYP3A4, or CYP3A5 (2 nmol/mL), pHLM (pooled of 25 donors, 20 mg microsomal protein/mL, 330 pmol total P450/mg protein), pS9 (20 mg protein/mL, from 30 individual donors), UGT reaction mix solution A (25 mM UDP-glucuronic acid), and UGT reaction mix solution B (250 mM Tris–HCl, 40 mM MgCl$_2$, and 0.125 mg/mL alamethicin) were obtained from Corning (Amsterdam, Netherlands). After delivery, the pooled human liver microsomes, insect cell microsomes, and pS9 were thawed at 37°C, aliquoted, snap-frozen in liquid nitrogen, and stored at -80°C until use.

2.2 | In vitro drug metabolism studies using pS9

Incubations using pS9 were performed according to Richter et al.[5,20] Briefly, pS9 was used at a final protein concentration of 2 mg/mL. The incubation was performed after a 10-minute preincubation at 37°C with 25 μg/mL alamethicin (UGT reaction mix solution B), 90 mM phosphate buffer (pH 7.4), 2.5 mM Mg^{2+}, 2.5 mM isocitrate, 0.6 mM NADP$^+$, 0.8 U/mL isocitrate dehydrogenase, 100 U/mL superoxide dismutase, 0.1 mM AcCoA, 2.3 mM acetyl carnitine, and 8 U/mL carnitine acetyltransferase. Subsequently, 2.5 mM UDP-glucuronic acid (UGT reaction mix solution A), 40 μM aqueous PAPS, 1.2 mM SAM, 1 mM DTT, 10 mM GSH, and 25 μM substrate in distilled water were added. The final volume of the incubation mixture was 150 μL. All given concentrations are final concentrations. Reactions were started by the addition of substrate and incubated for a maximum of 480 minutes. After 60 minutes, 60 μL of the mixture was transferred into a reaction tube and reactions were terminated by addition of 20 μL ice-cold acetonitrile containing 5 μM alpha-PVP as an internal standard. The remaining mixture was incubated for additional 7 hours and then stopped by the addition of 30 μL ice-cold acetonitrile containing 5 μM alpha-PVP. Additionally, blank samples not containing pS9 were incubated to identify compounds of non-metabolic origin. Every incubation was performed once for every substance. The solutions were cooled for 30 minutes at -18°C, centrifuged for 2 minutes at 14,000 × g, and finally 60 μL of the supernatants were transferred into an autosampler vial. One μL supernatant was injected onto the liquid chromatography–high resolution–tandem mass spectrometry (LC–HR–MS/MS) system as described in the following section.

2.3 | Microsomal incubations

Incubations were performed according to previous publications.[21] The incubation was conducted at 37°C using 25 μM substrate and 75 pmol/mL of CYP1A2, CYP2A6, CYP2B6, CYP2C8, CYP2C9, CYP2C19, CYP2D6, CYP2E1, CYP3A4, CYP3A5, or 50 mg protein/mL pHLM. The final incubation volume was 50 μL and consisted of 90 mM phosphate buffer, 5 mM isocitrate, 5 mM Mg^{2+}, 1.2 mM NADP+, 200 U/mL superoxide dismutase, and 0.5 U/mL isocitrate

FIGURE 1 Chemical structures of the investigated compounds

dehydrogenase. For incubations with CYP2A6 and CYP2C9, phosphate buffer was replaced with Tris-buffer, according to the manufacturer's manual. The incubation was performed for 30 minutes, reaction was started by the addition of a pre-warmed mixture of isocitrate dehydrogenase, isocitrate, $MgCl_2$, and $NADP^+$. The reaction was stopped by adding 50 μL of ice-cold acetonitrile. These incubations were performed twice for every enzyme. The mixture was centrifuged for 2 minutes at 14,000 x g and 70 μL of the supernatant were transferred to an autosampler vial and 1 μL was injected onto the LC–HR–MS/MS using the conditions as described in the following section.

2.4 | Kinetic studies

Kinetic studies were based on previous publications.[22,23] The incubations were performed for 10 minutes except for alpha-PBP, which was incubated for 5 minutes with CYP2C9, alpha-PVT for 2 minutes with CYP2B6, alpha-PHP for 5 minutes with CYP1A2, and alpha-POP for 5 minutes with CYP1A2. Protein concentrations were between 10 and 30 pmol/mL. The incubation time and enzyme concentrations were chosen to be within a linear range of metabolite formation. This was determined by preceding incubations of the substances with either varying incubation time or protein concentration. The formation of the metabolite was monitored and the range of linear correlation between the varied factor and the peak area of the metabolite was determined by visual inspection of the plot. Substrate concentrations used in this study were for alpha-PBP and alpha-PHP from 1 to 1500 μM, for alpha-PVT and alpha-PEP from 1 to 1000 μM, and for alpha-POP from 0.5 to 250 μM. Every substrate concentration was incubated twice with an additional blank sample containing no enzyme to exclude artificial metabolite formation, while all other parameters were the same as for the microsomal incubations described earlier. The reactions were stopped with 50 μL ice-cold acetonitrile containing 5 μM alpha-PVP as an internal standard. After sample preparation, 10 μL was injected onto the LC–MS^n system as described later. The relative amount of formed metabolites was determined by the product area ratio (PAR) of the metabolite and the internal standard. Determination of relative amounts was a suitable approach for the calculation of the relative net hepatic clearances.[22] Curve fitting and calculation of enzyme kinetic constants was performed by a nonlinear regression model using GNU R (https://www.r-project.org). The Michaelis-Menten equation (Equation 1) was used to calculate apparent K_m and V_{max} values for single-enzyme systems.

$$V = \frac{V_{max} \times [S]}{K_m + [S]} \quad (1)$$

The relative activity factor (RAF)[24,25] approach was used to account for differences in the functional levels of redox partners between the 2 enzyme sources. The turnover rates of the investigated CYP enzymes in ICM and pHLM were taken from the supplier's data sheets. The RAFs were calculated according to Equation 2.

$$RAF_{enzyme} = \frac{TR_{PS} \text{ in pHLM}}{TR_{PS} \text{ in ICM}} \quad (2)$$

The enzyme velocities V_{enzyme} (Equation 1) for the respective metabolic reactions were calculated at the median plasma levels of alpha-PVP at 64 ng/mL as published by Beck et al.,[26] since no plasma concentrations of the investigated compounds could not be identified. The enzyme velocities were then multiplied with the corresponding RAF leading to a value, which is defined as "contribution" (Equation 3). V_{max} and K_m values (Equation 1) were obtained from the incubations with isolated CYP enzymes.

$$contribution_{enzyme} = RAF_{enzyme} \times V_{enzyme} \quad (3)$$

$$clearance_{enzyme}[\%] = \frac{contribution_{enzyme}}{\sum contribution_{enzyme}} \times 100 \quad (4)$$

From these corrected activities (contributions), the percentages of net clearance by a particular CYP enzyme at a certain substrate concentration can be calculated according to Equation 4.

2.5 | LC–HR–MS/MS apparatus for the identification of metabolites

The analysis was performed using a Thermo Fisher Scientific (TF, Dreieich, Germany) Dionex UltiMate 3000 RS pump consisting of a degasser, a quaternary pump and an UltiMate Autosampler, coupled to a TF Q-Exactive Plus system equipped with a heated electrospray ionization HESI-II source. Mass calibration was done prior to analysis according to the manufacturer's recommendations using external mass calibration. The conditions were set according to published procedures.[5,27,28] Gradient elution was performed on a TF Accucore PhenylHexyl column (100 mm × 2.1 mm, 2.6 μm). The mobile phases consisted of 2 mM aqueous ammonium formate containing acetonitrile (1%, v/v) and formic acid (0.1%, v/v, pH 3, eluent A) and ammonium formate solution with acetonitrile: methanol (1:1, v/v) containing water (1%, v/v) and formic acid (0.1%, v/v, eluent B). The flow rate was set from 1 to 10 minutes to 500 μL/minute and from 10 to 13.5 minutes to 800 μL/minute using the following gradient: 0–1.0 minutes 99% A, 1–10 minutes to 1% A, 10–11.5-minute hold 1% A, 11.5–13.5-minute hold 99% A. The HESI-II source conditions were as follows: ionization mode, positive; sheath gas, 53 AU; auxiliary gas, 14 AU; sweep gas, 3 AU; spray voltage, 3.50 kV; heater temperature, 438°C; ion transfer capillary temperature, 320°C; and S-lens RF level, 60.0. Mass spectrometry was performed using full scan (FS) data and subsequent data-dependent acquisition (DDA). The settings for FS data acquisition were as follows: resolution, 35,000; microscans, 1; automatic gain control (AGC) target, 1e6; maximum injection time, 120 ms; and scan range, m/z 50–750. The settings for the DDA mode were as follows: dynamic exclusion, 0.1 s; resolution, 17,500; microscans, 1; loop count, 5; AGC target, 2e4; maximum injection time, 250 ms; isolation window, m/z 1.0; high collision dissociation (HCD) with stepped normalized collision energy (NCE), 17.5, 35, and 52.5%; spectrum data type, profile; and underfill ratio, 1%. TF Xcalibur Qual Browser software version 3.0.63 was used for data handling.

2.6 | LC–MS^n apparatus for the determination of enzyme kinetics

The samples from the kinetic study incubations were analyzed using a TF LXQ linear ion trap MS equipped with an HESI-II source and

coupled to a TF Accela ultra HPLC (UPLC) system consisting of a degasser, a quaternary pump, and an autosampler. The LC and MS conditions were modified from Welter et al.[21] Gradient elution was performed on a TF Hypersil GOLD C18 column (100 × 2.1 mm, 1.9 μm). The mobile phases consisted of 10 mM aqueous ammonium formate containing formic acid (0.1%, v/v, pH 3, eluent A) or acetonitrile containing formic acid (0.1%, v/v, eluent B). The flow rate was set to 500 μL/minute using the following gradient: 0 minutes 98% A,

0–3 minutes to 60% A, 3–4 minutes to 10% A, 4–5-minute hold 10% A, 5–6 minutes to 98% A, 6–7-minute hold 98% A. The HESI-II source conditions were as follows: ionization mode, positive; sheath gas, 34 AU; auxiliary gas, 11 AU; sweep gas, 3 AU; spray voltage, 3.0 kV; heater temperature, 250° C; ion transfer capillary temperature, 300°C; and S-lens RF level, 80.0. MS[1] was performed in the full scan mode (m/z 100–800). MS[2] spectra were generated with separate scan events for each mass of the parent substance, the hydroxy metabolite,

TABLE 1 Detection of investigated compounds and their metabolites as described in literature.[11,15-19] Three most abundant analytes of every model are bold, except for alpha-PEP in humans since no ranking is available in literature[11] (a: alpha-PBP, b: alpha-PVT, c: alpha-PHP, d: alpha-PEP, e: alpha-POP, HLM: human liver microsomes, PHH: primary human hepatocytes, pS9: pooled S9 fraction)

		Name	pHLM[19]	pS9 1 h	pS9 8 h	PHH[11,18] 0.5 h	PHH[11,18] 2 h	Human[11,15-18] urine
		Parent compound	**a, b, c, d, e**	**a, b, c, d, e**	**a, b, c, d, e**	**b, d**	**b, d**	**a, b, c, d, e**
Phase I	M1	Dehydro				d	d	
	M2	Dehydro (iminium)				d	d	
	M3	Dihydro-N,N-dealkyl						c
	M4	N,N-Dealkyl				d	d	c, d
	M5	Dihydro				b, d	b, d	**a, b, c, e**
	M6	Alkyl-oxo	e	d, e	d, e			**e**
	M7	Pyrrolidine-oxo						c
	M8	Pyrrolidine-oxo (lactam)	b, c, d, e	**a, b, c, d, e**	**a, b, c, d, e**	b	b	**a, b, c, d, e**
	M9	Thiophene-oxo						**b**
	M10	Dihydro-alkyl-oxo						e
	M11	Dihydro-pyrrolidine-oxo				b	b	b
	M12	Dihydro-pyrrolidine-oxo (lactam)				d	d	
	M13	Alkyl-HO	b, c, d, e	d, e	**d, e**	b, d	b, d	b, c, d, e
	M14	N-Oxide				d	d	d
	M15	Pyrrolidine-HO	**a, b, c, d, e**	b, c, d, e	b, c, d, e	b, d	b, d	b, c, d
	M16	Thiophene-HO	**b**	b	**b**	b	**b**	
	M17	Dihydro-alkyl-HO				d	d	c, d, e
	M18	Dihydro-pyrrolidine-HO				b	b	b, c
	M19	N-dealkyl-pyrrolidine-HO				d	d	d
	M20	Dihydro-N-dealkyl-COOH						c
	M21	N-Dealkyl-dehydro-pyrrolidine-HO-aldehyde						c
	M22	N-Dealkyl-COOH						c
	M23	Alkyl-HO-pyrrolidine-oxo		e	e			
	M24	Alkyl-HO-pyrrolidine-oxo (lactam)		e	e			e
	M25	N-dealkyl-pyrrolidine-HO-aldehyde						**c**
	M26	Alkyl-HO-pyrrolidine-HO				d	d	d
	M27	Pyrrolidine-di-HO		**a, b, c, d, e**	a, b, c, d, e	**b, d**	**b, d**	b
	M28	Dihydro-alkyl-aldehyde-N-dealkyl-pyrrolidine-HO-aldehyde						c
	M29	Dihydro-alkyl-COOH						e
	M30	Alkyl-COOH		e	d, e	d	d	c, e
	M31	Alkyl-HO-pyrrolidine-di-HO			c			
	M32	Pyrrolidine-tri-HO			a			
	M33	N-dealkyl-pyrrolidine-di-HO-COOH						c
Phase II	M34	Dihydro Gluc						a, c, d, e
	M35	Dehydro-pyrrolidine-HO Gluc						b
	M36	N-dealkyl-pyrrolidine-HO Gluc						d
	M37	Alkyl-HO Gluc						c, d
	M38	Dihydro-alkyl-HO Gluc						c
	M39	Dihydro-pyrrolidine-HO Gluc						b, c
	M40	Alkyl-COOH Gluc						c, e

the oxo metabolite and the internal standard. Normalized wideband collision energy was 35.0 % for MS^2. TF Xcalibur 2.0.7 software was used for data acquisition.

3 | RESULTS AND DISCUSSION

The metabolites formed by the various assays were identified by HR–MS/MS by comparing the spectra of the parent compound to those of the putative metabolites based on the detailed interpretation of the fragmentation patterns. The corresponding spectra are listed as Supporting Information in Figures S1–S5 that were used for comparing the results obtained using the different systems.

3.1 | Proposed fragmentation patterns in LC–HR–MS/MS and tentative identification of metabolites

Every parent compound underwent an elimination of the pyrrolidine ring resulting in the fragment ions with m/z 147.0804 ($C_{10}H_{11}O$) for alpha-PBP, m/z 167.0525 ($C_9H_{11}OS$) for alpha-PVT, m/z 175.1114 ($C_{12}H_{15}O$) for alpha-PHP, m/z 189.1274 ($C_{13}H_{17}O$) for alpha-PEP, and m/z 203.1430 ($C_{14}H_{19}O$) for alpha-POP. In addition, alpha-cleavage by eliminating phenylmethanone resulted in the fragment ions at m/z 112.1121 ($C_7H_{14}N$) for alpha-PBP, m/z 126.1277 ($C_8H_{16}N$) for alpha-PVT, m/z 140.1434 ($C_9H_{18}N$) for alpha-PHP, m/z 154.1590 ($C_{10}H_{20}N$) for alpha-PEP, and m/z 168.1747 ($C_{11}H_{22}N$) for alpha-POP. Because of the alpha-cleavage, every substance formed the fragment ion with m/z 105.0335 (C_7H_5O), except for alpha-PVT, which formed the fragment ion with m/z 110.9900 (C_5H_3OS). After further fragmentation, every substance formed the fragment ion with m/z 91.0542 (C_7H_7) representing a tropylium cation, except for alpha-PVT, which formed the fragment ion with m/z 97.0107 (C_5H_5S). This fragment might be a 2H-thiopyranium cation corresponding to the tropylium cation. The pyrrolidine ring was detected in every substance as the fragment ion with m/z 70.0657 (C_4H_8N) for the protonated dehydro pyrrolidine ring and the fragment ion with m/z 72.0808 ($C_4H_{10}N$) for the protonated ring. Pyrrolidine hydroxylation (spectra 3, 8, 13, 16, 19, and 29 in Figures S1–S5) was

determined by the formation of the fragment ion with m/z 86.0600 (C_4H_8NO) as a result of the introduction of oxygen (+15.9960 u). The elimination of water (-18.0106 u) did not lead to the expected fragment ion with m/z 68.0500 (C_4H_6N) representing dehydro-pyrrolidine in its radical form, but to the fragment ion with m/z 70.0657 (C_4H_8N) for the protonated dehydro-pyrrolidine ring. Nevertheless, the fragment ion with m/z 68.0500 (C_4H_6N) was detectable with a very

TABLE 3 Determined Michaelis-Menten values for pyrrolidine hydroxylation (alpha-PBP and alpha-PHP), thiophene hydroxylation (alpha-PVT), and alkyl chain hydroxylation (alpha-PEP and alpha-POP) by corresponding CYP enzymes. All K_m values were given in μM, V_{max} in PAR/min/pmol

Substance	Enzyme	K_m	V_{max}
alpha-PBP	CYP2B6	561	2E-04
	CYP2C19	32	8E-05
	CYP2D6	88	5E-04
alpha-PVT	CYP1A2	199	3E-04
	CYP2C9	23	4E-04
	CYP2C19	210	6E-04
	CYP2D6	8	9E-05
alpha-PHP	CYP1A2	50	4E-04
	CYP2B6	65	1E-04
	CYP2C9	34	1E-04
	CYP2C19	1563	3E-04
	CYP3A4	288	4E-05
alpha-PEP	CYP1A2	49	7E-04
	CYP2B6	36	2E-04
	CYP2C9	43	3E-04
	CYP2C19	88	3E-04
	CYP2D6	63	5E-05
	CYP3A4	122	3E-04
alpha-POP	CYP1A2	28	1E-03
	CYP2B6	17	2E-04
	CYP2C8	8	7E-04
	CYP2C9	681	3E-03
	CYP2C19	8	4E-04
	CYP2D6	3	2E-04
	CYP3A4	66	3E-04

TABLE 2 CYP enzymes identified for different metabolic steps in microsomal incubations with isolated CYP enzymes for the investigated substances

	Pyrrolidine ring hydroxylation	Alkyl chain hydroxylation	Thiophene ring hydroxylation	Lactam formation	Alkyl chain oxo group formation
alpha-PBP	CYP2B6, CYP2C19, CYP2D6			CYP2D6	
alpha-PVT	CYP2B6, CYP2D6		CYP1A2, CYP2B6, CYP2C9, CYP2C19, CYP2D6		
alpha-PHP	CYP2B6, CYP2C9, CYP2C19			CYP1A2, CYP2B6, CYP2C19, CYP3A4	
alpha-PEP	CYP2B6, CYP2C19	CYP1A2, CYP2B6, CYP2C19, CYP2D6, CYP3A4		CYP1A2, CYP3A4	CYP2C19, CYP3A4
alpha-POP	CYP2B6, CYP2C9 CYP2C19, CYP3A4	CYP1A2, CYP2B6, CYP2C8 CYP2C9, CYP2C19, CYP2D6, CYP3A4		CYP1A2, CYP2B6, CYP2C19, CYP3A4	CYP1A2, CYP2C9, CYP2C19, CYP2D6, CYP3A4

low abundance. Alkyl chain hydroxylated metabolites (spectra 12, 18, 27, and 28 in Figures S3–S5) resulted also in specific fragments formed by water elimination. Another indication was the exclusion of hydroxylation of the pyrrolidine, thiophene, or phenyl ring. These positions were excluded by the absence of the fragment ion with the m/z 86.0605 (C_4H_8NO) for the hydroxylated pyrrolidine ring, the fragment ion with the m/z 113.0061 (C_5H_5OS) for the hydroxylated thiophene ring, and the fragment ion with the m/z 107.0496 (C_7H_7O) for the hydroxy tropylium ion. The occurrence of the fragment ion with m/z 113.0056 (C_5H_5OS) in combination with that with m/z 72.0808 ($C_4H_{10}N$) indicated hydroxylation of the thiophene ring (spectra 7 in Figure S2). According to Gramec et al.,[29] oxidation of thiophene rings should mainly result in hydroxylations of the ring system. Formation of oxo groups at the pyrrolidine ring (spectra 2, 6, 11, 16, and 26 in Figures S1–S5) was determined by the occurrence of the fragment ion with m/z 86.0600 (C_4H_8NO) representing the protonated oxo-pyrrolidine ring. According to the hydroxylation of the pyrrolidine ring, the elimination of the oxo group resulted in a fragment ion with the 70.0657 (C_4H_8N) making the discrimination of hydroxy and oxo metabolites only possible by the mass of the parent ion. In metabolites with an oxo group at the pyrrolidine ring the formation of a lactam was considered to be most likely since Vickers and Polsky showed that nitrogen containing xenobiotics are preferably metabolized to lactams.[30] The determination as lactam was also made referring to their retention time. In previous studies lactams eluted after the parent compound while oxo metabolites eluted before the parent compound.[11,16,18,31] Keto group formation of the alkyl chain (spectra 16 and 23–25 in Figures S4 and S5) was determined by a shift of +13.9793 u for the initial fragment after pyrrolidine ring elimination. For example, in case of alpha-PEP-M (oxo-) isomer 1, oxidation of the alkyl chain resulted in the fragment m/z 203.1067 ($C_{13}H_{15}O_2$). All other metabolites were determined likewise.

3.2 | In vitro metabolism using pS9

Results of the incubations using pS9 are summarized in the Supporting Information (Table S2–S6). All investigated substances underwent multiple hydroxylations and formation of lactam groups. Differences were found in the part of the molecule where the hydroxylation took place. alpha-PBP was solely hydroxylated at the pyrrolidine ring resulting in mono- and dihydroxy metabolites and alpha-PVT was
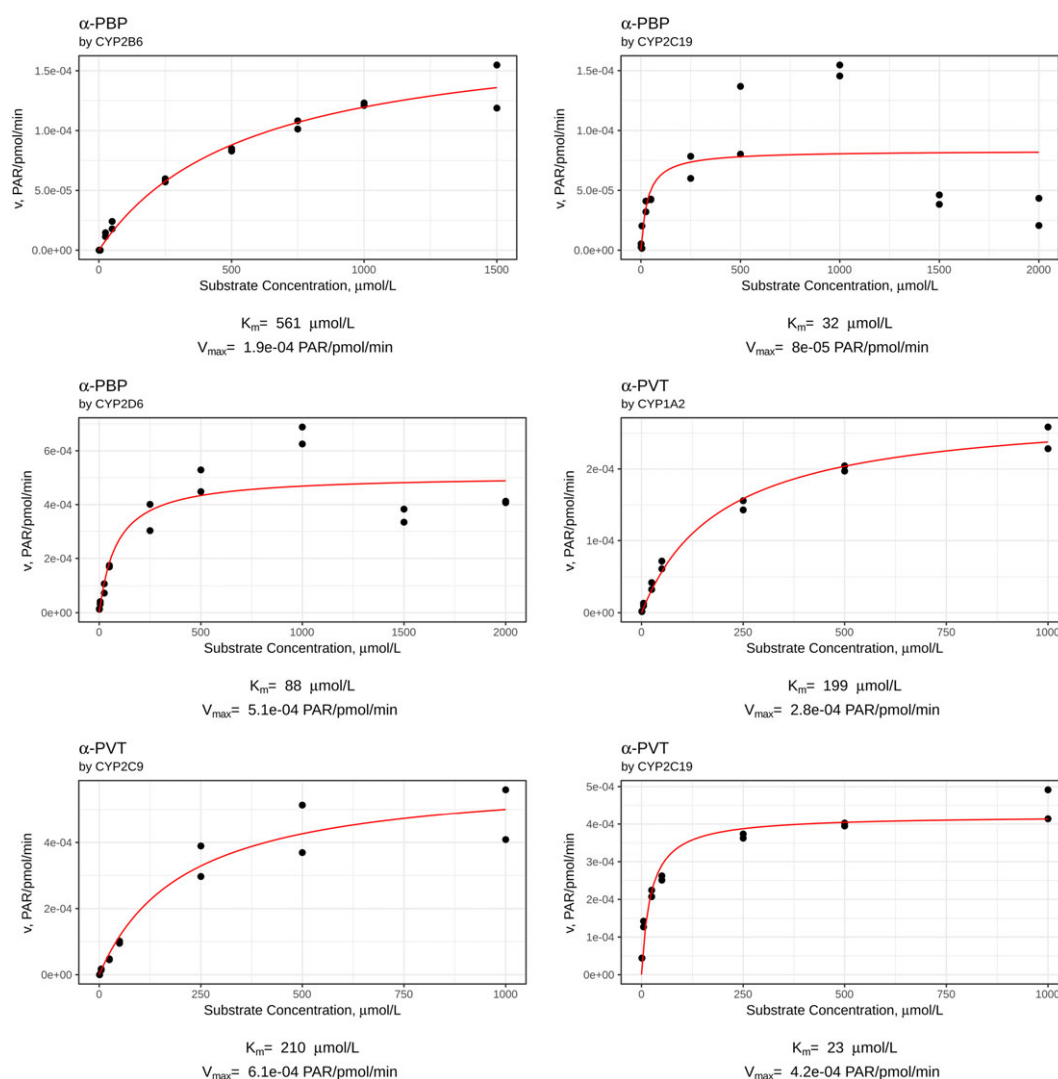

FIGURE 2 a-e, Enzyme kinetic plots for formation of hydroxy metabolites of alpha-PBP, alpha-PVT, alpha-PHP, alpha-PEP, and alpha-POP. Data points represent one incubation [Colour figure can be viewed at wileyonlinelibrary.com]

mainly hydroxylated at the thiophene ring but mono- and dihydroxy metabolites were found as well. Mono and bis-hydroxylation were observed for alpha-PHP, alpha-PEP, and alpha-POP as well as additional hydroxylation at the alkyl chain. alpha-PEP and alpha-POP were further oxidized at the side chain to an oxo and a carboxy metabolite. alpha-POP formed another pyrrolidine oxo metabolite. The metabolic steps found for each substance correlated with their kinetic characteristics as discussed in the following section.

In contrast to metabolites described in literature, glucuronides were not found. This might be the consequence of the low abundance of phase I metabolites that were formed in this experiment. Glucuronosyltransferases are known for their rather low substrate affinity (high K_m value).[32] Dihydro metabolites formed by reduction of the alpha-keto group detected in PHH incubations[11,15,16,18] could not be found in the pS9 incubations, which is consistent with results reported in previous studies.[5]

3.3 | In vitro metabolism using pHLM

Metabolites found in pHLM are summarized in the Supporting Information (Table S1). The parent compound was the most abundant analyte in every incubation. alpha-PBP was hydroxylated at the pyrrolidine ring and alpha-PVT hydroxylated at the thiophene ring and oxidized at the pyrrolidine ring to a lactam species. alpha-PHP, alpha-PEP, and alpha-POP were hydroxylated at the pyrrolidine ring and at the alkyl chain as well as oxidized at the pyrrolidine ring to a lactam. In addition, alpha-POP was further oxidized at the side chain to the corresponding oxo metabolite. The number of metabolites increased with the length of the alkyl chain. This was also in agreement with the results collected from the kinetic studies, in which the maximum enzyme velocity and the affinity to CYP enzymes increased within the homologous chain.

Takayama et al. already published the pHLM metabolism of alpha-PVT.[19] Their results corresponded to those described here. They also found hydroxylation of the thiophene ring or the pyrrolidine ring, but they did not observe the lactam formation. They could not determine whether the pyrrolidine ring or the alkyl chain was hydroxylated for lack of particular fragmentation, namely the missing fragment ion with m/z 167 representing the molecule after elimination of the pyrrolidine ring. However, in the present study, this fragment was observed in all investigated compounds after pyrrolidine ring hydroxylation.
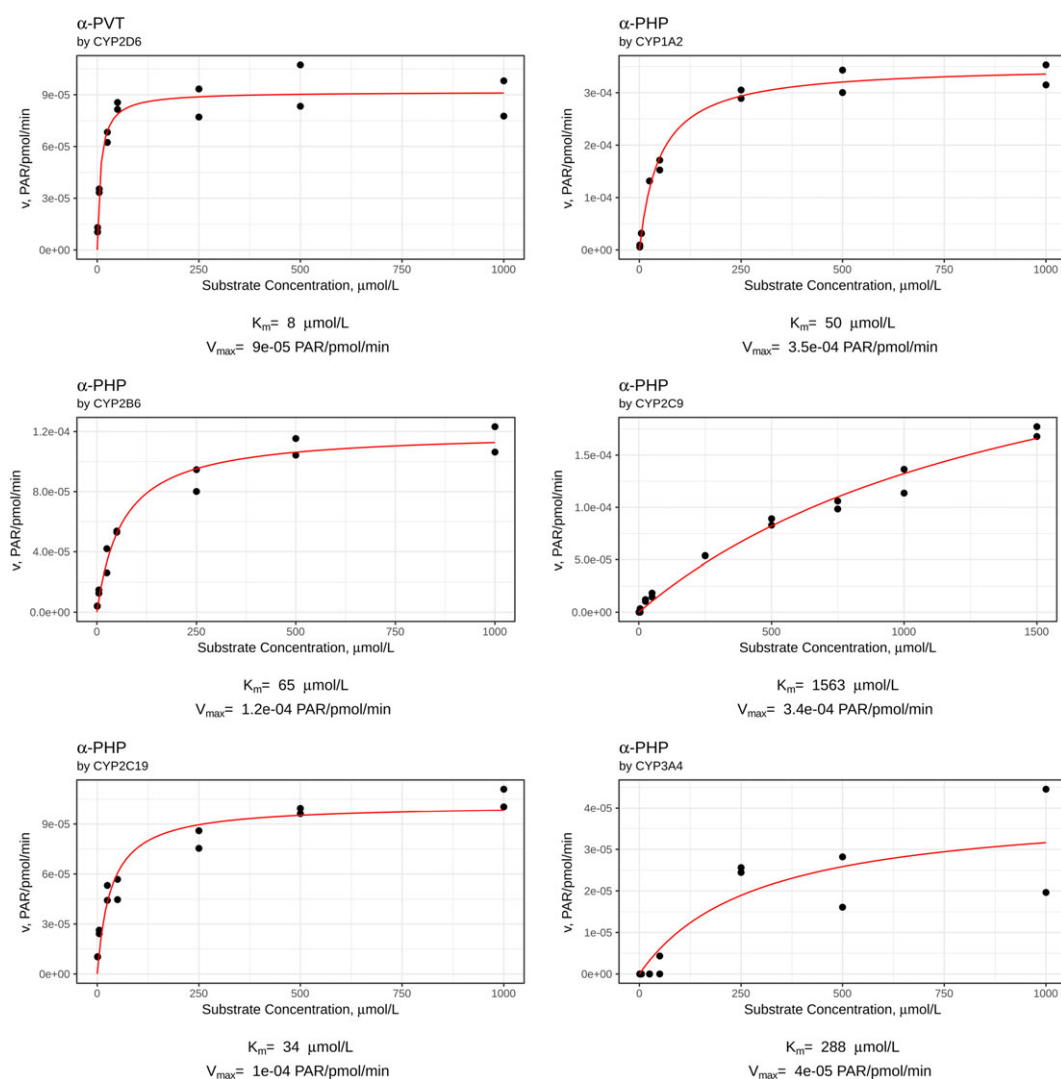

FIGURE 2 Continued.

3.4 | Comparison of different models

An overview of the metabolites described in literature and those found in the present study using pHLM and pS9 incubations are listed in Table 1. Takayama et al[19] published a study investigating the metabolism of alpha-PVT using pHLM. With the exception of the alkyl chain hydroxylation (M13), all steps could be confirmed by pHLM and pS9. In contrast, lactam formation (M8) and dihydroxylation (M27) could only be observed in the present pS9 incubations for alpha-PVT.

Incubations using PHH were published by Swortwood et al..[11,18] for alpha-PVT and alpha-PEP. The pathways observed in the present pS9 incubations were also described for PHH. Among further metabolites, particularly those formed by beta-ketone reduction (M5, M11–12, M17–18) could not be detected in pHLM and pS9. These metabolites were prominent in human urine of most cathinones (M3, M5, M10–11, M17-18, M20, M29, M34, M35, M38, and M39), but lactams formed by pHLM and pS9 were also excreted into urine. Nevertheless, the metabolic profile of PHH for the investigated alpha-cathinones was very close to that of the human urine. This is

in accordance to Richter et al, comparing different in vitro models for 4-methoxy-alpha-pyrrolidinovalerophenone.[20]

However, the most abundant compounds found in all incubations were the parent compounds indicating that cathinones were metabolized only to a minor extent. This is in accordance with urine findings for alpha-PHP and alpha-PVT.[16,18] The main metabolites found in every compared model were the lactam (M8) and the pyrrolidine hydroxy metabolite (M15). Glucuronidation (M34–40) was merely found in authentic human urine samples. Sulfation was not detectable in any of the experiments, possibly due to the lack of aromatic hydroxylations of these substances. The complexity of a whole organism for the metabolism of the investigated substances was best represented by PHH, which was the only investigated in vitro model that was able to elucidate every metabolic step that was also observed in human urine. Nevertheless, in accordance to previously published studies,[20] pooled human liver fractions and especially pS9 were able to form metabolites of the investigated substances that were identified as most suitable targets for monitoring them in human urine screenings. At least all results from in vitro models should be confirmed by authentic human urine.
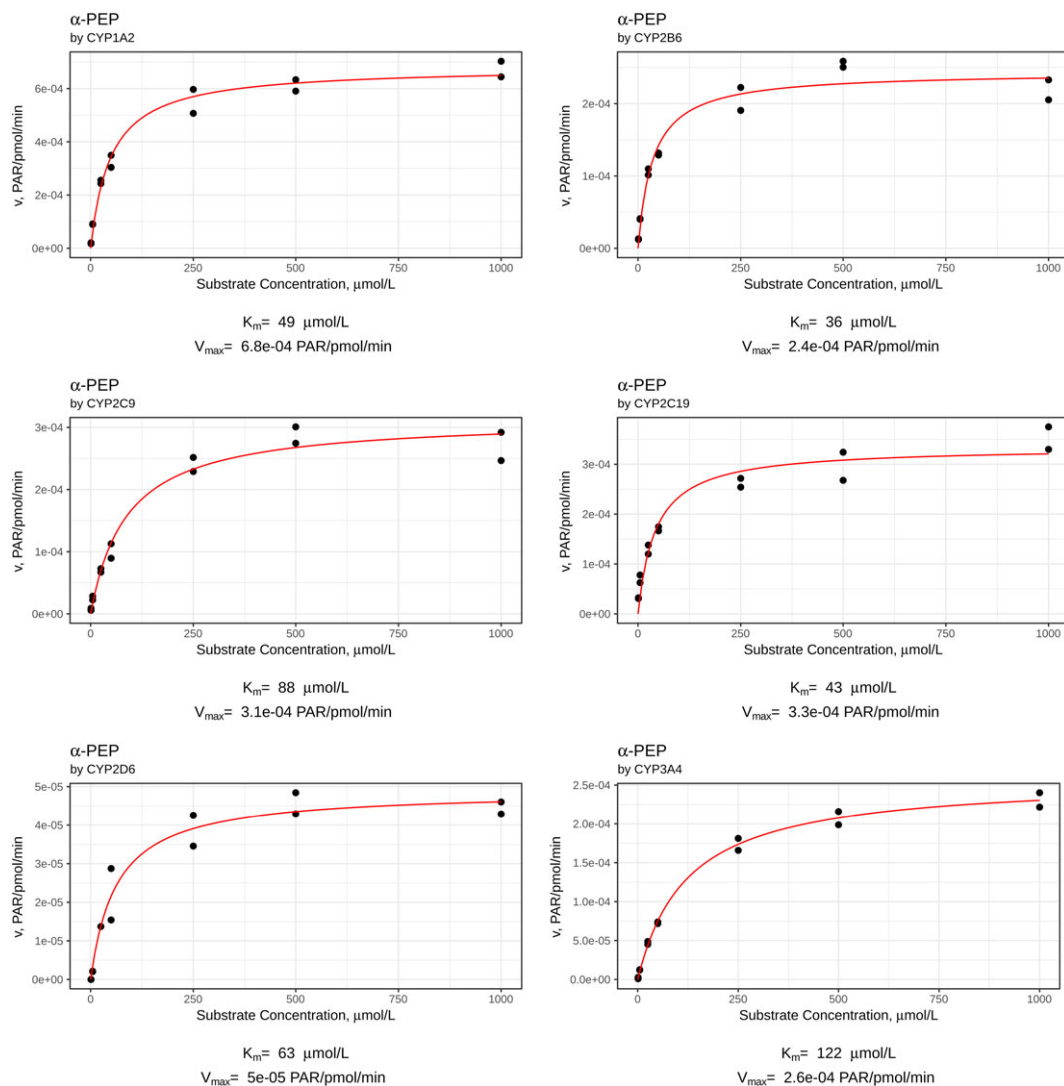

FIGURE 2 Continued.

3.5 | Microsomal incubations with isolated CYP enzymes

The results of the incubations with isolated CYP enzymes are summarized in Table 2. Pyrrolidine ring hydroxylations were catalyzed by CYP2B6, CYP2C9, CYP2C19, CYP2D6, and CYP3A4. CYP1A2 additionally catalyzed alkyl chain hydroxylations. The thiophene ring hydroxylation was catalyzed by CYP1A2, CYP2B6, CYP2C9, CYP2C19, and CYP2D6. Lactam formation was catalyzed by CYP1A2, CYP2B6, CYP2C19, CYP2D6, and CYP3A4. The formation of an oxo

group at the alkyl chain was catalyzed by CYP1A2, CYP2B6, CYP2C19, CYP2D6, and CYP3A4.

3.6 | CYP enzyme kinetics and calculation of hepatic net clearance

The monitored reaction for the determination of the kinetic parameters K_m and V_{max} was the most frequently metabolic step found in the CYP initial screening and kinetic incubations. The K_m and V_{max} values are
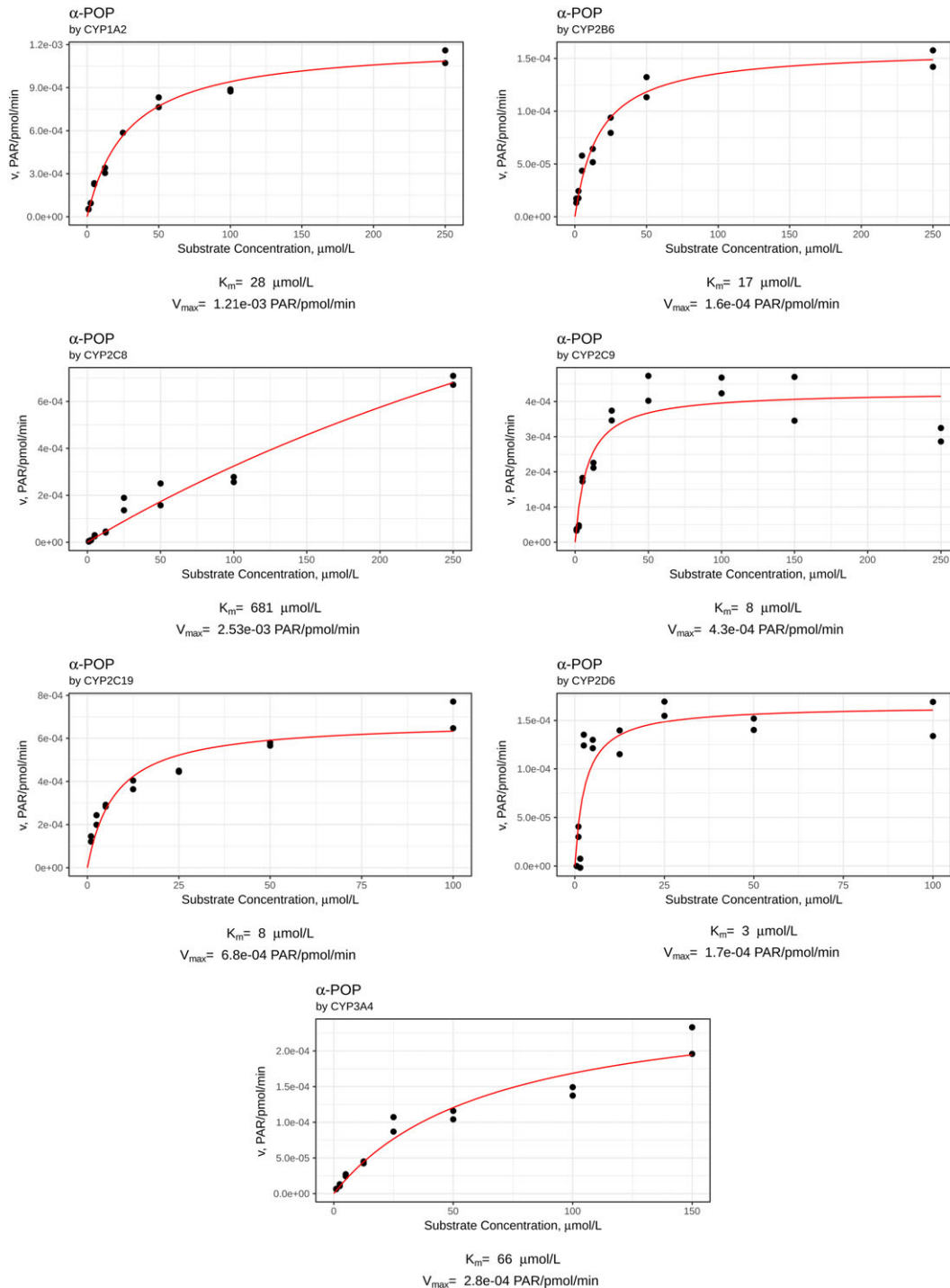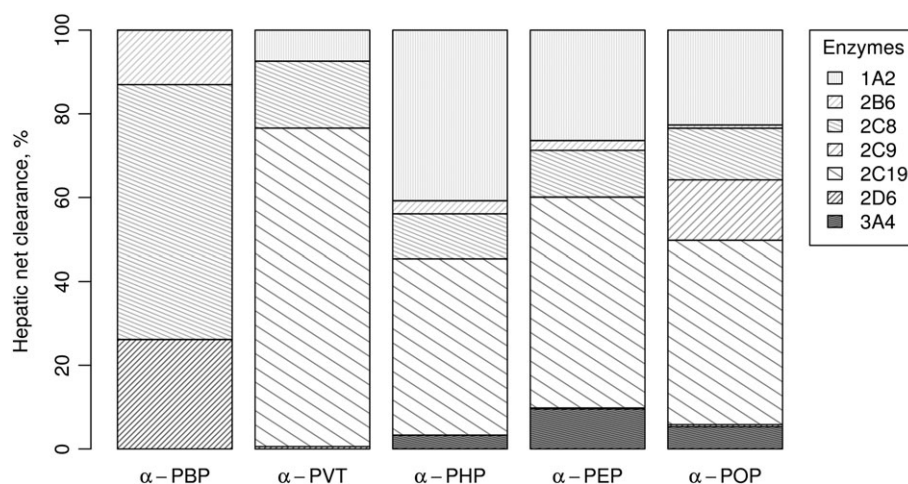

FIGURE 2 Continued.

FIGURE 3 Relative activity factor (RAF) corrected, calculated hepatic total net clearances of CYP1A2, CYP2B6, CYP2C8, CYP2C9, CYP2C19, CYP2D6, and CYP3A4 at a concentration of 64 ng/mL for the hydroxylation of the pyrrolidine ring (alpha-PBP and alpha-PHP), the thiophene ring (alpha-PVT), or the alkyl chain (alpha-PEP and alpha-POP)

summarized in Table 3. All profiles of metabolite formation followed classic Michaelis-Menten kinetics (Figures 2. a–e), except for product formation of alpha-PHP by CYP2C9 and alpha-POP by CYP2C8. There is reasonable suspicion that these product formations followed biphasic kinetics when comparing them to general atypical kinetics described by Korzekwa et al.[33] Results of the calculation of the in vivo hepatic net clearance are shown in Figure 3. Concerning alpha-PBP, CYP2B6 catalyzed the hydroxylation of the pyrrolidine ring by about 13%, CYP2C19 by 61%, and CYP2D6 by 26%. The data point shown in Figure 2a. for the CYP2C19/2D6 catalyzed reaction indicated substrate inhibition at very high substrate concentrations, which is expected not to be of practical relevance as the used alpha-PBP concentration should not be reached in vivo. For alpha-PVT, the parameters were calculated for the hydroxylation of the thiophene ring. Although CYP2B6 also catalyzed this reaction, the amount of the formed metabolite was too low to be monitored. Thiophene hydroxylation was catalyzed by CYP1A2 by about 7%, CYP2C9 by 76%, CYP2C19 by 16%, and by CYP2D6 by 1%. alpha-PHP was mainly hydroxylated at the pyrrolidine ring. This was catalyzed by CYP2B6 by about 5%, CYP2C9 by 71%, CYP2C19 by 18%, and CYP3A4 by 6%. The most observed reaction for alpha-PEP was the hydroxylation of the side chain. This was catalyzed by CYP1A2 by about 26%, CYP2B6 by 2%, CYP2C9 by 50%, CYP2C19 by 11%, CYP2D6 by 0.5%, and CYP3A4 by 9.5%. The same reaction was used for the determination of the hepatic net clearance of alpha-POP. CYP1A2 catalyzed this reaction by about 23%, CYP2B6 by 1%, CYP2C8 by 14%, CYP2C9 by 44%, CYP2C19 by 12%, CYP2D6 by 0.5%, and CYP3A4 by 5.5%. As already observed in incubations with isolated CYP enzymes, hydroxylation of the side chain was catalyzed by CYP1A2, CYP2C19, and CYP3A4 to a large extent. The results also indicated that CYP2C9 was responsible for the main part of the CYP-mediated hepatic clearance. In addition, the involvement of CYP1A2 for side chain oxidation increased with the length of the side chain. In general, these results could be explained by the increasing lipophilic character of the homologous chain of the investigated compounds. alpha-PBP and alpha-PVT had in relation to the homologous chain of the investigated compounds high K_m and V_{max} values, which reflected the comparatively few metabolites that were

found after incubation with pS9. alpha-PEP and alpha-POP had kinetic characteristics that pointed to extensive metabolism and this was confirmed by the number of metabolites found in this experiment. Besides the number of the metabolites, the kind of metabolism also correlates with the incubations with isolated CYP enzymes. Pyrrolidine hydroxylation was a dominant metabolic step for alpha-PBP, thiophene hydroxylation for alpha-PVT, and alkyl chain hydroxylation for alpha-PEP and alpha-POP. alpha-PHP, which represents a comparatively medium-length homologous chain, was mainly metabolized at the pyrrolidine ring. These results indicated that the overall metabolism and the preferred metabolic step of the investigated CYP enzymes concerning hydroxylation of the side chain increased with the length of the alkyl chain. These findings did especially apply for CYP1A2, CYP2C19, and CYP3A4. CYP2C9, CYP2C19, and CYP2D6 are polymorphically expressed enzymes that can cause interindividual variability concerning the hepatic clearance.[34] Apart from alpha-PBP, a wide range of CYP enzymes was involved in the metabolism of these substances, which suggests that variabilities in the metabolizing phenotype may be balanced by other CYP enzymes involved in the metabolism. However, for compounds such as alpha-PVT and alpha-POP mainly undergoing non-CYP mediated metabolism based on human urine findings, the RAF approach for CYP enzymes only may not be of great value as some of the important clearance pathways are not accounted for.

4 | CONCLUSION

Under in vitro conditions, the investigated substances underwent hydroxylation at different structural locations of the molecule depending on the length of the alkyl chain. Longer alkyl chains resulted in alkyl chain hydroxylation instead of pyrrolidine ring hydroxylation. For alpha-PVT, the hydroxylation of the thiophene ring was predominant compared to what was observed at the pyrrolidine ring. Comparing these results with published data obtained using pHLM, PHH, and authentic human urine samples, PHH provided the broadest pattern of metabolites for the investigated substances. Nevertheless, pooled human liver fractions and especially pS9 were able to form metabolites

of the investigated substances that are important targets for monitoring in a human urine screening approach. The kinetic studies revealed that the main CYP enzymes responsible for the hepatic net clearance were CYP1A2, CYP2C9, and CYP2C19 except for alpha-PBP, which was mainly metabolized by CYP2C19 and CYP2D6. The affinity of the investigated enzymes to their substrate increased with the length of the side chain and was reflected in the decreasing K_m values for the homologous chain.

ORCID

Sascha K. Manier http://orcid.org/0000-0002-7126-5263
Hans H. Maurer http://orcid.org/0000-0003-4579-4660
Markus R. Meyer http://orcid.org/0000-0003-4377-6784

REFERENCES

1. Sinz MA. In vitro and in vivo models of drug metabolism. In: *Encyclopedia of Drug Metabolism and Interactions.* John Wiley & Sons, Inc.; 2012.

2. Maurer HH, Meyer MR. High-resolution mass spectrometry in toxicology: current status and future perspectives. *Arch Toxicol.* 2016;90(9):2161-2172.

3. Peters FT, Meyer MR. In vitro approaches to studying the metabolism of new psychoactive compounds. *Drug Test Anal.* 2011;3(7–8):483-495.

4. Jia L, Liu X. The conduct of drug metabolism studies considered good practice (II): in vitro experiments. *Curr Drug Metab.* 2007;8(8):822-829.

5. Richter LHJ, Flockerzi V, Maurer HH, Meyer MR. Pooled human liver preparations, HepaRG, or HepG2 cell lines for metabolism studies of new psychoactive substances? A study using MDMA, MDBD, butylone, MDPPP, MDPV, MDPB, 5-MAPB, and 5-API as examples. *J Pharm Biomed Anal.* 2017;143:32-42.

6. Sinz MW, Kim S. Stem cells, immortalized cells and primary cells in ADMET assays. *Drug Discov Today Technol.* 2006;3(1):79-85.

7. Liu X, Jia L. The conduct of drug metabolism studies considered good practice (I): analytical systems and in vivo studies. *Curr Drug Metab.* 2007;8(8):815-821.

8. EMCDDA. *EMCDDA–Europol Joint Report on a new psychoactive substance: 1-phenyl-2-(1-pyrrolidinyl)-1-pentanone (α-PVP).* European Monitoring Centre for Drugs and Drug Addiction; 2015.

9. Kudo K, Usumoto Y, Kikura-Hanajiri R, Sameshima N, Tsuji A, Ikeda N. A fatal case of poisoning related to new cathinone designer drugs, 4-methoxy PV8, PV9, and 4-methoxy PV9, and a dissociative agent, diphenidine. *Leg Med (Tokyo).* 2015;17(5):421-426.

10. Odoardi S, Romolo FS, Strano-Rossi S. A snapshot on NPS in Italy: Distribution of drugs in seized materials analysed in an Italian forensic laboratory in the period 2013-2015. *Forensic Sci Int.* 2016;265:116-120.

11. Swortwood MJ, Ellefsen KN, Wohlfarth A, et al. First metabolic profile of PV8, a novel synthetic cathinone, in human hepatocytes and urine by high-resolution mass spectrometry. *Anal Bioanal Chem.* 2016;408(18):4845-4856.

12. Marusich JA, Antonazzo KR, Wiley JL, Blough BE, Partilla JS, Baumann MH. Pharmacology of novel synthetic stimulants structurally related to the "bath salts" constituent 3,4-methylenedioxypyrovalerone (MDPV). *Neuropharmacology.* 2014;87:206-213.

13. Coppola M, Mondola R. Synthetic cathinones: chemistry, pharmacology and toxicology of a new class of designer drugs of abuse marketed as "bath salts" or "plant food". *Toxicol Lett.* 2012;211(2):144-149.

14. Kolanos R, Solis E Jr, Sakloth F, De Felice LJ, Glennon RA. "Deconstruction" of the abused synthetic cathinone methylenedioxypyrovalerone (MDPV) and an examination of effects at the human dopamine transporter. *ACS Chem Neurosci.* 2013;4(12):1524-1529.

15. Matsuta S, Shima N, Kamata H, et al. Metabolism of the designer drug alpha-pyrrolidinobutiophenone (alpha-PBP) in humans: identification and quantification of the phase I metabolites in urine. *Forensic Sci Int.* 2015;249:181-188.

16. Paul M, Bleicher S, Guber S, Ippisch J, Polettini A, Schultis W. Identification of phase I and II metabolites of the new designer drug alpha-pyrrolidinohexiophenone (alpha-PHP) in human urine by liquid chromatography quadrupole time-of-flight mass spectrometry (LC–QTOF–MS). *J Mass Spectrom.* 2015;50(11):1305-1317.

17. Shima N, Kakehashi H, Matsuta S, et al. Urinary excretion and metabolism of the alpha-pyrrolidinophenone designer drug 1-phenyl-2-(pyrrolidin-1-yl)octan-1-one (PV9) in humans. *Forensic Toxicol.* 2015;33(2):279-294.

18. Swortwood MJ, Carlier J, Ellefsen KN, et al. In vitro, in vivo and in silico metabolic profiling of alpha-pyrrolidinopentiothiophenone, a novel thiophene stimulant. *Bioanalysis.* 2016;8(1):65-82.

19. Takayama T, Suzuki M, Todoroki K, et al. UPLC/ESI-MS/MS-based determination of metabolism of several new illicit drugs, ADB-FUBINACA, AB-FUBINACA, AB-PINACA, QUPIC, 5F-QUPIC and alpha-PVT, by human liver microsome. *Biomed Chromatogr.* 2014;28(6):831-838.

20. Richter LHJ, Maurer HH, Meyer MR. New psychoactive substances: Studies on the metabolism of XLR-11, AB-PINACA, FUB-PB-22, 4-methoxy-alpha-PVP, 25-I-NBOMe, and meclonazepam using human liver preparations in comparison to primary human hepatocytes, and human urine. *Toxicol Lett.* 2017;280:142-150.

21. Welter J, Meyer MR, Wolf EU, Weinmann W, Kavanagh P, Maurer HH. 2-methiopropamine, a thiophene analogue of methamphetamine: studies on its metabolism and detectability in the rat and human using GC-MS and LC-(HR)-MS techniques. *Anal Bioanal Chem.* 2013;405(10):3125-3135.

22. Meyer GM, Meyer MR, Wink CS, Zapp J, Maurer HH. Studies on the in vivo contribution of human cytochrome P450s to the hepatic metabolism of glaucine, a new drug of abuse. *Biochem Pharmacol.* 2013;86(10):1497-1506.

23. Meyer MR, Vollmar C, Schwaninger AE, Wolf E, Maurer HH. New cathinone-derived designer drugs 3-bromomethcathinone and 3-fluoromethcathinone: studies on their metabolism in rat urine and human liver microsomes using GC-MS and LC-high-resolution MS and their detectability in urine. *J Mass Spectrom.* 2012;47(2):253-262.

24. Crespi CL, Miller VP. The use of heterologously expressed drug metabolizing enzymes--state of the art and prospects for the future. *Pharmacol Ther.* 1999;84(2):121-131.

25. Venkatakrishnan K, von Moltke LL, Court MH, Harmatz JS, Crespi CL, Greenblatt DJ. Comparison between cytochrome P450 (CYP) content and relative activity approaches to scaling from cDNA-expressed CYPs to human liver microsomes: ratios of accessory proteins as sources of discrepancies between the approaches. *Drug Metab Dispos.* 2000;28(12):1493-1504.

26. Beck O, Franzen L, Backberg M, Signell P, Helander A. Toxicity evaluation of alpha-pyrrolidinovalerophenone (alpha-PVP): results from intoxication cases within the STRIDA project. *Clin Toxicol (Phila).* 2016;54(7):568-575.

27. Caspar AT, Helfer AG, Michely JA, et al. Studies on the metabolism and toxicological detection of the new psychoactive designer drug 2-(4-iodo-2,5-dimethylphenyl)-N-[(2-methoxyphenyl)methyl]ethanamine (25I-NBOMe) in human and rat urine using GC-MS, LC-MS(n), and LC-HR-MS/MS. *Anal Bioanal Chem.* 2015;407(22):6697-6719.

28. Helfer AG, Michely JA, Weber AA, Meyer MR, Maurer HH. Orbitrap technology for comprehensive metabolite-based liquid chromatographic-high resolution-tandem mass spectrometric urine drug screening - exemplified for cardiovascular drugs. *Anal Chim Acta.* 2015;891:221-233.

29. Gramec D, Peterlin Masic L, Sollner DM. Bioactivation potential of thiophene-containing drugs. *Chem Res Toxicol.* 2014;27(8): 1344-1358.

30. Vickers S, Polsky SL. The biotransformation of nitrogen containing xenobiotics to lactams. *Curr Drug Metab.* 2000;1(4):357-389.

31. Shima N, Kakehashi H, Matsuta S, et al. Urinary excretion and metabolism of the α-pyrrolidinophenone designer drug 1-phenyl-2-(pyrrolidin-1-yl)octan-1-one (PV9) in humans. *Forensic Toxicology.* 2015;33(2):279-294.

32. Kanayama N, Kanari C, Masuda Y, Ohmori S, Ooie T. Drug-drug interactions in the metabolism of imidafenacin: role of the human cytochrome P450 enzymes and UDP-glucuronic acid transferases, and potential of imidafenacin to inhibit human cytochrome P450 enzymes. *Xenobiotica.* 2007;37(2):139-154.

33. Korzekwa KR, Krishnamachary N, Shou M, et al. Evaluation of atypical cytochrome P450 kinetics with two-substrate models: evidence that multiple substrates can simultaneously bind to cytochrome P450 active sites. *Biochemistry.* 1998;37(12):4137-4147.

34. Bozina N, Bradamante V, Lovric M. Genetic polymorphism of metabolic enzymes P450 (CYP) as a susceptibility factor for drug response, toxicity, and cancer risk. *Arh Hig Rada Toksikol.* 2009;60(2):217-242.

SUPPORTING INFORMATION

Additional Supporting Information may be found online in the supporting information tab for this article.

3.2 Automated optimization of XCMS parameters for improved peak picking of liquid chromatography–mass spectrometry data using the coefficient of variation and parameter sweeping for untargeted metabolomics (DOI: 10.1002/dta.2552)[95]

RESEARCH ARTICLE

Automated optimization of XCMS parameters for improved peak picking of liquid chromatography–mass spectrometry data using the coefficient of variation and parameter sweeping for untargeted metabolomics

Sascha K. Manier[1] [iD] | Andreas Keller[2] | Markus R. Meyer[1] [iD]

[1] Department of Experimental and Clinical Toxicology, Institute of Experimental and Clinical Pharmacology and Toxicology, Saarland University, Center for Molecular Signaling (PZMS), 66421 Homburg, Germany

[2] Chair of Clinical Bioinformatics, Saarland University, Saarbruecken, Germany

Correspondence
Markus R. Meyer, Department of Experimental and Clinical Toxicology, Center for Molecular Signaling (PZMS), Saarland University, 66421 Homburg, Germany.
Email: markus.meyer@uks.eu

Abstract

Accurate peak picking and further processing is a current challenge in the analysis of untargeted metabolomics using liquid chromatography–mass spectrometry (LC–MS) data. The optimization of these processes is crucial to obtain proper results. This study investigated and optimized the detection of peaks by XCMS, a widely used R package for peak picking and processing of high-resolution LC–MS metabolomics data by their coefficient of variation using neat standard solutions of drug like compounds. The obtained results were additionally verified by using fortified pooled plasma samples. Settings of the mass spectrometer were optimized by recommendations in literature to enable a reliable detection of the investigated analytes. XCMS parameters were evaluated using a comprehensive parameter sweeping approach. The optimization steps were statistically evaluated and further visualized after principal component analysis (PCA). Concerning the lower concentrated solution in methanol samples, the optimization of both mass spectrometer and XCMS parameters improved the median coefficient of variation from 24% to 7%, retention time fluctuation from 9.3 seconds to 0.54 seconds, and fluctuation of the mass to charge ratio (m/z) from m/z 0.00095 to m/z 0.00028. The number of parent compounds and their related species annotated by CAMERA increased from 88 to 113 while the total amount of features decreased from 3282 to 428. Optimized MS settings such as increased resolution led to a higher specificity of peak picking. PCA supported these findings by showing the best clustering of samples after optimization of both mass spectrometer and XCMS parameters. The results implied that peak picking needs to be individually adapted for the experimental set up. Reducing unwanted variation in the data set was most successful after combining high resolving power with strict peak picking settings.

KEYWORDS

LC–HRMS/MS, parameter optimization, untargeted metabolomics, XCMS

1 | INTRODUCTION

Studies on the metabolome (metabolomics) by liquid chromatography–mass spectrometry (LC–MS) are still an analytical challenge. They are meant to be comprehensive studies on the metabolism of an organism with the aim to identify biomarkers for non-physiological conditions such as diseases or intoxications amongst others.[1,2]

There are generally two approaches used to achieve this. The first is called targeted metabolomics, the analysis of a set of already known metabolites. This enables a specific monitoring of metabolites that are suspected to have an influence on the studied condition. Such an approach assumes that the investigator already has a certain amount of knowledge about the metabolic pathways that are affected. This knowledge is not always present and the prediction what might be affected is hard to achieve.[1]

Untargeted metabolomics avoids the problem of not having any knowledge about the affected pathways. It provides an impartial approach for the study of the metabolome by not monitoring specific metabolites but as many as possible.[2,3] This aspect of comprehensiveness bears its own difficulties and involves not only huge amounts of data but also complex statistical methods that are necessary to distinguish relevant information from irrelevant information.[4]

For untargeted metabolomics, several preprocessing pipelines are currently used for the detection of chromatographic peaks, their alignment, and annotation such as MZmine 2,[5] Metalign,[6] and XCMS.[7] Different publications performed comparisons of these tools and concluded that XCMS might be one of the best solutions for high resolution LC–MS.[8-10] The choice of appropriate preprocessing software is not a guarantee for proper results. Since preprocessing software usually offers many parameters to adjust peak picking and alignment algorithms, it is crucial to optimize them.[11-13] Thus several approaches have been published to optimize peak picking parameters by design of experiment approaches,[13,14] discriminant analysis,[11] as well as multiple feature extraction and subsequent merging.[15] All of these approaches improved the obtained data significantly, but were also time consuming taking from 33 days[13] down to 40 hours.[14] Libiseller et al[16] published an optimization approach based on isotopic patterns using naturally occurring ^{13}C isotopes. It is notable that almost none of the published approaches was evaluated using defined substance mixtures but rather biological samples containing an unmanageable number of compounds.

The present optimization approach uses variance to minimize unwanted variability in the data set. As a straightforward and common measure, we decided to compute the coefficient of variation (CV) as a standardized measure that considers variance in relation to the mean and is more robust to outlier than standard deviation. Data sets of untargeted metabolomics are influenced by several sources of variability such as instrument instability or variability in sample conditions as well as actual biological variability. Variability within and between groups is an important aspect of untargeted data sets since statistical methods such as principal component analysis (PCA) only reveal group structure when variation within groups is sufficiently less than between groups.[4] Concerning preprocessing of untargeted metabolomics, such variability can also be introduced by an inappropriate choice of algorithm parameters that lead to the detection of chromatographic noise,[17] insufficient aligning, and production of artifacts. The aim of this study was therefore to evaluate the CV as an optimization parameter that reflects the variability of the data set and additionally to optimize mass spectrometer settings for an optimal result.

2 | EXPERIMENTAL

2.1 | Chemicals and reagents

All experiments were conducted using two neat standard mixtures. The first mixture (Mix High) was a one-point spike solution for the quantitation of drugs in blood plasma as described by Michely et al.[18] The second mixture was the corresponding lower concentrated solution (Mix Low). Both mixtures were prepared in methanol as well as in pooled plasma as described elsewhere.[18] They contained 40 of the published 45 substances, leaving out those which appeared to be unstable. Every substance of the mixture is listed in Table S1 with its corresponding concentrations in both mixtures. The reference standards of the studied drugs and metabolites were kindly provided by the corresponding pharmaceutical companies. Trimipramine-d_3 was obtained from LGC Standards (Wesel, Germany). Acetonitrile (LC–MS grade), and methanol (LC–MS grade) were obtained from VWR (Darmstadt, Germany). Water was purified using a Millipore filtration unit (18.2 $\Omega \times$ cm water resistance). Ammonium formate and formic acid were obtained from Sigma (Taufkirchen, Germany). Pooled plasma samples (stabilized by citrate) were obtained from a regional blood bank.

2.2 | LC–HRMS/MS apparatus and optimization of mass spectrometer settings

The analysis was performed using a Thermo Fisher Scientific (TF, Dreieich, Germany) Dionex UltiMate 3000 RS pump consisting of a degasser, a quaternary pump and an UltiMate Autosampler, coupled to a Q-Exactive Plus system equipped with a heated electrospray ionization HESI-II source. Mass calibration was done prior to analysis according to the manufacturer's recommendations using external mass calibration. Additionally before each experiment, the apparatus' spray shield and capillary was thoroughly cleaned before each experiment. The performance of the column and the mass spectrometer was tested using a test mixture as described by Maurer et al[19,20] prior to every experiment. The starting conditions were set according to published procedures.[21-23] Ionization mode was set to positive, since none of the investigated substances required negative ionization and the injection volume was set to 1 μL. Gradient elution was performed on a TF Accucore PhenylHexyl column (100 mm × 2.1 mm, 2.6 μm). The mobile phases consisted of 2mM aqueous ammonium formate containing acetonitrile (1%, v/v) and formic acid (0.1%, v/v, pH 3, eluent A) and ammonium formate solution with acetonitrile: methanol (1:1, v/v) containing water (1%, v/v) and formic acid (0.1%, v/v, eluent B). The flow rate was set from 1–10 minutes to 500 μL/min and from 10–13.5 minutes to 800 μL/min using the following gradient: 0–1-.0 minutes 99% A, 1–10 minutes to 1% A, 10–11.5-minute hold 1% A, 11.5–13.5-minute hold 99% A. The HESI-II source conditions were

as follows: ionization mode, positive; sheath gas, 53 AU; auxiliary gas, 14 AU; sweep gas, 3 AU; spray voltage, 3.50 kV; heater temperature, 438°C; ion transfer capillary temperature, 320°C; and S-lens RF level, 60.0. Mass spectrometry was performed using full scan (FS) data and subsequent data-dependent acquisition (DDA). The settings for FS data acquisition were as follows: resolution, 35 000; microscans, 1; automatic gain control (AGC) target, 1e6; maximum injection time, 120 ms; and scan range, m/z 50–750. The settings for the DDA mode were as follows: dynamic exclusion, 0.1 seconds; resolution, 17 500; microscans, 1; loop count, 5; AGC target, 2e4; maximum injection time, 250 ms; isolation window, m/z 1.0; high collision dissociation (HCD) with stepped normalized collision energy (NCE), 17.5, 35, and 52.5%; spectrum data type, profile; and underfill ratio, 1%. Xcalibur Qual Browser software version 3.0.63 was used for data handling. The optimization was conducted regarding previously published investigations for LC–HRMS/MS metabolomics in matters of scan mode, resolution of the mass spectrometer and cycle time.[24-26] The obtained results were evaluated regarding the recovery of the investigated compounds as well as peak shapes.

2.3 | Data processing and optimization of XCMS parameters

The source code and related data were made available on GitHub (https://github.com/saskema/centWaveOpt). LC–HRMS/MS .RAW files were converted into mzXML files and subsequently centroided using Proteo Wizard.[27] Peak picking was performed using XCMS in an R environment[7,28] and annotation of isotopes, adducts, and artifacts was performed using the R package CAMERA.[29] The parameter sweeping consisted of consecutive loops, one for every parameter of the centWave algorithm as well as the bandwidth parameter for the grouping of features using the group.density algorithm.[7] The parameter sweeping started with the standard parameters of XCMS Online for the Q-Exactive[30] and was conducted within certain ranges using the corresponding step size as described in Table 1. Each parameter was altered independently, while the rest remained at the initial level. The three values of each parameter that led to the lowest median CV were additionally combined and processed in every possible combination to

TABLE 1 Ranges for the parameter sweeping and their step sizes conducted using the centWave algorithm. ppm = allowed ppm deviation of mass traces for peak picking, snthresh = signal-to-noise threshold, mzdiff = minimum difference in m/z for two peaks to be considered as separate, bw = bandwidth for grouping of peaks across separate chromatograms

Parameter	Minimum	Maximum	Step Size
Peakwidth, minimum	1	10	0.1
Peakwidth, maximum	10	100	1
ppm	1	2.5	0.1
snthresh	1	100	0.1
mzdiff	−0.1	0.1	0.002
Prefilter, scan number	1	100	1
Prefilter, scan abundance	100	10000	100
bw	0.5	5	0.5

investigate cross effects. XCMS Online suggested the following parameters: minimum peakwidth, 5 seconds; maximum peakwidth, 20 seconds; ppm deviation, 5 ppm; signal-to-noise threshold (snthresh), 4; minimum difference in exact mass for putative overlapping peaks (mzdiff), mass to charge ratio (m/z) 0.01; minimum of scan points per peak in prefilter, 3; minimum of peak intensity in prefilter, 100; bandwidth for grouping peaks of different samples (bandwidth), 5. After peak picking the distribution of the CV was calculated for those features that appeared in every replicate and the applied values for the individual parameters were sorted by the median of their CV. Peak picking was also benchmarked by recording the time for the execution of the algorithm. This enabled an evaluation of the prefilter parameters of the centWave algorithm as intended by Tautenhahn et al.[31] This optimization was conducted on the Mix Low samples. After peak picking every feature with a retention time lower than 60 seconds or higher than 720 seconds was removed, since they were acquired during column acquisition or washing phase of the chromatography. According to Wehrens et al,[32] feature abundances with a value of zero were replaced by the lowest measured abundance as a surrogate LOD, subsequently log10 transformed and mean centered. The transformed data set was subsequently analyzed using PCA.

2.4 | Recovery of analytes in technical replicates

The identification after peak picking process was conducted by manual inspection of the obtained feature lists using the monoisotopic mass of the substances and their retention time. For a substance to be filed as found, the corresponding feature needed to fulfill the following requirements: deviation of the monoisotopic mass, 5 ppm or lower; deviation of the retention time to that of the peak apex in Xcalibur, 10 seconds or lower; and detection in every analytical run. Isotopes, adducts, and artifacts of the investigated analytes were assumed when CAMERA suggested them. The measurements of the mixtures were performed in ten replicates. The optimization process was additionally evaluated by the distribution of the CV as well as the fluctuation of integrated masses and retention times within replicates. The results were verified using fortified plasma samples that were analyzed as described in 2.2 and 2.3.

2.5 | Metabolomic-like analysis

Metabolomic-like studies of neat standard solutions and fortified plasma samples were conducted using the initial and the optimized apparatus settings. Peak picking for both experiments was performed using the initial settings and the optimized settings obtained from technical replicates. The experiments were performed using both mixtures as well as not fortified methanol or plasma, representing a control group. Every solution was injected five times in a randomized sequence. Statistical evaluation was conducted using GNU R. For every feature fold change between the groups as well as the corresponding p-value after, Welch's two sample t-test was calculated. Those features with a fold change >2 and a corresponding p-value <0.001 were annotated as significant. Afterwards they were filtered and only those detected in every of the five Mix Low samples were

considered as relevant. Features with a retention time lower than 60 seconds and higher than 720 seconds were also removed since they were recorded during column equilibration or washing section of the chromatography. The remaining features were statistically evaluated using PCA.

3 | RESULTS AND DISCUSSION

The nomenclature of the results in the following sections refers to Figure 1. The measurement of both mixtures using the starting conditions of the mass spectrometer and the starting parameters from XCMS Online is defined as experiment A. Applying the optimized XCMS parameters to the aforementioned measurement is defined as experiment B, the measurement of both mixtures using optimized settings of the mass spectrometer without optimized XCMS parameters is defined as experiment C, and using both optimized settings for the mass spectrometer and XCMS is defined as experiment D.

3.1 | Optimization of mass spectrometer settings

Mass spectrometry after the optimization process was performed using full scan (FS) only. The settings for FS data acquisition were as
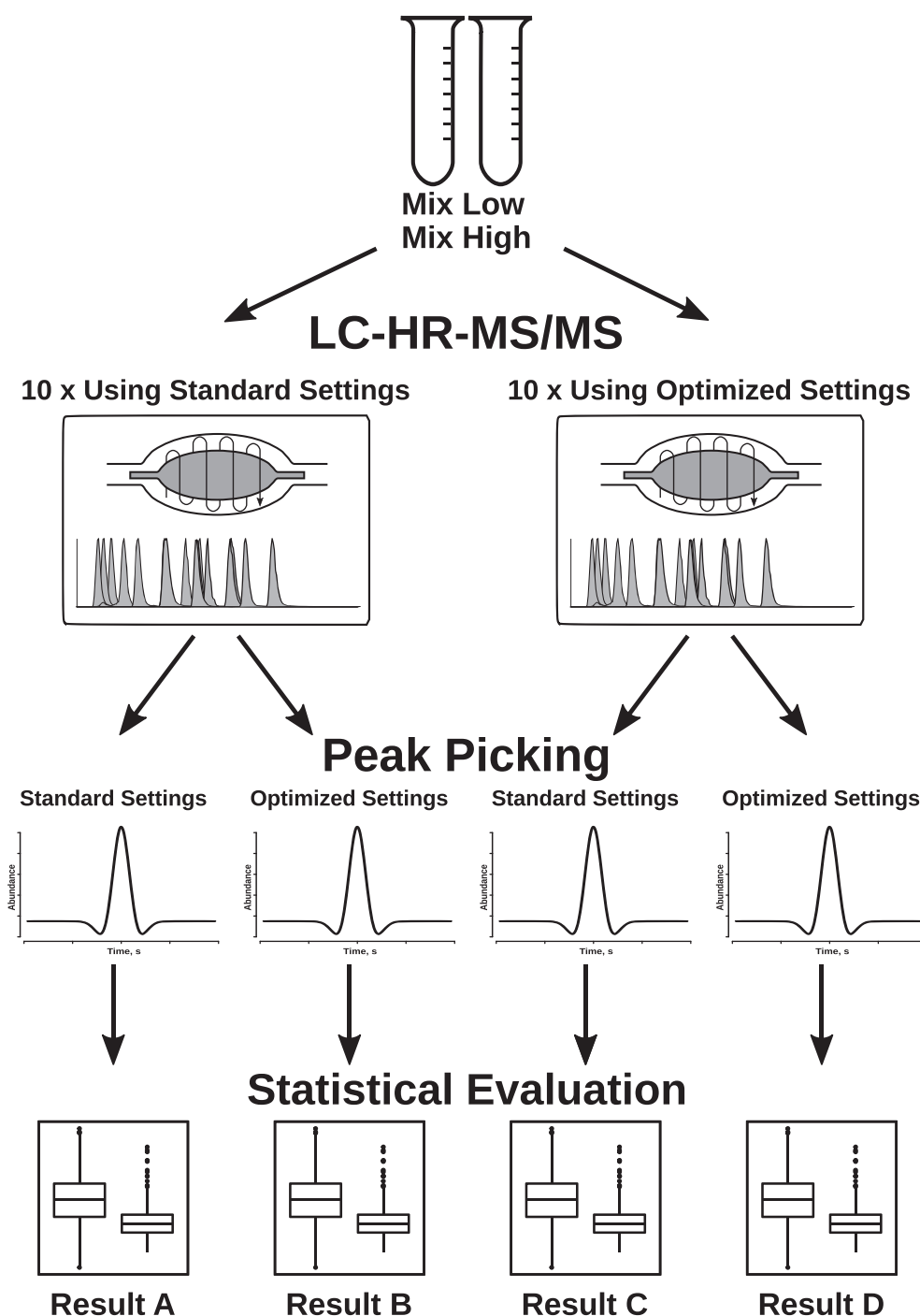

FIGURE 1   Schematic summary of conducted experiments

follows: resolution, 140 000 full width at half maximum (fwhm); microscans, 1; automatic gain control (AGC) target, 5×10^5; maximum injection time, 200 ms; scan range, m/z 50–750; spectrum data type, centroid. The chromatography settings were not altered. These settings were used for experiments C and D.

The starting conditions of the mass spectrometer provided 772 scan points during the analysis and the optimized conditions 1159. Maximum injection time and AGC target were also optimized to enable a precise acquisition of the m/z without having the risk of space-charge effects as described by Ganqiang et al.[33]

An increase in the resolving power of the mass spectrometer can enable a differentiated detection of peaks with small differences in their monoisotopic masses but is also associated with a loss in sensitivity. The number of scan points is important for the detection of peaks by the centWave algorithm. Fewer scan points make it necessary to use looser parameter settings and thus increase the risk of picking random detector fluctuations as well as baseline drifts. This is especially necessary for peaks that have a small chromatographic width as it is the case in modern chromatographic systems which can provide widths of 10 seconds or less. A high number of scans per peak allows a precise representation of the peak in the chromatogram.[1] The median peak width of the investigated substances was 10 seconds which resulted in approximately 16 scan points per peak.

The relevance of high resolving power for metabolomic studies was investigated by Najdekr et al.[25] Although recommending a range of 60 000 to 120 000 fwhm in positive mode due to restrictions in the number of scans per peak and to limit the detection of "noise features,"[25] they did not specify the data acquisition mode applied for their studies. Additionally, they did not adapt the applied parameter settings for peak picking using XCMS which might explain why they detected more noise features using a higher resolving power. These restrictions concerning scan points using Orbitrap mass analyzers are avoidable by using merely FS mode for data acquisition.

3.2 | Optimization of XCMS parameters

For the optimized peak picking, several parameter suggestions were used and evaluated. The conducted approach revealed that those parameter values that led to the second-lowest median CV led to

the highest recovery. If this was the case for several parameter values, we applied that value which included more features (eg, lowest minimum peakwidth, highest maximum peakwidth). Using parameter values that caused the lowest median CV did result in feature abundances with low variation, but they also led to not detecting analytes. This fact can be explained by considering that excluding features from the evaluation also means excluding sources of variability. The investigation of cross effects by combining several parameter values with a low CV did not result in significant change of the CV or the recovery (data not shown).

When planning metabolomics experiments the duration of several phases of the project is an important factor for the development of a schedule. During the parameter sweeping, 609 iterations were performed taking 15 hours of calculation time for the data set using optimized mass spectrometer conditions and 14 hours for the data set using the original conditions. These calculation times can vary with the deployed hardware and several other factors but are likely to remain within one day of optimization time.

The obtained parameters after optimization as well as the initial parameters are listed in Table 2. The distribution of the CV before and after the optimization processes of methanol samples is displayed in Figure 2. The median CV for Mix Low was reduced from 24% in result A to 13% in experiment B ($p = 3.2 \times 10^{-11}$) and from 22% in experiment C to 7% in experiment D ($p < 2.2 \times 10^{-16}$). The reduction of the median CV from experiment B to experiment D was significant as well ($p = 1.0 \times 10^{-15}$). For Mix High, the median CV was reduced from 21% in result A to 11% in experiment B ($p < 2.2 \times 10^{-16}$) and from 18% in experiment C to 6% in experiment D ($p < 2.2 \times 10^{-16}$). The reduction of the median CV from experiment B to experiment D was also significant in Mix High ($p < 2.2 \times 10^{-16}$).

The reduction of the median CV did also have an influence on the retention time ranges and the range of the m/z within feature groups of XCMS (Figures S1 and S2). Concerning retention time, the median range within feature groups decreased in Mix Low from 9.3 seconds in experiment A to 2.1 seconds in experiment B ($p < 2.2 \times 10^{-16}$) and from 2.0 seconds in experiment C to 0.54 seconds in experiment D ($p < 2.2 \times 10^{-16}$). The median retention time in Mix High decreased from 6.5 seconds in experiment A to 1.5 seconds in experiment B ($p < 2.2 \times 10^{-16}$) and from 1.2 seconds in experiment C to 0.53 seconds in experiment D ($p < 2.2 \times 10^{-16}$). The reduction of retention time

TABLE 2 XCMS parameters obtained after the optimization as well as the initial parameters as provided by XCMS Online.[30] Experiment B: Initial MS settings and optimized XCMS parameters, experiment D: Optimized MS settings and optimized XCMS parameters, ppm = allowed ppm deviation of mass traces for peak picking, snthresh = signal-to-noise threshold, mzdiff = minimum difference in m/z for two peaks to be considered as separate, bw = bandwidth for grouping of peaks across separate chromatograms

Parameter	XCMS Online	Methanol		Plasma	
		Experiment B	Experiment D	Experiment B	Experiment D
Peakwidth, minimum	5	3.7	8.9	3.8	9
Peakwidth, maximum	20	12	13	14	11
ppm	5	1.8	1.9	1.6	1.3
snthresh	4	37	54	6	33
mzdiff	0.01	0.024	0.088	0.022	0.014
Prefilter, scan number	3	7	8	5	9
Prefilter, scan abundance	100	8800	9100	9200	7800
bw	5	0.5	0.5	2	1
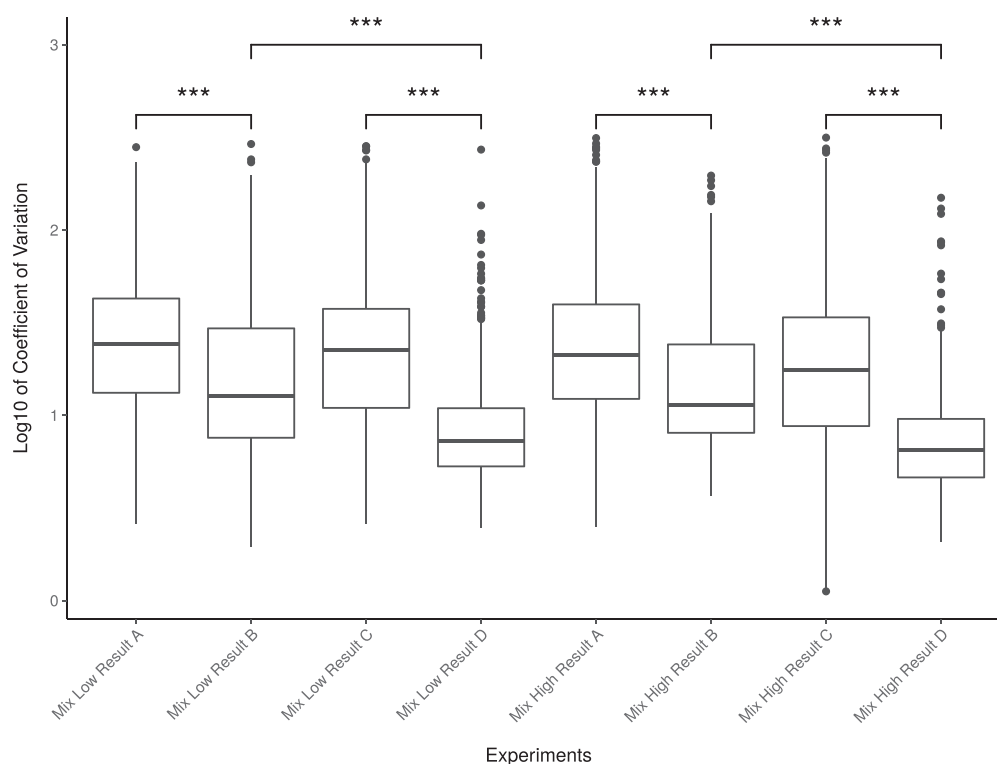
Welch Two Sample t-test				
Groups	Mean Diff.	95.00% CI of Diff.	Significant?	P-Value
Mix Low Result A vs Mix Low Result B	851.3	6.40 to 11.68	Yes	3.18e-11
Mix Low Result C vs Mix Low Result D	1217.1	17.67 to 22.29	Yes	< 2.22e-16
Mix Low Result B vs Mix Low Result D	1022.7	9.44 to 15.43	Yes	1.05e-15
Mix High Result A vs Mix High Result B	851.3	6.40 to 11.68	Yes	3.18e-11
Mix High Result C vs Mix High Result D	2293.5	16.88 to 20.46	Yes	< 2.22e-16
Mix High Result B vs Mix High Result D	1262.7	9.59 to 13.50	Yes	< 2.22e-16

FIGURE 2 Coefficient of variation observed after measurement of methanol replicates. Significance level was obtained by performing Welch's two sample t-test. Lines indicate which groups were compared. * = $p < 0.05$, ** = $p < 0.01$, *** = $p < 0.001$

ranges was significant for both mixtures from experiment B to experiment D (both with $p < 2.2 \times 10^{-16}$).

The median integrated mass range decreased for Mix Low from m/z 0.00095 in experiment A to m/z 0.00019 in experiment B ($p = 2.2 \times 10^{-9}$) and from m/z 0.00040 in experiment C to m/z 0.00028 in experiment D ($p < 2.2 \times 10^{-16}$). Similar results were obtained for Mix High were the median integrated mass range decreased from m/z 0.00097 in experiment A to m/z 0.00024 in experiment B ($p < 2.2 \times 10^{-16}$) and from m/z 0.00041 in experiment C to m/z 0.00020 in experiment D ($p < 2.2 \times 10^{-16}$). The reduction was again significant for both mixtures from experiment B to experiment D (both with $p < 2.2 \times 10^{-16}$).

These results were validated by investigations of fortified plasma samples and led to similar results even though an increase of the median m/z range from experiment B to D was not observable (Figures S3–S5). The applied optimization approach led to significant improvements in the precision of peak picking. This improvement was achieved for both investigated mass spectrometer settings but was most successful for the one using a higher resolving power (experiment D). Comparing the results from experiment B and C does

also imply that a higher resolving power of the mass spectrometer alone does not lead to a higher precision during peak picking if not combined with proper XCMS parameters.

3.3 | Recovery of analytes in technical replicates

The results of the recovery are summarized in Table 3 and 4. It is worth noting that even in neat standard solutions the number of true positive features for comparison is not fully accessible since it is not predictable how many adducts, artifacts, or isotopes the device will generate or is able to detect. Also impurities and products of aging processes will appear as features. Regarding the methanol samples in Table 3, the optimization of XCMS parameters as conducted by this study led to a slight decrease in the number of parent compounds and species annotated by CAMERA for Mix Low and an increase for Mix High. Since the total number of features for both mixtures was reduced by approximately 80%, the optimization lead to an increase in specificity compared to those parameters deployed by XCMS Online. Comparing the results from experiment C and D, an increase

TABLE 3 Recovery of analytes after peak picking in methanol. Isotopes, adducts, and artifacts are those of the investigated compounds and were annotated by CAMERA. A: Starting conditions, B: Optimized XCMS parameters, C: Optimized MS parameters, D: Optimized MS parameters and XCMS settings, Mix High: Mixture containing high concentration of analytes, Mix Low: Mixture containing low concentration of analytes

Species	Mix Low Result A	Mix High Result A	Mix Low Result B	Mix High Result B	Mix Low Result C	Mix High Result C	Mix Low Result D	Mix High Result D
Parent compounds	38	35	36	37	35	33	36	38
Annotated isotopes	44	66	35	61	64	74	68	83
Annotated adducts	6	14	9	12	7	8	9	19
Annotated artifacts	0	0	1	1	0	1	0	2
Total number of features	3282	3470	616	793	1818	1959	428	549

TABLE 4 Recovery of analytes after peak picking in fortified plasma. Isotopes, adducts, and artifacts are those of the investigated compounds and were annotated by CAMERA. A: Starting conditions, B: Optimized XCMS parameters, C: Optimized MS parameters, D: Optimized MS parameters and XCMS settings, Mix High: Mixture containing high concentration of analytes, Mix Low: Mixture containing low concentration of analytes

Species	Mix Low Result A	Mix High Result A	Mix Low Result B	Mix High Result B	Mix Low Result C	Mix High Result C	Mix Low Result D	Mix High Result D
Parent compounds	27	27	30	39	32	35	38	40
Annotated isotopes	18	35	25	55	49	67	53	68
Annotated adducts	3	3	10	18	13	12	12	14
Annotated artifacts	0	1	0	2	1	2	1	3
Total number of features	8212	7635	1814	2013	3993	3809	637	736

in both sensitivity and specificity was observed. The total number of features was reduced by 80% for Mix Low and 70% for Mix High, while the amount of correctly detected parent compounds rose. The best results regarding sensitivity and specificity was found for experiment D concerning both mixtures.

The results of the analysis of fortified plasma samples in Table 4 revealed an increase in both sensitivity and specificity after applying optimized XCMS parameters as well as after using the optimized mass spectrometer settings. Optimized XCMS parameters lead to an average reduction of the data set by 80% for both mixtures. The amount of isotopes, adducts, and artifacts that were annotated by CAMERA rose in almost every case after applying optimized XCMS parameters as well as optimized mass spectrometer settings. The best results were again obtained in experiment D, most likely because of the higher scan rate by using merely FS mode in combination with a higher resolving power.

It is important to take into account that the evaluation of the here described optimization approach was merely evaluated using drug-like compounds. Although metabolomic studies on biomatrices are often investigated using normal and reversed phase columns as well as multiple extraction steps to ensure an appropriate chromatography of the analytes of interest, the results of mixtures with a wide range of peakwidths may differ.

3.4 | Metabolomic-like analysis

The results of the metabolomic-like evaluation are summarized in Figures 3 and 4. The size of the data matrix for each PCA was 15 × 918 (Figure 3A), 15 × 121 (Figure 3B), 15 × 1000 (Figure 3C), and 15 × 245 (Figure 3D), 15 × 5585 (Figure 4A), 15 × 3496

(Figure 4B), 15 × 4281 (Figure 4C), and 15 × 2687 (Figure 4D). Metabolomic data sets are usually not evaluated without filtering unwanted variation. The features detected by XCMS were therefore filtered due to their occurrence in Mix Low to enable a more realistic assessment of the four experiments. This filtering is usually followed by a PCA for dimension reduction and to identify important features. PCA is one of the most widely used multivariate analysis for metabolomics. It uses a linear combination with the aim to preserve as much variance of the original data set as possible in the lower dimensional output.[4] The variance subsequently enables the identification of patterns and classes in the data set.

Since this study used merely neat standard mixtures or fortified pooled plasma samples, one would expect to obtain clear results indicating that the clustering of samples is caused by the investigated analytes only. The scores in Figures 3 and 4 confirmed the expectation of a clear clustering of the sample groups in all four experiments. Most of the variance in the investigated data sets was reflected by the first principal component. Especially the first principal component of Figure 3D that accounted for more than 90% of the variance suggested a high linear relationship. Differences in the clustering of groups in the different experiments are small but show an reduction of variance within the groups Mix Low and Mix High after applying optimized XCMS parameters. Although not absolutely necessary, the loadings of the analysis, displayed in Figures S6 and S7, indicate the distribution of the variance among the investigated factors. The displayed categorization of features as significant or not significant based on their fold change and p-value revealed a huge amount of features that were not identified as a parent compound or annotated by CAMERA in both methanol and plasma samples. The total amount of features/amount of significant features after filtering in methanol samples was 918/259 for experiment A, 141/96 for experiment B,
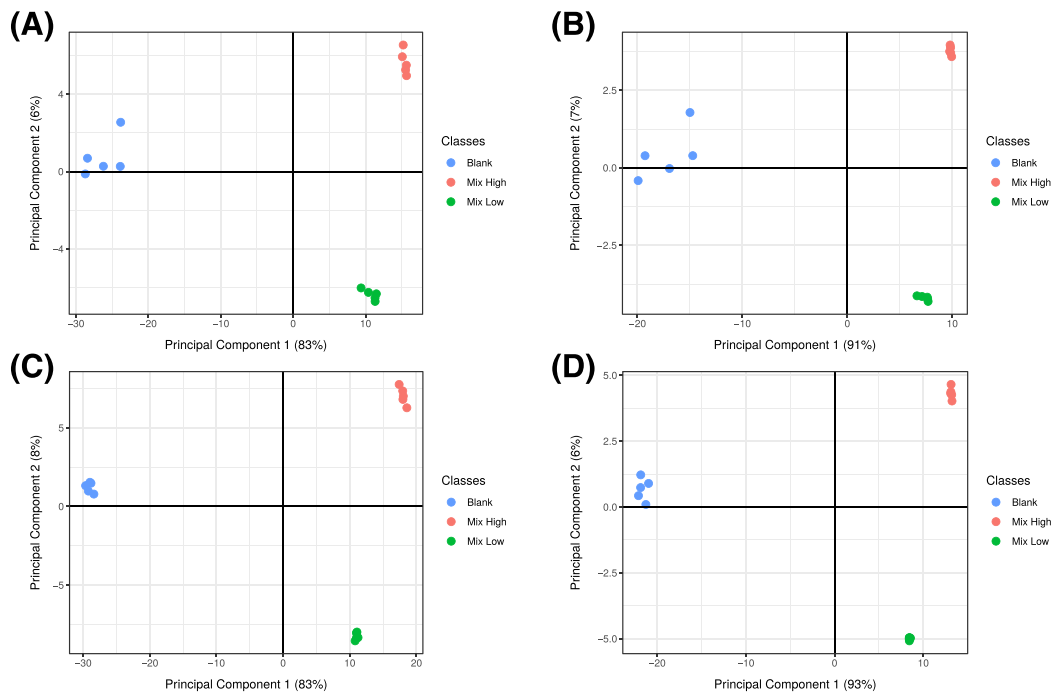
FIGURE 3 Scores of the metabolomic-like analysis using both mixtures in methanol as well as unspiked methanol as blank. A, Starting conditions. B, Optimized XCMS parameters, C, Optimized MS parameters, D, Optimized MS parameters and XCMS settings [Colour figure can be viewed at wileyonlinelibrary.com]
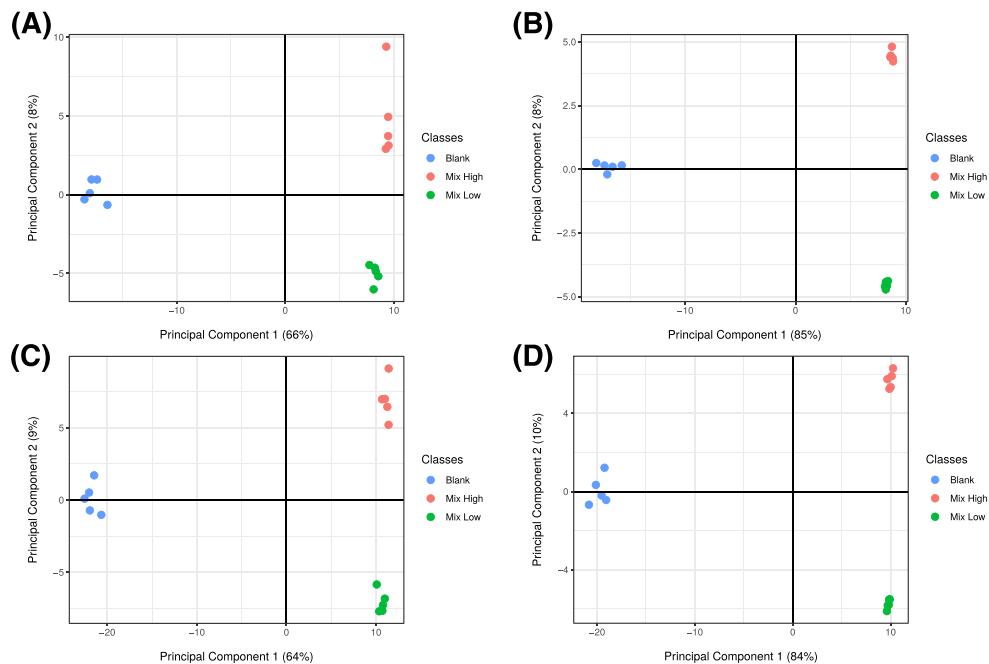

FIGURE 4 Scores of the metabolomic-like analysis using plasma samples as well as unfortified plasma as blank. A, Starting conditions. B, Optimized XCMS parameters. C, Optimized MS parameters. D, Optimized MS parameters and XCMS settings [Colour figure can be viewed at wileyonlinelibrary.com]

1000/381 for experiment C, and 245/178 for experiment D. In plasma samples, amounts were 1753/185 for experiment A, 765/183 for experiment B, 1927/273 for experiment C, and 881/243 for experiment D. These findings imply that the highest sensitivity for features with a significant fold change can be achieved by using the here described optimized mass spectrometer settings in combination with peak picking parameters from XCMS online. However, the absolute

loadings of the four experiments after PCA revealed a more differentiated contribution of significant features to the variance of the data set. Since it is usually not possible to obtain technical replicates from unknown analytes, this optimization could be conducted using pooled sample quality controls. All of the described results implicated that a method for untargeted metabolomics benefits from a high resolving power concerning the analysis but also indicate that this requires

stricter setting for peak picking and are in accordance to the literature considered for the optimization of the mass spectrometer settings.[24-26] It should also be noted that this approach was intended to be a dynamic optimization approach for individual experiments, which should be run in prior to every preprocessing using XCMS. The presented approach does not provide a universal result for peak picking.

4 | CONCLUSION

Optimization of XCMS parameters using technical replicates based on the CV of the measurement revealed to be an effective method for individual experiments. Variation of the data set was minimized by using stricter peak picking parameters and was most successful after applying optimized mass spectrometer settings. The investigation of known analytes from neat standard solutions and fortified pooled plasma samples demonstrated that using a higher resolving power alone was not sufficient to increase the precision of the preprocessing and the recovery of the investigated substances by peak picking. The application of optimized XCMS parameters led to an increase in sensitivity and specificity of XCMS preprocessing. Metabolomic-like experiments with fortified methanol and fortified pooled plasma samples revealed that generalized parameters of XCMS Online led to the highest total number of features but also to the highest number of features without a significant fold change. The best classification of sample groups by PCA of was found after combining optimized mass spectrometer settings and optimized peak picking parameters. These findings might be useful if the optimization process was applied to pooled samples quality controls to reduce variability at the level of the peak picking.

CONFLICT OF INTEREST

The authors declare that there are no conflicts of interest.

ORCID

Sascha K. Manier ![ORCID] http://orcid.org/0000-0002-7126-5263
Markus R. Meyer ![ORCID] https://orcid.org/0000-0003-4377-6784

REFERENCES

1. Barnes S, Benton HP, Casazza K, et al. Training in metabolomics research. I. Designing the experiment, collecting and extracting samples and generating metabolomics data. *J Mass Spectrom.* 2016;51(7):ii-iii.

2. Gowda GA, Djukovic D. Overview of mass spectrometry-based metabolomics: opportunities and challenges. *Methods Mol Biol.* 2014;1198:3-12.

3. Dudzik D, Barbas-Bernardos C, Garcia A, Barbas C. Quality assurance procedures for mass spectrometry untargeted metabolomics. A review. *J Pharm Biomed Anal.* 2018;147:149-173.

4. Worley B, Powers R. Multivariate analysis in metabolomics. *Curr Metabolomics.* 2013;1(1):92-107.

5. Katajamaa M, Miettinen J, Oresic M. MZmine: toolbox for processing and visualization of mass spectrometry based molecular profile data. *Bioinformatics.* 2006;22(5):634-636.

6. Lommen A. MetAlign: interface-driven, versatile metabolomics tool for hyphenated full-scan mass spectrometry data preprocessing. *Anal Chem.* 2009;81(8):3079-3086.

7. Smith CA, Want EJ, O'Maille G, Abagyan R, Siuzdak G. XCMS: processing mass spectrometry data for metabolite profiling using nonlinear peak alignment, matching, and identification. *Anal Chem.* 2006;78(3):779-787.

8. Coble JB, Fraga CG. Comparative evaluation of preprocessing freeware on chromatography/mass spectrometry data for signature discovery. *J Chromatogr a.* 2014;1358:155-164.

9. Myers OD, Sumner SJ, Li S, Barnes S, Du X. Detailed investigation and comparison of the XCMS and MZmine 2 chromatogram construction and chromatographic peak detection methods for preprocessing mass spectrometry metabolomics data. *Anal Chem.* 2017;89(17):8689-8695.

10. Lange E, Tautenhahn R, Neumann S, Gropl C. Critical assessment of alignment procedures for LC-MS proteomics and metabolomics measurements. *BMC Bioinformatics.* 2008;9(1):375.

11. Brodsky L, Moussaieff A, Shahaf N, Aharoni A, Rogachev I. Evaluation of peak picking quality in LC-MS metabolomics data. *Anal Chem.* 2010;82(22):9177-9187.

12. Dunn WB, Broadhurst D, Brown M, et al. Metabolic profiling of serum using ultra performance liquid chromatography and the LTQ-Orbitrap mass spectrometry system. *J Chromatogr B Analyt Technol Biomed Life Sci.* 2008;871(2):288-298.

13. Eliasson M, Rannar S, Madsen R, et al. Strategy for optimizing LC-MS data processing in metabolomics: a design of experiments approach. *Anal Chem.* 2012;84(15):6869-6876.

14. Zheng H, Clausen MR, Dalsgaard TK, Mortensen G, Bertram HC. Time-saving design of experiment protocol for optimization of LC-MS data processing in metabolomic approaches. *Anal Chem.* 2013;85(15):7109-7116.

15. Uppal K, Soltow QA, Strobel FH, et al. xMSanalyzer: automated pipeline for improved feature detection and downstream analysis of large-scale, non-targeted metabolomics data. *BMC Bioinformatics.* 2013;14(1):15.

16. Libiseller G, Dvorzak M, Kleb U, et al. IPO: a tool for automated optimization of XCMS parameters. *BMC Bioinformatics.* 2015;16(1):118.

17. Ettre LS. Nomenclature for chromatography. *Pure Appl Chem.* 1993;65(4):819-872.

18. Michely JA, Maurer HH. A multi-analyte approach to help in assessing the severity of acute poisonings - development and validation of a fast LC-MS/MS quantification approach for 45 drugs and their relevant metabolites with one-point calibration. *Drug Test Anal.* 2018;10(1):164-176.

19. Maurer HH, Pfleger K, Weber AA. *Mass spectral data of drugs, poisons, pesticides, pollutants and their metabolites.* Weinheim: Wiley-VCH; 2016.

20. Maurer HH, Meyer MR, Helfer AG, Weber AA. *Maurer/Meyer/Helfer/Weber MMHW LC-HR-MS/MS library of drugs, poisons, and their metabolites.* Weinheim, Germany: Wiley-VCH; 2018.

21. Caspar AT, Helfer AG, Michely JA, et al. Studies on the metabolism and toxicological detection of the new psychoactive designer drug 2-(4-iodo-2,5-dimethoxyphenyl)-N-[(2-methoxyphenyl)methyl] ethanamine (25I-NBOMe) in human and rat urine using GC-MS, LC-MS(n), and LC-HR-MS/MS. *Anal Bioanal Chem.* 2015;407(22):6697-6719.

22. Helfer AG, Michely JA, Weber AA, Meyer MR, Maurer HH. Orbitrap technology for comprehensive metabolite-based liquid chromatographic-high resolution-tandem mass spectrometric urine drug screening - exemplified for cardiovascular drugs. *Anal Chim Acta.* 2015;891:221-233.

23. Richter LHJ, Flockerzi V, Maurer HH, Meyer MR. Pooled human liver preparations, HepaRG, or HepG2 cell lines for metabolism studies of new psychoactive substances? A study using MDMA, MDBD,

butylone, MDPPP, MDPV, MDPB, 5-MAPB, and 5-API as examples. *J Pharm Biomed Anal*. 2017;143:32-42.

24. Evans AM, Bridgewater BR. High resolution mass spectrometry improves data quantity and quality as compared to unit mass resolution mass spectrometry in high-throughput profiling metabolomics. *J Postgenomics Drug Biomarker Dev*. 2014;4(2):1-7.

25. Najdekr L, Friedecky D, Tautenhahn R, et al. Influence of mass resolving power in orbital ion-trap mass spectrometry-based metabolomics. *Anal Chem*. 2016;88(23):11429-11435.

26. Zou W, She J, Tolstikov VV. A comprehensive workflow of mass spectrometry-based untargeted metabolomics in cancer metabolic biomarker discovery using human plasma and urine. *Metabolites*. 2013;3(3):787-819.

27. Adusumilli R, Mallick P. Data conversion with ProteoWizard msConvert. *Methods Mol Biol*. 2017;1550:339-368.

28. *R: A Language and Environment for Statistical Computing* [Computer Dent Prog]. Version 3.4.1: R Foundation for Statistical Comput Secur; R Core Team.

29. Kuhl C, Tautenhahn R, Bottcher C, Larson TR, Neumann S. CAMERA: an integrated strategy for compound spectra extraction and annotation of liquid chromatography/mass spectrometry data sets. *Anal Chem*. 2012;84(1):283-289.

30. Tautenhahn R, Patti GJ, Rinehart D, Siuzdak G. XCMS online: a web-based platform to process untargeted metabolomic data. *Anal Chem*. 2012;84(11):5035-5039.

31. Tautenhahn R, Bottcher C, Neumann S. Highly sensitive feature detection for high resolution LC/MS. *BMC Bioinform*. 2008;9(1):504.

32. Wehrens R, Hageman JA, van Eeuwijk F, et al. Improved batch correction in untargeted MS-based metabolomics. *Metabolomics*. 2016;12(5):88.

33. Gangqiang L, Yixiang D, Hieftje GM. Space-charge effects and ion distribution in plasma source mass spectrometry. *J Mass Spectrom*. 1995;30(6):841-848.

SUPPORTING INFORMATION

Additional supporting information may be found online in the Supporting Information section at the end of the article.

How to cite this article: Manier SK, Keller A, Meyer MR. Automated optimization of XCMS parameters for improved peak picking of liquid chromatography–mass spectrometry data using the coefficient of variation and parameter sweeping for untargeted metabolomics. *Drug Test Anal*. 2018;1–10. https://doi.org/10.1002/dta.2552

3.3 Untargeted metabolomics by high resolution mass spectrometry coupled to normal and reversed phase liquid chromatography as a tool to study the in vitro biotransformation of new psychoactive substances (DOI: 10.1038/s41598-019-39235-w)[96]

SCIENTIFIC REP⊙RTS

OPEN

Untargeted metabolomics by high resolution mass spectrometry coupled to normal and reversed phase liquid chromatography as a tool to study the in vitro biotransformation of new psychoactive substances

Sascha K. Manier [ID]1, Andreas Keller [ID]2, Jan Schäper3 & Markus R. Meyer1

In 2016, several synthetic cathinones were seized by the State Bureau of Criminal Investigation Bavaria in Germany. Due to their previous appearances in other countries their metabolism was already investigated in human urine as well as different *in vitro* models. These investigations were conducted using ordinary metabolism studies for drugs of abuse by using general knowledge about drug metabolism and visual comparison of mass spectra. The present study aimed to use untargeted metabolomics to support and improve those methods that highly depend on the investigators experience. Incubations were conducted using pooled human liver microsomes (pHLM) and the two cathinones 1-phenyl-2-(1-pyrrolidinyl)-1-butanone and 1-phenyl-2-(1-pyrrolidinyl)-1-heptanone. Samples were analyzed by LC-HRMS/MS using a metabolomics workflow consisting of a reversed phase or normal phase separation followed by electrospray ionization and full scan in positive or negative mode. LC-MS data was afterwards statistically evaluated using principal component analysis, t-distributed stochastic neighborhood embedding, and hierarchical clustering. Significant features were then identified using MS/MS. The workflow revealed 24 significant features after 1-phenyl-2-(1-pyrrolidinyl)-1-butanone and 39 after 1-phenyl-2-(1-pyrrolidinyl)-1-heptanone incubation, consisting of adducts, artifacts, isomers, and metabolites. The applied untargeted metabolomics strategy was able to find almost all of the metabolites that were previously described for 1-phenyl-2-(1-pyrrolidinyl)-1-butanone in literature as well as three additional metabolites. Concerning 1-phenyl-2-(1-pyrrolidinyl)-1-heptanone biotransformation in pHLM, merely four metabolites described in primary human hepatocytes and human urine were not found. This study revealed that untargeted metabolomics workflows are well suited to support biotransformation studies at least of the investigated compounds in pHLM.

Knowledge about the metabolism of abused drugs is often essential for a reliable confirmation of an intake by patients in clinical and forensic toxicology[1]. This can especially be the case if metabolites are the only targets for their detection in urine[2]. According to the World Drug Report 2018[3,4], 803 new psychoactive substances (NPS)

1Department of Experimental and Clinical Toxicology, Institute of Experimental and Clinical Pharmacology and Toxicology, Saarland University, Center for Molecular Signaling (PZMS), 66421, Homburg, Germany. 2Chair of Clinical Bioinformatics, Saarland University, Saarbruecken, Germany. 3State Bureau of Criminal Investigation Bavaria, München, Germany. Correspondence and requests for materials should be addressed to M.R.M. (email: markus.meyer@uks.eu)
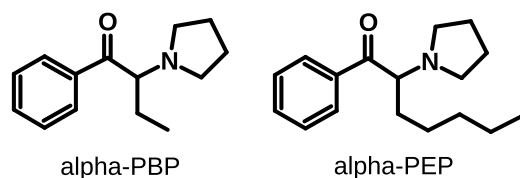
Figure 1. Chemical structures of the investigated compounds.

were reported between 2009 and 2017. These substances are often legally available while the health risk they entail remains unknown. This implies that continuous metabolism studies are necessary. Due to the lack of authentic human urine, such studies are often performed in advance using different *in vitro* and *in vivo* models such as pooled human liver microsomes (pHLM), pooled human liver S9 fraction (pS9), or rat urine[2,5]. pHLM is the most frequently used *in vitro* model, since it is easily accessible and the majority of drugs undergoes merely cytochrome P450 (CYP) mediated oxidation as well as uridine 5′-diphospho-glucuronosyltransferase mediated glucuronidation[6]. Both enzyme classes are located at the smooth endoplasmic reticulum that is part of the microsomal fraction[5]. The identification of metabolites is then conducted by comparing the fragmentation pattern of the parent compound with that of putative metabolites after mass spectrometry (MS) coupled to liquid (LC)- or gas chromatography (GC)[2,7–9]. Metabolism leads to changes in the chemical structure that can be identified by specific shifts in the fragmentation pattern[1]. This approach of discovering and identifying metabolites relies on the individual skills of the scientist that classifies a compound as a metabolite, based on the experience and knowledge of drug metabolism and interpretation of mass spectra.

The dependency on the experience of individuals is a drawback that might at least be avoided concerning the relevance of an analyte by application of metabolomics techniques, amongst others. Metabolomics in general means the analysis of the whole metabolome (e.g. in urine) and thus aims to detected as many metabolites as possible[10]. In case of human urine this includes metabolites that arise from food, physiological processes, or the gut microbiome[10] and very likely also may include NPS metabolites. Metabolomics can be divided into two groups. The first one, targeted metabolomics, aims to analyze certain metabolites found relevant and often also quantify their changes. This implies that the metabolites of interest are already known and their relevance has been confirmed. For the investigation of the metabolism of abused drugs (e.g. NPS), such an approach is usually not appropriate since the metabolic pathways still need to be revealed. The identification of relevant metabolites is carried out by untargeted metabolomics (UM). This kind of study provides an impartial approach on every peak that was recorded during the mass spectral analysis. It uses statistical evaluation of the peak abundances to highlight significant changes between two or more investigated groups[11]. After the detection by an algorithm, chromatographic peaks are usually called features that are statistically assessed.

This study aimed to evaluate untargeted metabolomics strategies for the identification of metabolites of NPS. The evaluation was conducted by investigating the metabolism of the two synthetic cathinones alpha-PBP (1-phenyl-2-(1-pyrrolidinyl)-1-butanone) and alpha-PEP (1-phenyl-2-(1-pyrrolidinyl)-1-heptanone, see Fig. 1) in pHLM incubations and compare the findings to previous metabolism studies[12–14]. Those previous studies revealed that both substances form several CYP-mediated metabolites. Furthermore, glucuronides were found in human urine.

Experimental

Chemicals and reagents.   alpha-PBP and alpha-PEP were provided by the Bavarian State Criminal Police Office (Munich, Germany). NADP-Na$_2$, acetonitrile (LC-MS grade), and methanol (LC-MS grade) were obtained from VWR (Darmstadt, Germany), MgCl$_2$, K$_2$HPO$_4$, K$_3$PO$_4$, superoxide dismutase, isocitrate dehydrogenase, isocitrate, ammonium formate, ammonium acetate, and formic acid from Sigma (Taufkirchen, Germany). Water was purified with a Millipore filtration unit (18.2 $\Omega \times$ cm water resistance). pHLM (pool of 25 donors, 20 mg microsomal protein/mL) were obtained from Corning (Amsterdam, The Netherlands). After delivery, the pHLM were thawed at 37 °C, aliquoted, snap-frozen in liquid nitrogen, and stored at −80 °C until use.

Microsomal incubations.   Incubations using pHLM were performed according to Welter *et al.*[15] alpha-PBP and alpha-PEP were freshly dissolved in 100 mM phosphate buffer and subsequently diluted to obtain the required concentrations in prior to the experiment. For UM, incubations were conducted at 37 °C using 0 (group Blank), 12.5 (group Low), or 25 μM (group High) substrate and 50 mg protein/mL pHLM. The final incubation volume was 50 μL and consisted of 90 mM phosphate buffer, 5 mM isocitrate, 5 mM Mg^{2+}, 1.2 mM NADP$^+$, 200 U/mL superoxide dismutase, and 0.5 U/mL isocitrate dehydrogenase. The mixture was preincubated for 10 min, reaction was started by the addition of substrate. After 60 min the reaction was stopped by adding 50 μL of ice-cold acetonitrile and the mixture was subsequently centrifuged for 2 min at 14,000 × g. These incubations were performed in five replicates for every group. 10 μL of each incubation were transferred into one MS vial. This pooled sample mixture (group QC) was used for optimization of peak picking and batch correction as described below. 70 μL of the remaining supernatant were transferred into separate MS vials.

For the identification of significant features, incubations were repeated in duplicates using 0 (substrate blank), 12.5, and, 25 μM of substrate. Additionally, incubations were performed not containing pHLM but corresponding amounts of phosphate buffer and 25 μM substrate (enzyme blank). Each of these incubations was conducted as described above.

LC-HRMS/MS apparatus. The analysis was performed using a Thermo Fisher Scientific (TF, Dreieich, Germany) Dionex UltiMate 3000 RS pump consisting of a degasser, a quaternary pump, and an UltiMate Autosampler, coupled to a TF Q-Exactive Plus system equipped with a heated electrospray ionization HESI-II source. Mass calibration was done prior to analysis according to the manufacturer's recommendations using external mass calibration. Additionally before each experiment the apparatus' spray shield and capillary was cleaned. The performance of the column and the mass spectrometer was tested using a test mixture as described by Maurer et al.[1,16] in prior to every experiment. The conditions were set according to published procedures[17,18]. Gradient reversed phase elution was performed on a TF Accucore PhenylHexyl column (100 mm × 2.1 mm, 2.6 μm) or a normal phase Macherey-Nagel (Düren, Germany) HILIC Nucleodur column (125 × 3 mm, 3 μm). The mobile phases for gradient elution using the PhenylHexyl column consisted of 2 mM aqueous ammonium formate containing acetonitrile (1%, v/v) and formic acid (0.1%, v/v, pH 3, eluent A), as well as 2 mM ammonium formate solution with acetonitrile:methanol (1:1, v/v) containing water (1%, v/v) and formic acid (0.1%, v/v, eluent B). The flow rate was set from 1–10 min to 500 μL/min and from 10–13.5 min to 800 μL/min using the following gradient: 0–1.0 min 99% A, 1–10 min to 1% A, 10–11.5 min hold 1% A, 11.5–13.5 min hold 99% A. The gradient elution using the HILIC column was performed using aqueous ammonium acetate (200 mM, eluent C) and acetonitrile containing formic acid (0.1%, v/v, eluent D). The flow rate was set to 500 μL/min using the following gradient: 0–1 min 2% C, 1–5 min 20% C, 5–8.5 min 60% C, 8.5–10 min hold 60% C. 10–12 min hold 2% C. For preparation and cleaning of the injection system isopropanol:water (90:10, v/v) was used. The following settings were used: wash volume, 100 μL; wash speed, 4000 nL/s; loop wash factor, 2. Every analysis was performed at 40 °C column temperature, maintained by a Dionex UltiMate 3000 RS analytical column heater. The injection volume for every analysis was 1 μL. The HESI-II source conditions for every experiment were as follows: ionization mode, positive or negative; sheath gas, 60 AU; auxiliary gas, 10 AU; sweep gas, 3 AU; spray voltage, 3.50 kV in positive mode and −4.0 kV in negative mode; heater temperature, 320 °C; ion transfer capillary temperature, 320 °C; and S-lens RF level, 50.0. Mass spectrometry for UM was performed according to a previously optimized workflow using full scan (FS) only[19]. The settings for FS data acquisition were as follows: resolution, 140,000 fwhm; microscans, 1; automatic gain control (AGC) target, 5×10^5; maximum injection time, 200 ms; scan range, m/z 50–750; polarity, negative or positive; spectrum data type, centroid. Significant features were identified using parallel reaction monitoring (PRM). Settings for PRM data acquisition were as follows: resolution, 70,000 fwhm; microscans, 1; AGC target, 5×10^5; maximum injection time, 200 ms; isolation window, 0.4 m/z; normalized collision energy (NCE), 35 eV; spectrum data type, centroid. The inclusion list contained the monoisotopic masses of all significant features and a time window of their retention time ±30 s. TF Xcalibur software version 3.0.63 was used for data handling. The analysis was performed using a randomized sequence order with five injections of pure methanol (PhenylHexyl column) or eluent D (HILIC column) samples at the beginning of the sequence for apparatus equilibration, followed by five injections of the pooled QC sample. Additionally, one QC injection was performed every five samples to monitor batch effects as described by Wehrens et al.[20].

Data processing. Thermo Fisher LC-HRMS/MS RAW files were converted into mzXML files using Proteo Wizard[21]. Peak picking was performed using XCMS in an R environment[22,23], annotation of isotopes, adducts, and artifacts was performed using the R package CAMERA[24]. Optimization of XCMS parameters was in accordance to a previously optimized strategy[19]. Peak picking and alignment parameters are summarized in Table S1. After peak picking, fold changes of features between the groups Blank and Low, Blank and High, as well as Low and High were calculated. A corresponding p-value was calculated using Welsh's two sample t-test. The data set was filtered keeping merely those features with a fold change <-1.5 or >1.5 and a corresponding p-value of <0.001 in one of the group comparisons. Additionally, every feature with a retention time lower than 60 s or higher than 600 s was removed, since they were acquired during column acquisition or washing phase of the chromatography. According to Wehrens et al.[20] feature abundances with a value of zero were replaced by the lowest measured abundance as a surrogate LOD and subsequently log10 transformed. A batch correction was performed for those features that were detected in every QC sample. The corresponding feature abundance was corrected using a linear model to extrapolate its abundance drift between QC samples[20]. Patterns in the data set were subsequently investigated using principal component analysis (PCA), t-distributed stochastic neighborhood embedding (t-SNE)[25,26] and hierarchical clustering. Names of the features were adopted from XCMS using "M" followed by the rounded mass and "T" followed by the retention time in seconds (e.g. "M218T216" as given in Table 1 for protonated alpha-PBP at m/z 218.1540 and a retention time of 216 s using a PhenylHexyl column).

Results and Discussion
Untargeted metabolomics.
Volcano plots of detected features are shown in Figures S1–S8, Scores and Loadings of the PCA in Figures S9 and S10. Results of t-SNE and heat maps of hierarchical clustering are presented in Figs 2 and 3. The first of five QC samples that were analyzed before samples from the different incubation groups during the analysis of alpha-PEP using HILIC and positive ionization mode had to be excluded due to a high sensitivity loss of the MS during the analysis. Almost none of the analyses using negative mode revealed significant features. An exception was the analysis of alpha-PEP in HILIC/negative mode (Figure S8). PCA revealed that more than 95% of the variance was stored in the first principal component leading to the conclusion that the data is characterized by a high amount of collinearity (Fig. S9A–D). This is not a surprise regarding the high amount of parent compound in relation to other substances within the incubation mixture. Samples of the group Blank also persistently displayed a high variability within their group throughout most of the analyses indicating a high variance in the measured peak abundances. Such high variance is also explainable by the study design since the variance in the data set primarily originated from the addition of parent compound and the subsequent formation of metabolites. If a peak was detected and integrated by XCMS it also reintegrated the same region in other samples where they were originally not detected. Regarding that samples of the group

Polarity	Feature	measured mass, *m/z*	retention time, s	Identity
pos	M216T214	216.1383	214	alpha-PBP artifact (dehydro-)
pos	M217T214	217.1415	214	alpha-PBP artifact (dehydro-) ^{13}C isotope
pos	M218T216	218.1540	216	alpha-PBP
pos	M219T216	219.1572	216	alpha-PBP ^{13}C-isotope
pos	M220T226	220.1695	226	**alpha-PBP-M (dihydro-)**
pos	M221T226	221.1728	226	alpha-PBP-M (dihydro-) ^{13}C-isotope
pos	M232T343	232.1331	343	**alpha-PBP-M (oxo-)**
pos	M236T214	236.1643	214	**alpha-PBP-M (dihydro-HO-)**
pos	M237T214	237.1676	214	alpha-PBP-M (dihydro-HO-) ^{13}C-isotope
pos	M250T215	250.1435	215	**alpha-PBP-M (di-HO-)**

Table 1. Significant features of alpha-PBP after untargeted analysis using a reversed phase (PhenylHexyl) column. Features are ordered by *m/z* and retention time. Isotopes were annotated by the R package CAMERA and not further identified. Metabolites are indicated by bold font. pos = positive.

Blank did not contain any parent compound or metabolite, XCMS merely integrated noise that resulted in peak areas with a high variance between different samples which is visible in these score plots. An exception was the analysis of alpha-PEP using HILIC in negative mode (Fig. S9E). Since neither the parent compounds nor their metabolites did contain any structural elements such as halogen atoms or carboxylic acids that can be ionized in negative mode under the given conditions, the above-mentioned restrictions did not apply here. The corresponding loadings (Figure S10 E) showed that the three features that were found significant in this analysis contributed evenly to the group separation.

These findings implied that even though PCA is a widely used technique for untargeted metabolomics, it was not suitable for those experiments where the substrate and its metabolites were detectable. Patterns in the data were therefore investigated using t-SNE, a dimension reduction algorithm that visualized similarities in the data set[26]. The t-SNE plots resulted in a more appropriate clustering of the groups (Fig. 1) with evenly distributed distances. QC samples appear very close or within the cluster of samples from the group Low. This is not surprising since the pooled sample QC consists of a mixture of every incubation sample and thus contains parent compound and its metabolites in an approximate concentration of the samples from group Low. Differences between both group Low and QC might appear due to inaccuracy when preparing the pooled sample QC or a nonlinear metabolite formation in the given concentrations during incubation.

Clustering patterns of t-SNE corresponded to those obtained by hierarchical clustering (Fig. 2). Every analysis in positive mode showed a clear discrimination between samples from the group Blank and the remaining ones. The only exception again was the analysis of alpha-PEP using HILIC (Fig. 2E), were QC samples appeared in the same class as samples from the group Blank. The corresponding z-scores indicated a correlation of the features' peak abundances with the clustering. It is noteworthy that in the analysis of alpha-PBP in positive mode using the PhenylHexyl column (Fig. 2A), the feature M217T214 showed a positive z-score in the groups Blank and High, but a negative z-score in the groups Low and QC what implied a corresponding decrease of the peak abundances. However, this feature was annotated by CAMERA as a ^{13}C isotope (see Table 1) whose peak abundance should increase with increasing concentrations of the parent compound. Inspection of the chromatograms as detected by XCMS revealed a coeluting peak and the beginning of a baseline drift[27] that artificially increased the peak abundance of those peaks from the group Blank.

Identification of significant features. The results of the identification of significant features is summarized in Tables 1–4. Isotopes that were annotated by CAMERA were not further analyzed. Every other feature was analyzed as described above using a PRM method and the resulting mass spectra are shown in Figures S9-S13. The Metabolomics Standards Initiative proposed minimum information that need to be supplied when reporting metabolomics experiments[28]. These include a classification of the identification level by four categories. The first category is the most valid identification level using two orthogonal data sets. The last category means an unidentified metabolite. Due to the lack of reference compounds, the proposed structural formulas were deduced by comparing the spectra of the metabolites with those of the parent compounds or reference spectra using the METLIN and Human Metabolome Database (HMDB)[28,29]. This approach is referred to as category two in the above mentioned publication, meaning a putatively annotated compound. It applies to all of the identified compounds except for M417T103 and M434T104 in Table 4 which are yet unknown and therefore category four. The fragmentation of both substances was already described in previous publications[14] and will not further be discussed here. Concerning the incubations using alpha-PBP, significant features consisted of six isotopes, three artifacts, five metabolites, one adduct, and one impurity. alpha-PBP itself formed one in-source artifact (M216T214 in Table 1 and M216T347 in Table 2). It was the result of an oxidation of the pyrrolidine ring. The formation of the artifact within the ion source was assumed since its retention time was similar to that of the parent compound. The oxidation of the pyrrolidine ring was additionally found at a different retention time using HILIC (M216T114 in Table 2) implying that this compound was not formed within the ion source. Since it was also contained in the enzyme blank but not in the substrate blank sample it is very likely that this compound is an impurity of the powder that was seized by the Bavarian State Criminal Police Office. In addition to the in-source artifact there were two further compounds that are presumably artifacts of different origin (M215T328 and M243T80 in Table 2).
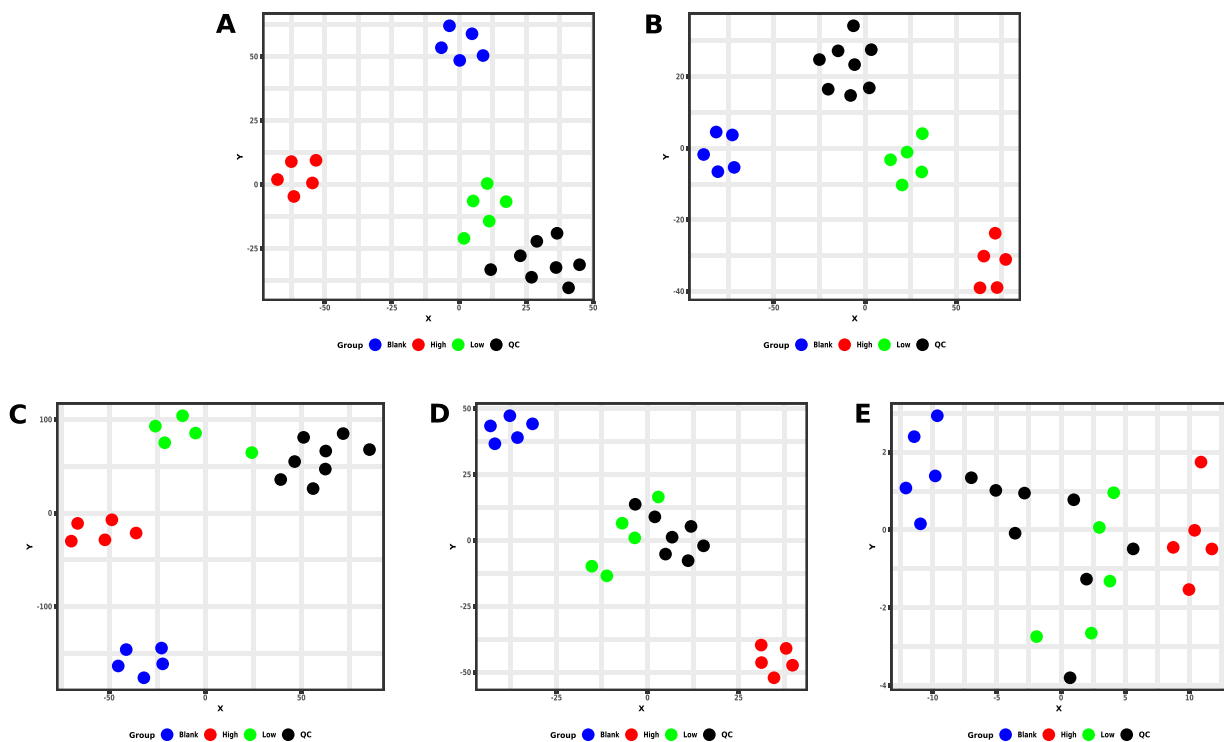
Figure 2. Results of t-SNE. **A** = alpha-PBP, PhenylHexyl column, positive mode; **B** = alpha-PBP, HILIC column, positive mode; **C** = alpha-PEP, PhenylHexyl column, positive mode; **D** = alpha-PEP, HILIC column, positive mode; **E** = alpha-PEP, HILIC column, negative mode.
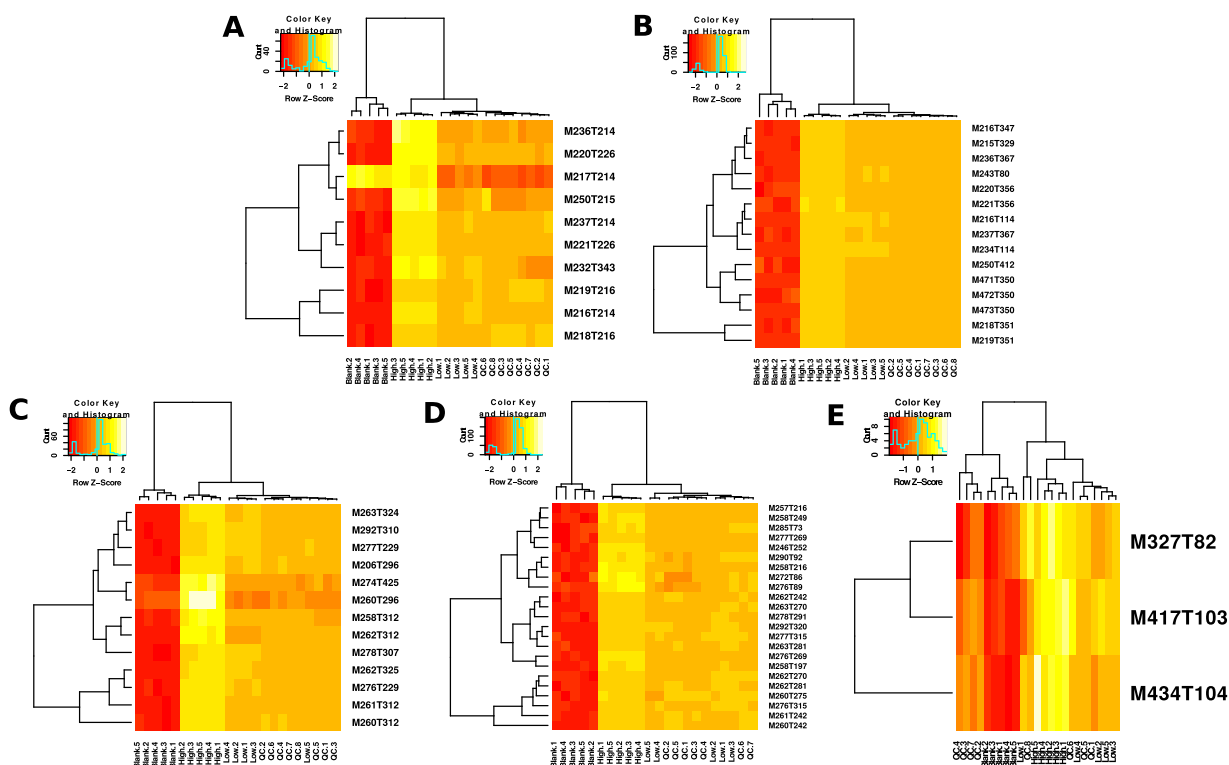

Figure 3. Heat maps of hierarchical clustering. **A** = alpha-PBP, PhenylHexyl column, positive mode; **B** = alpha-PBP, HILIC column, positive mode; **C** = alpha-PEP, PhenylHexyl column, positive mode; **D** = alpha-PEP, HILIC column, positive mode; **E** = alpha-PEP, HILIC column, negative mode.

Polarity	Feature	measured mass, *m/z*	retention time, s	Identity
pos	M215T328	215.1542	328	alpha-PBP impurity (dehydro-) artifact (imido-)
pos	M216T114	216.1383	114	alpha-PBP impurity (dehydro-)
pos	M216T347	216.1383	347	alpha-PBP artifact (dehydro-)
pos	M218T351	218.1541	351	alpha-PBP
pos	M219T350	219.1572	350	alpha-PBP ^{13}C-isotope
pos	M220T355	220.1694	355	**alpha-PBP-M (dihydro-)**
pos	M221T355	221.1726	355	alpha-PBP-M (dihydro-) ^{13}C-isotope
pos	M234T114	234.1488	114	**alpha-PBP-M (dihydro-oxo-)**
pos	M236T367	236.1643	367	**alpha-PBP-M (dihydro-HO-)**
pos	M237T367	237.1677	367	alpha-PBP-M (dihydro-HO-) ^{13}C-isotope
pos	M243T80	243.1492	80	alpha-PBP impurity (dehydro-) artifact (cyano-)
pos	M250T412	250.1436	412	**alpha-PBP-M (di-HO-)**
pos	M471T350	471.2771	350	alpha-PBP adduct $[2M+2H+Cl]^+$
pos	M472T350	472.2805	350	alpha-PBP adduct $[2M+2H+Cl]^+$ ^{13}C-isotope
pos	M473T350	473.2742	350	alpha-PBP adduct $[2M+2H+Cl]^+$ ^{13}C$_2$-isotope

Table 2. Significant features of alpha-PBP after untargeted analysis using a normal phase (HILIC) column. Features are ordered by *m/z* and retention time. Isotopes were annotated by the R package CAMERA and not further identified. Metabolites are indicated by bold font. pos = positive.

Polarity	Feature	measured mass, *m/z*	retention time, s	Identity
pos	M206T296	206.1538	296	**alpha-PEP-M (N,N-dealkyl-)**
pos	M258T312	258.1852	312	alpha-PEP artifact (dehydro-)
pos	M260T296	260.2008	296	alpha-PEP conformer 2
pos	M260T312	260.2009	312	alpha-PEP conformer 1
pos	M261T312	261.2042	312	alpha-PEP ^{13}C-isotope
pos	M262T312	262.2073	312	alpha-PEP ^{13}C$_2$-isotope
pos	M262T325	262.2165	325	**alpha-PEP-M (dihydro-)**
pos	M263T324	263.2197	324	alpha-PEP-M (dihydro-) ^{13}C-isotope
pos	M274T425	274.1799	425	**alpha-PEP-M (oxo-)**
pos	M276T229	276.1958	229	**alpha-PEP-M (HO-) isomer 2**
pos	M277T229	277.1990	229	alpha-PEP-M (HO-) isomer 2 ^{13}C-isotope
pos	M278T307	278.2113	307	**alpha-PEP-M (dihydro-HO-)**
pos	M292T310	292.1904	310	**alpha-PEP-M (di-HO-)**

Table 3. Significant features of alpha-PEP after untargeted analysis using a reversed phase (PhenylHexyl) column. Features are ordered by *m/z* and retention time. Isotopes were annotated by the R package CAMERA and not further identified. Metabolites are indicated by bold font. pos = positive.

The first one contains an imide group instead of a cathinone oxo group and an oxidized pyrrolidine ring. The introduction of an imide could theoretically be conducted by the inversion of a deamination reaction but such a metabolism step has never been reported before and was therefore classified as an artifact of the dehydro impurity. The second artifact contains a cyano group which cannot be introduced by human enzymes. The formation of this artifact might have been occurred within the ion source while using acetonitrile as an eluent or after terminating the incubation with acetonitrile. One dihydro metabolite (M220T355 in Table 2) was found, that was not sufficiently separated from the alpha-PBP isotope containing two ^{13}C atoms during the analysis using HILIC. The result of the PRM analysis was therefore a mixed MS^2 spectrum containing fragments from both parent ions (see Fig. S10). The separation of both compounds was possible after using an alternative chromatography with a flatter increase of eluent D. The employed gradient as well as the obtained chromatogram and MS^2 spectra are displayed in Figure S14.

The significant features identified in the incubations using alpha-PEP consisted of seven isotopes, four artifacts, nine metabolites, two impurities, one endogenous compound, and two yet unidentified compounds. For the parent compound of alpha-PEP two features with different abundances were found showing the same fragmentation but different abundances of the corresponding fragments (M260T312 and M260T296 in Table 3, as well as M260T243 and M260T276 in Table 4). A considerable difference between the MS^2 spectra is the huge intensity of the fragment at *m/z* 242.1901 in Fig. S11 and *m/z* 242.1903 in Fig. S12. This fragment occurs after the initial elimination of the cathinone oxo group and leads to the conclusion that these conformers arise from a different conformation of the pyrrolidine ring in relation to the oxo group. The analysis using HILIC revealed two

Polarity	Feature	measured mass, *m/z*	retention time, s	Identity
pos	M246T254	246.1849	254	alpha-PHP impurity
pos	M257T216	257.2008	216	alpha-PEP impurity (dehydro-) artifact (imido-)
pos	M258T198	258.1849	198	alpha-PEP impurity (dehydro-)
pos	M258T216	258.2042	216	alpha-PEP impurity (dehydro) artifact (imido-) C[13]-isotope
pos	M258T249	258.1849	249	alpha-PEP artifact (dehydro-)
pos	M260T243	260.2007	243	alpha-PEP conformer 1
pos	M260T276	260.2005	276	alpha-PEP conformer 2
pos	M261T243	261.2040	243	alpha-PEP ^{13}C-isotope
pos	M262T243	262.2071	243	alpha-PEP [13]C$_2$ isotope
pos	M262T271	262.2162	271	**alpha-PEP-M (dihydro-) diastereomer 1**
pos	M262T282	262.2162	282	**alpha-PEP-M (dihydro-) diastereomer 2**
pos	M263T270	263.2195	270	alpha-PEP-M (dihydro-) diastereomer 1 ^{13}C-isotope
pos	M263T282	263.2195	282	alpha-PEP-M (dihydro-) diastereomer 2 ^{13}C-isotope
pos	M272T87	272.1641	87	alpha-PEP-M (oxo-HO-) isomer 2 artifact
pos	M276T90	276.1954	90	**alpha-PEP-M (dihydro-oxo-)**
pos	M276T269	276.1954	269	**alpha-PEP-M (HO-) isomer 1**
pos	M276T316	276.1954	316	**alpha-PEP-M (HO-) isomer 2**
pos	M277T269	277.1987	269	alpha-PEP-M (HO-) isomer 1 ^{13}C-isotope
pos	M277T316	277.1987	316	alpha-PEP-M (HO-) isomer 2 ^{13}C-isotope
pos	M278T291	278.2110	291	**alpha-PEP-M (dihydro-HO-)**
pos	M285T74	285.1957	74	alpha-PEP impurity (dehydro-) artifact (cyano-)
pos	M290T93	290.1746	93	**alpha-PEP-M (oxo-HO-) isomer 1**
pos	M292T321	292.1901	321	**alpha-PEP-M (di-HO-)**
neg	M327T82	327.2323	82	Docosahexaenoic acid
neg	M417T103	417.1910	103	Unknown
neg	M434T104	434.1811	104	Unknown

Table 4. Significant features of alpha-PEP after untargeted analysis using a normal phase (HILIC) column. Features are ordered by *m/z* and retention time. Isotopes were annotated by the R package CAMERA and not further identified. Metabolites are indicated by bold font. pos = positive, neg = negative.

dihydro metabolites of alpha-PEP (M262T271 and M262T282 in Table 4). Since the reduction of the cathinone oxo group introduces an additional stereo center into the molecule, these two features are most likely different diastereomers of the same compound. Due to an insufficient separation, the analysis using a PhenylHexyl column merely revealed one feature identified as a dihydro metabolite (M262T325 in Table 3). One of the artifacts that were found in the analysis of alpha-PEP was also an in-source artifact of the parent compound and followed the same formation principle as that of alpha-PBP (M258T312 in Table 3, M258T249 in Table 4). An impurity with an oxidized pyrrolidine ring was also found (M246T254 in Table 4), forming the same artifacts as already described for the analysis of alpha-PBP (M257T216 and M285T74 in Table 4). Another feature was identified as compound with a shorter alkyl chain (M246T254in Table 4). Alkyl chain shortening may be a result of human fatty acid like metabolism. The the β-oxidation usually results in carboxylic acids that are further broken down by subsequent oxidation steps. However, the identified compound did not contain such structural elements leading to the conclusion that it might also be an impurity.

The analysis of alpha-PEP using HILIC and negative ionization mode revealed three significant features. The fragmentation of these features could not be explained by using the parent compound fragmentation leading to the assumption that these features might be endogenous compounds. For further identification, the METLIN and the HMDB were searched using the MS/MS search method of both databases and the respective MS^2 spectra. The precursor *m/z* deviation was set to a maximum of 5 ppm, the *m/z* deviation of the corresponding fragments was set to 0.01 Da for METLIN and 10 ppm for HMDB. One feature (M327T82 in Table 4) was identified as Docosahexaenoic acid (Metlin ID: 3457, HMDB0002183) with a METLIN score of 58 and a HMDB fit of 85%. Both databases matched the compound to experimental MS/MS data. Docosahexaenoic acid is an important structural component of the human brain, cerebral cortex, and the discs of the rod photoreceptor cells. It can be provided via animal fats or converted from alpha-linolenic acid and linoleic acid in the human liver[30]. Since docosahexaenoic acid was the only lipid that was found in this study the cause of its enrichment in incubations with alpha-PEP remains speculative. The remaining features (M417T103 and M434T104 in Table 4) are yet unknown since their spectra did not lead to any match in the above-mentioned databases. Their MS^2 spectra needed to be recorded using an isolation window of *m/z* 1 to obtain sufficient scan points. Since they could not be identified, their spectra were additionally recorded using an isolation window of *m/z* 1 to obtain sufficient scan points and collision energies of 10, 20, and 40 eV. Mass spectra were included in Figure S13 without the annotation of a putative composition and a corresponding ppm deviation.
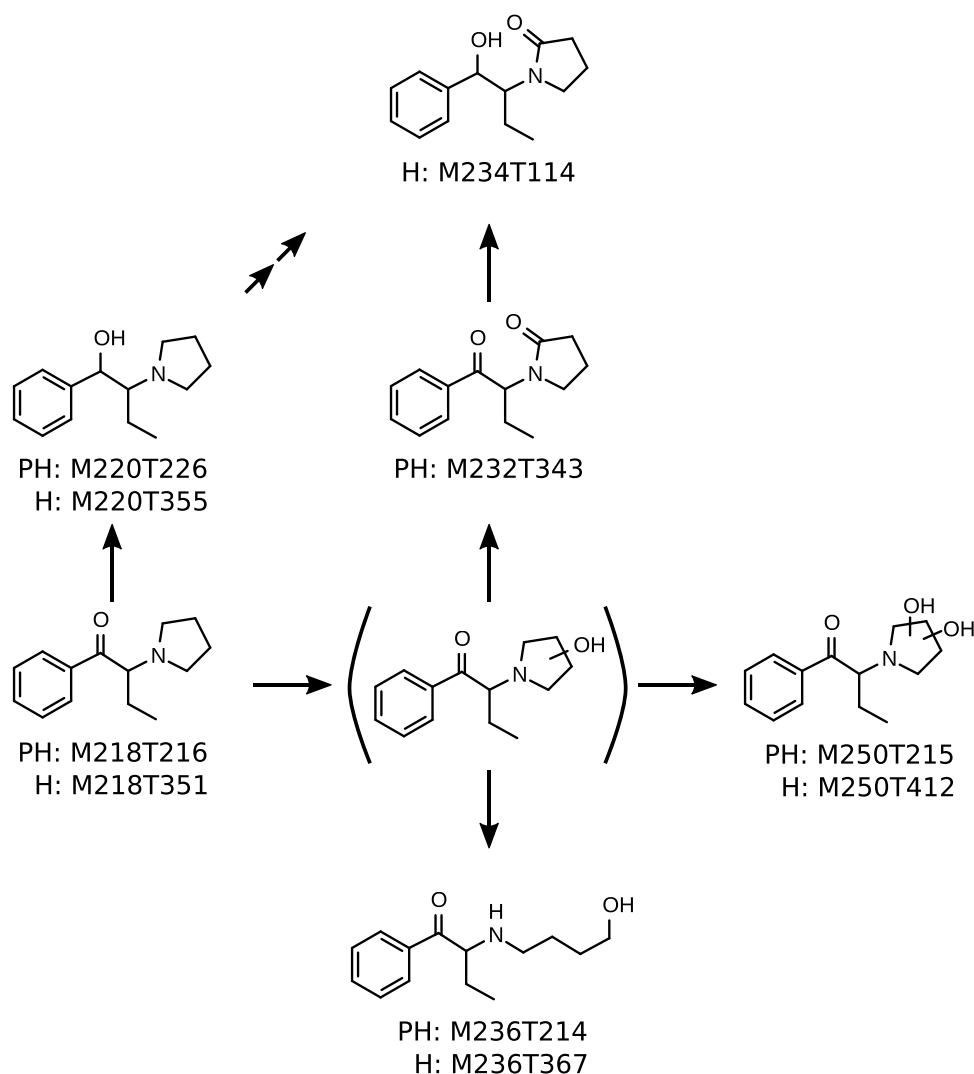
Figure 4. Metabolic pathways of alpha-PBP in pHLM. Undefined position of hydroxylation indicated by unspecific bonds. Two arrows indicate a pathway that contains multiple metabolism steps. Every metabolite is annotated with its feature identifier from untargeted metabolomics analyses. PH = PhenylHexyl column, H = HILIC column.

Metabolism of alpha-PBP and alpha-PEP in pHLM. The metabolic pathways of alpha-PBP and alpha-PEP in pHLM as elucidated by this study are represented by Figs 4 and 5. alpha-PBP was reduced at the cathinone oxo group resulting in a dihydro metabolite. The pyrrolidine ring underwent metabolism resulting in an oxo and a dihydroxy metabolite as well as a ring opened hydroxy metabolite. The oxo group was suggested to be in ortho position due to the retention time of the metabolite. The oxo metabolite was eluting later than the parent compound using a PhenylHexyl column and earlier using HILIC. This allowed the conclusion that this compound should be more lipophilic. Higher lipophilic properties of oxo metabolites can be explained by the existence of a lactam. This finding is in accordance to previous publications investigating the metabolism of alpha-cathinones and one study describing the biotransformation of nitrogen containing xenobiotics to lactams[13,31–34]. The opening of the pyrrolidine ring is very likely the result of a hydroxylation in ortho position of the pyrrolidine ring followed by a retro-hemiaminal reaction. The resulting aldehyde was finally reduced forming the hydroxy group. Additionally, a combination of the dihydro and the oxo metabolite was found. The metabolism of alpha-PBP in pHLM and pS9 has already been investigated by Manier *et al.*, as well as in human urine by Matsuta *et al.*[12,14]. Most metabolites found in this study were already described in these publications. Nevertheless, the UM approach was able to additionally identify a di-hydroxy metabolite, a ring opened dihydro hydroxy metabolite, as well as a dihydro oxo metabolite. The dihydro metabolite was not found in previous pHLM and pS9 investigations but in human urine. This might be due to the case, that the dihydro metabolite showed a similar retention time as the parent compound when using a PhenylHexyl column and is thus hard to distinguish from the parent compound isotope containing two ¹³C atoms. The above described mass spectrometer settings with a resolution of 140,000 fwhm however allowed to distinguishing both peaks. Matsuta *et al.* were able to separate the dihydro metabolite from the parent compound since they used gas chromatography[12]. The hydroxy metabolite
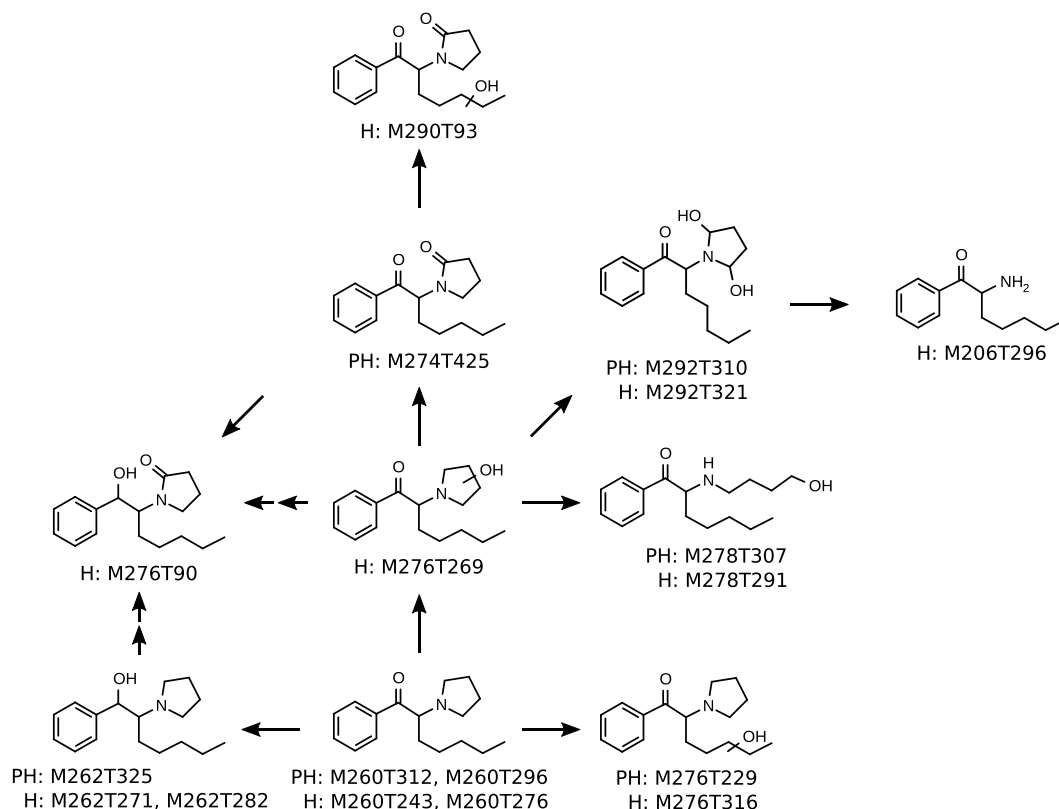
Figure 5. Metabolic pathways of alpha-PEP in pHLM. Undefined position of hydroxylation indicated by unspecific bonds. Two arrows indicate a pathway that contains multiple metabolism steps. Every metabolite is annotated with its feature identifier from untargeted metabolomics analyses. PH = PhenylHexyl column, H = HILIC column.

described by Manier *et al.* in previous studies was not found by the metabolomics approach used in this study. Considering that Matsuta *et al.* did not find a hydroxy metabolite in human urine[12] leads to the assumption that this metabolite is not a primary target and is formed only in very small amounts *in vitro*, which might explain the non-detection via automated peak picking.

alpha-PEP also underwent reduction of the cathinone oxo group resulting in a dihydro metabolite. The pyrrolidine ring was metabolized resulting in an oxo, two hydroxy, and one dihydroxy metabolite. The position of the oxo group was again determined in ortho to the pyrrolidine nitrogen due to the above-mentioned characteristics. The position of the hydroxy groups in the dihydroxy metabolite was determined as vicinal to the nitrogen in the pyrrolidine ring since it is likely that this metabolite leads to the *N,N*-dealkyl metabolite that was also detected. In addition to these pathways, alpha-PEP was hydroxylated at the alkyl chain leading to a mono hydroxy metabolite as well as a hydroxylated oxo metabolite. The formation of a ring opened hydroxy metabolite was found as well and likely resulted from the metabolism steps already described for alpha-PBP.

Previous investigations on the metabolism of alpha-PEP were performed by Manier *et al.* using pHLM and pS9 as well as Swortwood *et al.* using primary human hepatocytes (PHH) and human urine[13]. The metabolomic approach after pHLM incubation used in this study was able to reveal all of the metabolites previously found after incubations using pHLM and additionally most of those found in pS9, PHH, and human urine. Metabolites that were not found by the metabolomic approach were primarily those that resulted from dehydrogenation, as well as the carboxylic acid that likely resulted from hydrolysis of the lactam metabolite. This might have been the result of limitations of the chosen pHLM model in comparison to PHH and human urine.

Conclusions

In vitro metabolism studies using pHLM in combination with untargeted metabolomics resulted in the detection of 24 significant features for alpha-PBP and 39 significant features for alpha-PEP. Most of these features were artifacts, isotopes, conformers, diastereomers, or adducts. Nevertheless, metabolites were identified that corresponded well with those from previous investigations using pHLM, pS9, PHH, and human urine[12–14]. For alpha-PBP three metabolites were found that were not described in any of the previous publications. Investigations of alpha-PEP in pHLM revealed known metabolites but missed those additionally found in PHH and human urine, which is most likely due to enzymatic differences between pHLM and the other models. Besides metabolites of the parent compounds, this study was also able to reveal changes within the incubation mixture after exposure to the drugs. After the incubation of alpha-PEP, docosahexaenoic acid was found enriched, while two yet unidentified compounds showed a significant decrease in their peak abundances. This

study demonstrated that the developed untargeted metabolomics approach allows detection of *in vitro* metabolites of NPS after pHLM incubation besides the detection of further compounds by using an investigator independent approach.

Data Availability

Datasets generated during and/or analyzed during the current study are not publicly available but are available from the corresponding author on reasonable request.

References

1. Maurer, H. H., Pfleger, K. & Weber, A. A. *Mass spectral data of drugs, poisons, pesticides, pollutants and their metabolites*. (Wiley-VCH, 2016).
2. Caspar, A. T., Westphal, F., Meyer, M. R. & Maurer, H. H. LC-high resolution-MS/MS for identification of 69 metabolites of the new psychoactive substance 1-(4-ethylphenyl-)-N-[(2-methoxyphenyl)methyl] propane-2-amine (4-EA-NBOMe) in rat urine and human liver S9 incubates and comparison of its screening power with further MS techniques. *Anal Bioanal Chem* **410**, 897–912 (2018).
3. UNODC. (World Drug Report 2018).
4. UNODC. World Drug Report 2018. Booklet 3. Analysis of drug markets - opioids, cocaine, cannabis, synthetic drugs.
5. Peters, F. T. & Meyer, M. R. *In vitro* approaches to studying the metabolism of new psychoactive compounds. *Drug Test Anal* **3**, 483–495 (2011).
6. Sinz, M. A. & Lyubimov, A. V. In *Encyclopedia of Drug Metabolism and Interactions*. (John Wiley & Sons, Inc., 2011).
7. Michely, J. A. *et al*. New Psychoactive Substances 3-Methoxyphencyclidine (3-MeO-PCP) and 3-Methoxyrolicyclidine (3-MeO-PCPy): Metabolic Fate Elucidated with Rat Urine and Human Liver Preparations and their Detectability in Urine by GC-MS, "LC-(High Resolution)-MSⁿ" and "LC-(High Resolution)-MS/MS". *Curr Neuropharmacol* **15**, 692–712 (2017).
8. Michely, J. A. *et al*. Metabolism of the new psychoactive substances N,N-diallyltryptamine (DALT) and 5-methoxy-DALT and their detectability in urine by GC-MS, LC-MSn, and LC-HR-MS-MS. *Anal Bioanal Chem* **407**, 7831–7842 (2015).
9. Caspar, A. T. *et al*. Metabolism of the tryptamine-derived new psychoactive substances 5-MeO-2-Me-DALT, 5-MeO-2-Me-ALCHT, and 5-MeO-2-Me-DIPT and their detectability in urine studied by GC-MS, LC-MS(n), and LC-HR-MS/MS. *Drug Test Anal* **10**, 184–195 (2018).
10. Barnes, S. *et al*. Training in metabolomics research. I. Designing the experiment, collecting and extracting samples and generating metabolomics data. *J. Mass Spectrom.* **51**, ii–iii (2016).
11. Worley, B. & Powers, R. Multivariate Analysis in Metabolomics. *Curr Metabolomics* **1**, 92–107 (2013).
12. Matsuta, S. *et al*. Metabolism of the designer drug alpha-pyrrolidinobutiophenone (alpha-PBP) in humans: identification and quantification of the phase I metabolites in urine. *Forensic Sci Int* **249**, 181–188 (2015).
13. Swortwood, M. J. *et al*. First metabolic profile of PV8, a novel synthetic cathinone, in human hepatocytes and urine by high-resolution mass spectrometry. *Anal Bioanal Chem* **408**, 4845–4856 (2016).
14. Manier, S. K. *et al*. Different *In vitro* and *In vivo* tools for elucidating the human metabolism of alpha-cathinone-derived drugs of abuse. *Drug Test Anal*, https://doi.org/10.1002/dta.2355 (2018).
15. Welter, J. *et al*. 2-methiopropamine, a thiophene analogue of methamphetamine: studies on its metabolism and detectability in the rat and human using GC-MS and LC-(HR)-MS techniques. *Anal Bioanal Chem* **405**, 3125–3135 (2013).
16. Maurer, H. H., Meyer, M. R., Helfer, A. G. & Weber, A. A. *Maurer/Meyer/Helfer/Weber MMHW LC-HR-MS/MS library of drugs, poisons, and their metabolites*. (Wiley-VCH, 2018).
17. Helfer, A. G. *et al*. Orbitrap technology for comprehensive metabolite-based liquid chromatographic-high resolution-tandem mass spectrometric urine drug screening - exemplified for cardiovascular drugs. *Anal. Chim. Acta* **891**, 221–233 (2015).
18. Wagmann, L., Maurer, H. H. & Meyer, M. R. An easy and fast adenosine 5′-diphosphate quantification procedure based on hydrophilic interaction liquid chromatography-high resolution tandem mass spectrometry for determination of the *In vitro* adenosine 5′-triphosphatase activity of the human breast cancer resistance protein ABCG2. *J. Chromatogr. A* **1521**, 123–130 (2017).
19. Manier, S. K., Keller, A. & Meyer, M. R. Automated optimization of XCMS parameters for improved peak picking of liquid chromatography-mass spectrometry data using the coefficient of variation and parameter sweeping for untargeted metabolomics. *Drug Test Anal*, https://doi.org/10.1002/dta.2552 (2018).
20. Wehrens, R. *et al*. Improved batch correction in untargeted MS-based metabolomics. *Metabolomics* **12**, 88 (2016).
21. Adusumilli, R. & Mallick, P. Data Conversion with ProteoWizard msConvert. *Methods Mol Biol* **1550**, 339–368 (2017).
22. Smith, C. A. *et al*. XCMS: processing mass spectrometry data for metabolite profiling using nonlinear peak alignment, matching, and identification. *Anal. Chem.* **78**, 779–787 (2006).
23. R: A Language and Environment for Statistical Computing v. 3.4.1 (R Foundation for Statistical Computing, R Core Team).
24. Kuhl, C. *et al*. CAMERA: an integrated strategy for compound spectra extraction and annotation of liquid chromatography/mass spectrometry data sets. *Anal. Chem.* **84**, 283–289 (2012).
25. van der Maaten, L. Accelerating t-SNE using Tree-Based Algorithms. *J Mach Learn Res* **15**, 3221–3245 (2014).
26. van der Maaten, L. & Hinton, G. Visualizing Data using t-SNE. *J Mach Learn Res* **9**, 2579–2605 (2008).
27. Ettre, L. S. Nomenclature for Chromatography. *Pure Appl Chem* **65**, 819–872 (1993).
28. Sumner, L. W. *et al*. Proposed minimum reporting standards for chemical analysis Chemical Analysis Working Group (CAWG) Metabolomics Standards Initiative (MSI). *Metabolomics* **3**, 211–221 (2007).
29. Wishart, D. S. *et al*. HMDB: the Human Metabolome Database. *Nucleic Acids Res* **35**, D521–526 (2007).
30. Burdge, G. C. & Wootton, S. A. Conversion of alpha-linolenic acid to eicosapentaenoic, docosapentaenoic and docosahexaenoic acids in young women. *Br J Nutr* **88**, 411–420 (2002).
31. Vickers, S. & Polsky, S. L. The biotransformation of nitrogen containing xenobiotics to lactams. *Curr Drug Metab* **1**, 357–389 (2000).
32. Paul, M. *et al*. Identification of phase I and II metabolites of the new designer drug alpha-pyrrolidinohexiophenone (alpha-PHP) in human urine by liquid chromatography quadrupole time-of-flight mass spectrometry (LC-QTOF-MS). *J. Mass Spectrom.* **50**, 1305–1317 (2015).
33. Shima, N. *et al*. Urinary excretion and metabolism of the α-pyrrolidinophenone designer drug 1-phenyl-2-(pyrrolidin-1-yl)octan-1-one (PV9) in humans. *Forensic Toxicology* **33**, 279–294 (2015).
34. Swortwood, M. J. *et al*. *In vitro*, *in vivo* and in silico metabolic profiling of alpha-pyrrolidinopentiothiophenone, a novel thiophene stimulant. *Bioanalysis* **8**, 65–82 (2016).

Acknowledgements

Author Contributions

S.K.M., A.K., and M.R.M. designed the experiments, S.K.M. performed the experiments, S.K.M., A.K., and M.R.M. analyzed and interpreted the data, J.S. provided the compounds, S.K.M., A.K., and M.R.M. wrote and edited the manuscript, S.K.M. prepared the figures. S.K.M., A.K., M.R.M., and J.S. reviewed the manuscript.

Additional Information

Supplementary information accompanies this paper at https://doi.org/10.1038/s41598-019-39235-w.

Competing Interests: The authors declare no competing interests.

Publisher's note: Springer Nature remains neutral with regard to jurisdictional claims in published maps and institutional affiliations.

3.4 Impact of the used solvent on the reconstitution efficiency of evaporated biosamples for untargeted metabolomics studies (DOI: 10.1007/s11306-019-1631-1)[97]

SHORT COMMUNICATION

Impact of the used solvent on the reconstitution efficiency of evaporated biosamples for untargeted metabolomics studies

Sascha K. Manier[1] · Markus R. Meyer[1]

Abstract

Introduction Untargeted metabolomics intends to objectively analyze a wide variety of compounds. Their diverse physicochemical properties make it difficult to choose an appropriate reconstitution solvent after sample evaporation without influencing the chromatography or hamper column sorbent integrity.

Objectives The study aimed to identify the most appropriate reconstitution solvent for blood plasma samples in terms of feature recovery, four endogenous compounds, and one selected internal standard.

Methods We investigated several reconstitution solvent mixtures containing acetonitrile and methanol to resolve human plasma extract and evaluated them concerning the peak areas of tryptophan-d_5, glucose, creatinine, palmitic acid, and the phophatidylcholine PC(P-16:0/P-16:0), as well as the total feature count

Results Results indicated that acetonitrile containing 30% methanol was best suited to match all tested criteria at least for human blood plasma samples.

Conclusion Despite identifying the mixture of acetonitrile and methanol being suitable as solvent for human blood plasma extracts, we recommend to systematically test for an appropriate reconstitution solvent for each analyzed biomatrix.

Keywords Untargeted metabolomics · Reconstitution · Method validation · Recovery

1 Introduction

Untargeted metabolomics (UT) is a technique that aims to objectively analyze biosamples without any limitation to their composition (Barnes et al. 2016). This intention leads to several challenges concerning chromatographical separation of the analytes as well as their detectability. Typically, samples are separated into their constituent compounds using normal phase and reversed phase chromatography to give consideration to the diverse physicochemical properties that they inherit. There are publications that aim to standardize the development of untargeted metabolomics methods

✉ Markus R. Meyer
  markus.meyer@uks.eu

[1] Department of Experimental and Clinical Toxicology,
  Center for Molecular Signaling (PZMS), Institute
  of Experimental and Clinical Pharmacology and Toxicology,
  Saarland University, 66421 Homburg, Germany

as well as the reporting of the parameters in publications (Dudzik et al. 2018; Sumner et al. 2007). Concerning the laboratory workflow, these guideline include a comprehensive set of parameters from sample collection to metabolite extraction and matrix effects during ionization. One aspect that is usually not mentioned is the impact of the reconstitution solvent that is used to resolve the extract after its evaporation to dryness and which is usually the last step before injection onto the column of the chromatographic device. Lindahl et al. (2017) investigated the impact of several reconstitution solvents after extracting human plasma samples for separation using a reversed phase column. They came to the conclusion that the usage of pure water is most appropriate to resolve human plasma samples in their workflow to obtain an increased number of detected features as well as significant features. However as described above, typically untargeted metabolomics workflows use several column with physicochemical properties that are contrary to each other. The injection of pure water can lead to damages on normal phase columns such as those used for hydrophilic hydrophilic interaction liquid chromatography (HILIC). Acetonitrile is the only solvent that is recommended as a

part of the mobile phase by the manufacturers for each of the used columns in this study and was therefore the first choice as a reconstitution solvent. The aim of this study was therefore to systematically test for a reconstitution solvent mixture that is most appropriate for reversed phase chromatography as well as normal phase chromatography.

2 Experimental

2.1 Chemicals and reagents

Pooled plasma samples (stabilized by citrate) were obtained from a regional blood bank. Methanol, ethanol, and acetonitrile (all LC–MS grade) were obtained from VWR (Darmstadt, Germany), ammonium formate, ammonium acetate, and formic acid from Merck (Darmstadt, Germany). L-Tryptophan-d_5 was obtained from Alsachim (Illkirch-Graffenstaden, France). Water was purified with a Millipore filtration unit (18.2 $\Omega \times$ cm water resistance).

2.2 LC-HRMS/MS apparatus

Analysis was performed according to previously published studies (Helfer et al. 2015; Manier et al. 2018, 2019; Wagmann et al. 2017). Details can be found in the supplementary data.

2.3 Sample preparation

For each mixture of reconstitution solvents, 100 µL of pooled human plasma samples were transferred into a reaction tube and precipitated using 400 µL of a mixture of methanol and ethanol (1:1, v/v) as recommended elsewhere (Bruce et al. 2009). The mixture contained 50 µmol tryptophan-d_5 as internal standard. These samples were shaken for 2 min at 2000 rpm and subsequently centrifuged for 30 min at 15,000 rpm and 2 °C. 400 µL of the supernatant were transferred into a new reaction tube and evaporated to dryness using a vacuum centrifuge at 1400 rpm and room temperature. The obtained residues were reconstituted in different mixtures of acetonitrile and methanol containing 0, 10, 20, 30, 40, or 50% methanol. Each sample was prepared in triplicates. Quality Control (QC) samples that represent a common standard reconstitution solvent for each chromatographic condition used, were obtained by reconstituting the residue in eluent A and B (1:1, v/v) for analyses using a phenylhexyl column or eluent C and D (1:1, v/v) for analyses using HILIC. Five of these QC samples were prepared of each analysis. At last, a 1-µL aliquot was injected into the LC-HRMS/MS system.

2.4 Data processing

Thermo Fisher LC-HRMS/MS RAW files were converted into mzXML files using Proteo Wizard (Adusumilli and Mallick 2017). Peak picking was performed using XCMS in an R environment (Smith et al. 2006; R Core Team 2019). Optimization of XCMS parameters was in accordance to a previously optimized strategy (Manier et al. 2018). Peak picking and alignment parameters are summarized in Table S1 in the supplementary data. After peak picking, tryptophan-d_5 areas in full scan were evaluated for each sample group prepared with a different reconstitution mixture. To include a wider range of substance classes we additionally evaluated peak areas of creatinine and the phosphatidylcholine PC(P-16:0/P-16:0) for analyses using positive ionization, as well as glucose and palmitic acid for those using negative ionization mode. Total feature count was used to evaluate the number of features that were able to be detected by the analysis. For this parameter the number of features which peak area was not declared as not available ("NA") was summed up for each analysis. Statistical evaluation was carried out using one-way ANOVA for variances as well as Welch's two sample t-test for significance concerning group QC.

3 Results and discussion

Results of analyses using positive ionization are displayed in Figs. 1 and 2. Those of analyses using negative ionization are displayed in Figs. S1 and S2 in the supplementary data. In every analysis the peak areas of the investigated compounds indicated a tendency to increase with an increasing amount of methanol that was used. While they were usually only detectible to a very low extend using 0, 10, or 20% methanol their area clearly increased using more than 20% methanol in the reconstitution solvent. This effect diminished for most compounds after the use of 30% methanol. One exception is the peak area of creatinine after using a phenylhexyl column and positive ionization (Fig. 1a). Its area first increases after using 20% methanol and subsequently decreases with a higher fraction of methanol in the reconstitution solvent. This effect is very likely the result of the low retention time of creatinine on reversed phase columns. Since most hydrophilic compounds elute very early on this type of column there is an increased risk of ion suppression. It is notable that in the analysis using a phenylhexyl column and positive ionization mode (Fig. 1a), the area of tryptophan-d_5 decreases at first after using 10% methanol before it increases further. This effect is also notable for glucose using HILIC
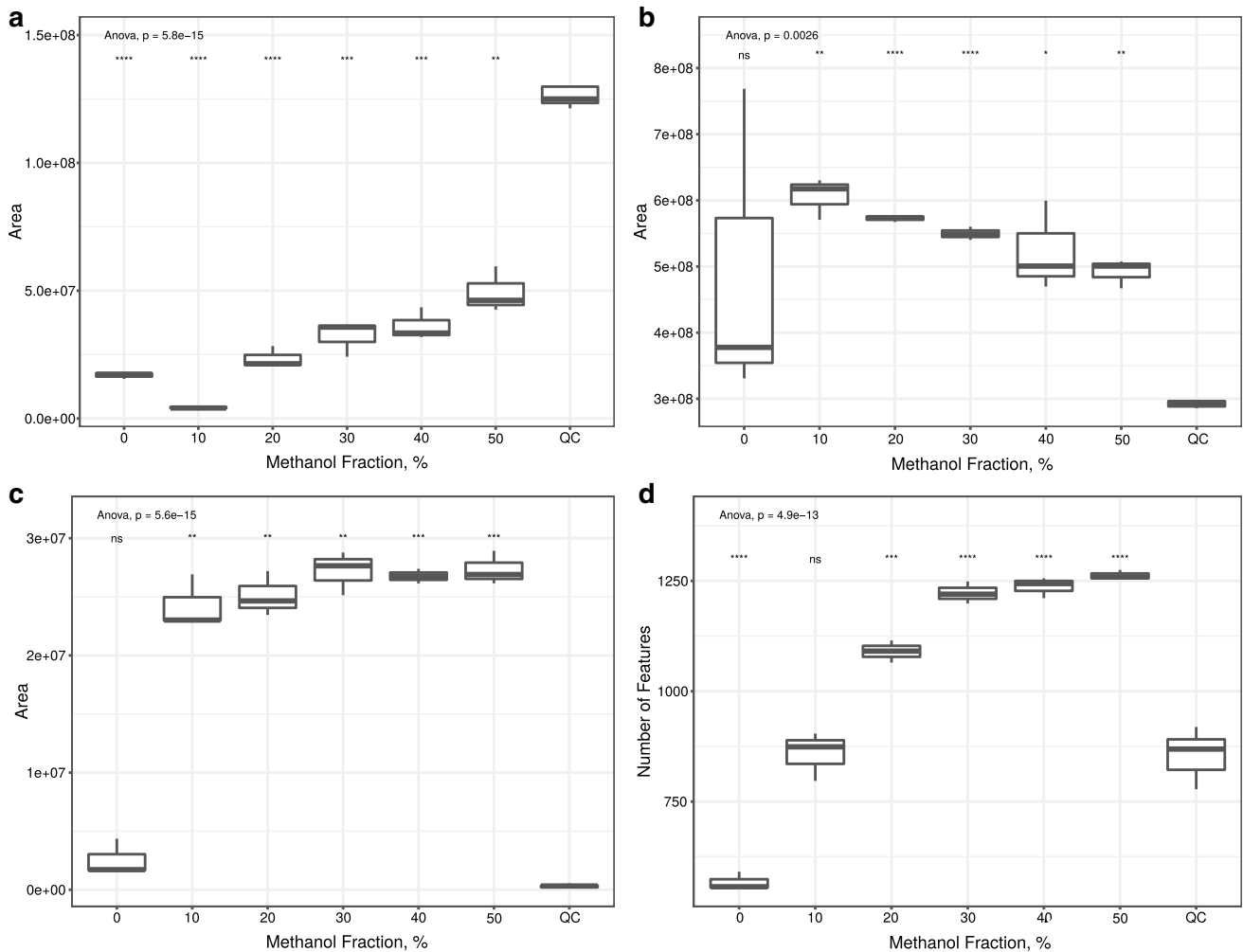
Fig. 1 Results of analysis using phenylhexyl column in positive mode. Statistical evaluation was performed using one-way ANOVA and Welch's two sample t-test comparing each group to QC. **a** Tryptophan-d$_5$. **b** Creatinine. **c** PC(P-16:0/P-16:0). **d** Total feature count. *ns* not significant; *p < 0.05; **p < 0.01; ***p < 0.001; ****p < 0.0001

in negative mode (Fig. S2a). This might be explained with the reconstitution solvent not only resolving the internal standard, but also other compounds that suppress the signal of tryptophan-d$_5$ and glucose during ionization. Since solubility varies from compound to compound, the increasing fraction of methanol in the reconstitution solvent might resolve more tryptophan-d$_5$ and glucose than the interfering analyte.

Concerning the total feature counts of these analyses, they also increase with higher amounts of methanol used for reconstitution. Again, this effect dimished after the usage of 30% methanol. These results underline the effect of methanol being beneficial for the reconstitution of analytes as seen above for those investigated in this study but indicate that this effect might not be limited to those analytes whose peak area has been monitored during this study but for several other analytes as well. This effect is most likely the reason of

the high polarity of acetonitrile that leads to it not being able to spread on the polypropylene surface of the reaction tubes. Methanol has a considerably lower electric dipole moment and might act as a spreading mediator. Additional effects such as solubility of analytes in the reconstitution solvent are very likely relevant as well.

The total feature count was recently described as an inappropriate parameter to compare different methods in untargeted metabolomics (Mahieu et al. 2014), since features are not only the result of detected metabolites, but also of their isotopes, adducts and artifacts. Since in this study we used a highly standardized procedure and applied almost the same conditions on each sample the variability of the total feature count that is the result of different mechanisms is rather small compared to the variability that is introduced by the different concentrations of the metabolites. Given these conditions, such an increase in total feature counts can only
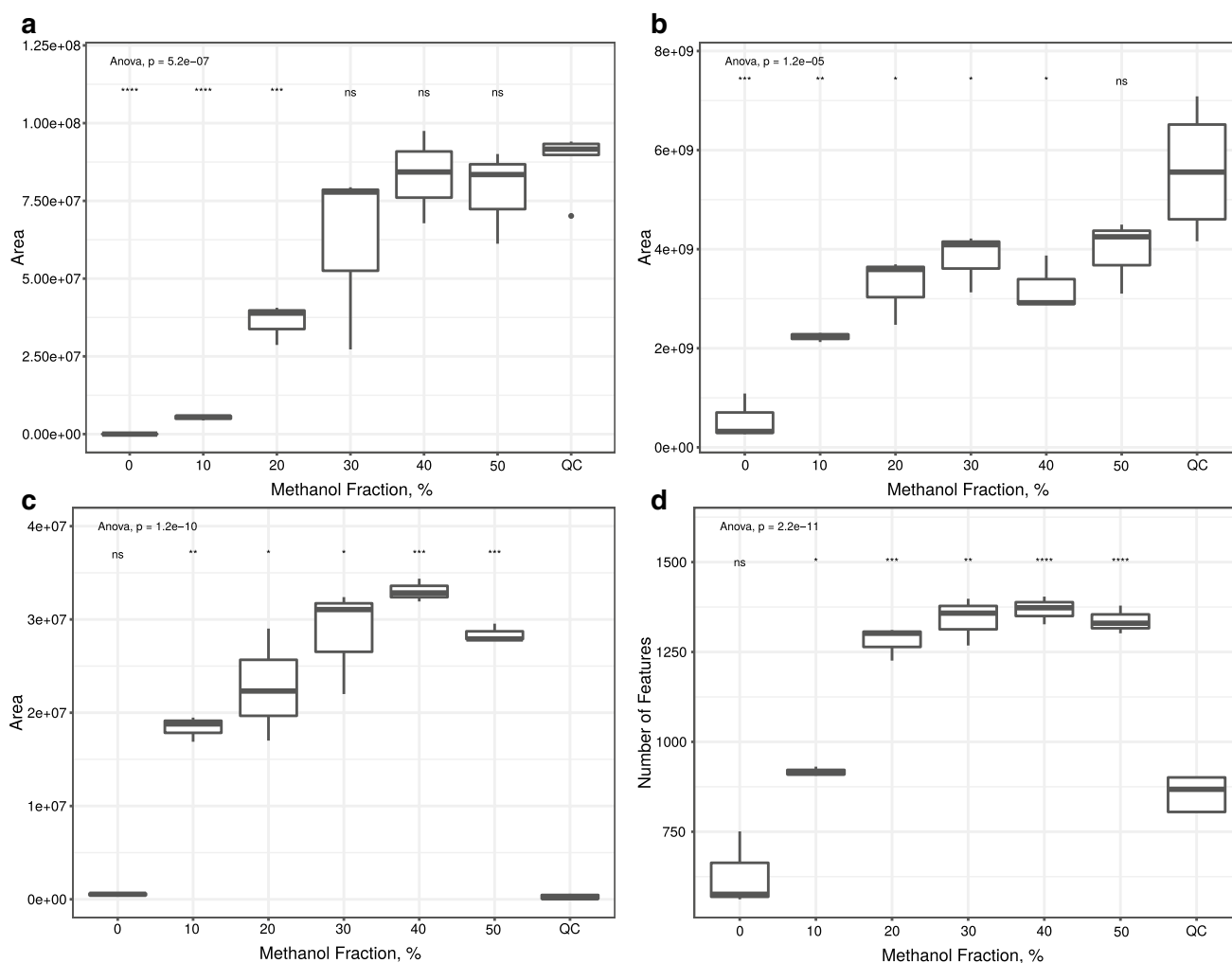
Fig. 2 Results of analysis using HILIC in positive mode. Statistical evaluation was performed using one-way ANOVA and Welch's two sample t-test comparing each group to QC. **a** Tryptophan-d$_5$. **b** Cre-atinine. **c** PC(P-16:0/P-16:0). **d** Total feature count. *ns* not significant; *p < 0.05; **p < 0.01; ***p < 0.001; ****p < 0.0001

hardly be explained by additional mechanisms of artifact formation that are introduced by adding methanol to a reconstitution solvent. In this study the increase of the total feature count is very likely the result of additional metabolites, that can be detected by adding methanol to the reconstitution solvent.

All of the above described results lead to the conclusion that different reconstitution mixtures have a huge effect on the recovery of analytes. Concerning the area of the investigated analytes, this even concerns the chromatography that is used. Nevertheless, using several reconstitution mixtures might not be practical under most circumstances, since it requires enough of the typically scarce sample material for several sample preparations. It also makes it necessary to invest a lot more time, effort, and material in the workup procedure. It therefore appears to be more appropriate to use reconstitution solvents that is optimized for every

chromatographical system that is used and agnostic to the analyzed chemical classes. As mentioned above, the choice of the reconstitution solvent can be challenging since UT are typically performed using reversed phase as well as normal phase columns with properties that are contrary to each other. The results of this study indicate that usage of methanol in the reconstitution solvent is beneficial for the analysis of blood plasma within the scope of this analysis workflow. Since the improvement of the peak areas of the investigated internal standard and the total feature count abated after using a methanol fraction of 30% we believe that this amount is most appropriate for further UT studies using the applied analysis workflow. Due to the fact that methanol has the second highest relative solvent strength in HILIC, higher amount of methanol might lead to unfavorable effects such as double peaks, especially at the beginning of the chromatography. The results of this study are clearly limited to the

biomatrix and analytes investigated. It is therefore not the aim of this study to describe a reconstitution solvent mixture that is universally applicable. This kind of study needs to be performed for each workflow to evaluate its most appropriate reconstitution solvent.

4 Conclusions

This study investigated the impact of different reconstitution mixtures on the peak area of tryptophan-d$_5$, glucose, creatinine, palmitic acid, and the phophatidylcholine PC(P-16:0/P-16:0), as well as the total feature count of the analyses. While acetonitrile appears to be the first choice for the here described chromatographical conditions, it was shown that the used internal standard was almost not detectable at all. In most cases it was only detectable after adding methanol to the reconstitution solvent with increasing peak areas for higher amounts of methanol. Total feature count did also increase with an increasing amount of methanol used, leading to the conclusion that this effect is not only relevant for the investigated analytes, but several other analytes as well. Since the improvement of both parameters fades at 30% methanol, we recommend this amount for the here described workflow. These results are in line with another published study describing pure water as the most appropriate reconstitution solvent for human serum samples their chromatographical conditions merely using a reversed phase column.

Since systematic testing of the reconstitution solvent is not required in any of the guidelines describing quality insurance for UT, we recommend to incorporate this parameter. We also recommend systematically testing for the most appropriate reconstitution solvent for the investigated biomatrix and used internal standards in prior to conducting any studies.

Compliance with ethical standards

were performed by the authors. Pooled plasma samples were obtained from a local blood bank.

References

Adusumilli, R., & Mallick, P. (2017). Data conversion with ProteoWizard msConvert. *Methods in Molecular Biology, 1550*, 339–368. https://doi.org/10.1007/978-1-4939-6747-6_23.

Barnes, S., et al. (2016). Training in metabolomics research. I. Designing the experiment, collecting and extracting samples and generating metabolomics data. *Journal of Mass Spectrometry, 51*, 2–3. https://doi.org/10.1002/jms.3672.

Bruce, S. J., Tavazzi, I., Parisod, V., Rezzi, S., Kochhar, S., & Guy, P. A. (2009). Investigation of human blood plasma sample preparation for performing metabolomics using ultrahigh performance liquid chromatography/mass spectrometry. *Analytical Chemistry, 81*, 3285–3296. https://doi.org/10.1021/ac8024569.

Dudzik, D., Barbas-Bernardos, C., Garcia, A., & Barbas, C. (2018). Quality assurance procedures for mass spectrometry untargeted metabolomics: A review. *Journal of Pharmaceutical and Biomedical Analysis, 147*, 149–173. https://doi.org/10.1016/j.jpba.2017.07.044.

Helfer, A. G., Michely, J. A., Weber, A. A., Meyer, M. R., & Maurer, H. H. (2015). Orbitrap technology for comprehensive metabolite-based liquid chromatographic-high resolution-tandem mass spectrometric urine drug screening-exemplified for cardiovascular drugs. *Analytica Chimica Acta, 891*, 221–233. https://doi.org/10.1016/j.aca.2015.08.018.

Lindahl, A., Sääf, S., Lehtiö, J., & Nordström, A. (2017). Tuning metabolome coverage in reversed phase LC–MS metabolomics of MeOH extracted samples using the reconstitution solvent composition. *Analytical Chemistry, 89*, 7356–7364. https://doi.org/10.1021/acs.analchem.7b00475.

Mahieu, N. G., Huang, X., Chen, Y. J., & Patti, G. J. (2014). Credentialing features: A platform to benchmark and optimize untargeted metabolomic methods. *Analytical Chemistry, 86*, 9583–9589. https://doi.org/10.1021/ac503092d.

Manier, S. K., Keller, A., & Meyer, M. R. (2018). Automated optimization of XCMS parameters for improved peak picking of liquid chromatography-mass spectrometry data using the coefficient of variation and parameter sweeping for untargeted metabolomics. *Drug Testing and Analysis,*. https://doi.org/10.1002/dta.2552.

Manier, S. K., Keller, A., Schaper, J., & Meyer, M. R. (2019). Untargeted metabolomics by high resolution mass spectrometry coupled to normal and reversed phase liquid chromatography as a tool to study the in vitro biotransformation of new psychoactive substances. *Scientific Reports, 9*, 2741. https://doi.org/10.1038/s41598-019-39235-w.

R Core Team. (2019). R: A language and environment for statistical computing. Vienna, Austria: R Foundation for Statistical Computing. https://www.R-project.org/.

Smith, C. A., Want, E. J., O'Maille, G., Abagyan, R., & Siuzdak, G. (2006). XCMS: Processing mass spectrometry data for metabolite profiling using nonlinear peak alignment, matching, and identification. *Analytical Chemistry, 78*, 779–787. https://doi.org/10.1021/ac051437y.

Sumner, L. W., et al. (2007). Proposed minimum reporting standards for chemical analysis Chemical Analysis Working Group (CAWG) Metabolomics Standards Initiative (MSI). *Metabolomics, 3*, 211–221. https://doi.org/10.1007/s11306-007-0082-2.

Wagmann, L., Maurer, H. H., & Meyer, M. R. (2017). An easy and fast adenosine 5'-diphosphate quantification procedure based on hydrophilic interaction liquid chromatography-high resolution tandem mass spectrometry for determination of the in vitro adenosine 5′-triphosphatase activity of the human breast cancer resistance protein ABCG2. *Journal of Chromatography A, 1521*, 123–130. https://doi.org/10.1016/j.chroma.2017.09.034.

Publisher's Note Springer Nature remains neutral with regard to jurisdictional claims in published maps and institutional affiliations.

3.5 Toxicometabolomics of the new psychoactive substances α-PBP and α-PEP studied in HepaRG cell incubates by means of untargeted metabolomics revealed unexpected amino acid adducts (DOI: 10.1007/s00204-020-02742-1)[98]

Toxicometabolomics of the new psychoactive substances α-PBP and α-PEP studied in HepaRG cell incubates by means of untargeted metabolomics revealed unexpected amino acid adducts

Sascha K. Manier[1] · Lea Wagmann[1] · Veit Flockerzi[2] · Markus R. Meyer[1]

Abstract

Toxicometabolomics, essentially applying metabolomics to toxicology of endogenous compounds such as drugs of abuse or new psychoactive substances (NPS), can be investigated by using different in vitro models and dedicated metabolomics techniques to enhance the number of relevant findings. The present study aimed to study the toxicometabolomics of the two NPS α-pyrrolidinobutiophenone (1-phenyl-2-(pyrrolidin-1-yl)butan-1-one, α-PBP) and α-pyrrolidinoheptaphenone (1-phenyl-2-(pyrrolidin-1-yl)heptan-1-one, α-PEP, PV8) in HepaRG cell line incubates. Evaluation was performed using reversed-phase and normal-phase liquid chromatography coupled with high-resolution mass spectrometry in positive and negative ionization mode, respectively, to analyze cells and cell media. Statistical evaluation was performed using one-way ANOVA, principal component discriminant function analysis, as well as hierarchical clustering. In general, the analysis of cells did not mainly reveal any features, but the parent compounds of the drugs of abuse. For α-PBP an increase in *N*-methylnicotinamide was found, which may indicate hepatotoxic potential of the substance. After analysis of cell media, significant features led to the identification of several metabolites of both compounds. Amino acid adducts with glycine and alanine were found, and these have not been described in any study before and are likely to appear in vivo. Additionally, significant changes in the metabolism of cholesterol were revealed after incubation with α-PEP. In summary, the application of metabolomics techniques after HepaRG cells exposure to NPS did not lead to an increased number of identified drug metabolites compared to previously published studies, but gave a wider perspective on the physiological effect of the investigated compounds on human liver cells.

Keywords Toxicometabolomics · HepaRG · Untargeted metabolomics · HPLC–HRMS/MS · New psychoactive substances

✉ Markus R. Meyer
markus.meyer@uks.eu

1   Department of Experimental and Clinical Toxicology, Institute of Experimental and Clinical Pharmacology and Toxicology, Center for Molecular Signaling (PZMS), Saarland University, 66421 Homburg, Germany

2   Department of Experimental and Clinical Pharmacology, Institute of Experimental and Clinical Pharmacology and Toxicology, Center for Molecular Signaling (PZMS), Saarland University, 66421 Homburg, Germany

Introduction

Several in vitro models have been developed and used for investigating the metabolism of drugs of abuse (DOA) and new psychoactive substances (NPS), and also for xenobiotics in general (Manier et al. 2018; Richter et al. 2017a, b; Sinz 2012; Sinz and Kim 2006). They are based on subcellular fractions such as pooled human liver microsomes (pHLM), pooled human liver cytosol, or pooled human liver S9 fraction (pHLS9), as well as hepatic cell lines such as HepG2 and HepaRG. Additionally, primary cells can be used after isolation from tissue by enzymatic digestion or mechanical force (Sinz and Kim 2006). Primary human hepatocytes are regarded as the most suitable in vitro model predict in vivo metabolism, since a high number of reactions can be observed such as those catalyzed by cytochrome P450 (CYP) enzymes and by flavin-containing monooxygenases

(FMOs), as well as conjugation with glucuronic acid, sulfate, and glutathione (Sinz and Lyubimov 2011). In subcellular fractions, only some of these reactions can be observed. For instance, pHLM are limited to reactions catalyzed by membrane-bound enzymes such as CYP enzymes, FMOs, and uridine 5′-diphospho-glucuronosyltransferases (UGTs). Since these reactions are the most relevant ones in drug metabolism, pHLM are widely applied in such studies (Sinz and Lyubimov 2011). Due to their limitations, pHLM still might fail to predict in vivo excretion products, particularly those that were subject to phase II metabolism other than glucuronidation or a combination of both phase I and II metabolism. In pHLS9, an unseparated mixture of cytosol and microsomes, both phase I and phase II metabolites, are present, but it generally suffers from lower enzyme activities compared to isolated fractions (Brandon et al. 2003; Zhang et al. 2012). Immortalized cell lines such as HepaRG and HepG2 are often applied to avoid the high costs of primary human hepatocytes and to apply a model that is better suited to represent the physiology of liver cells (Sinz and Kim 2006).

Metabolomics studies are dedicated to investigate the change of all detectable small molecules in a biological system on a global or network scale (Liu and Locasale 2017). This includes in silico methods such as automated peak detection and integration, as well as methods from uni- and multivariate statistics to evaluate the results and obtain an impartial image of the changes (Barnes et al. 2016a; Liu and Locasale 2017; Worley and Powers 2013). Metabolomics techniques are applied to investigate the response to pathophysiological stimuli or genetic modifications (Lindon et al. 2000) such as cancer (Dang et al. 2009), diseases (Wild et al. 2019), or intoxications (D'Elia et al. 2019). Metabolomics has lately also been used to study DOA or NPS, either with a focus on the drug metabolism (Manier et al. 2019a; Mortele et al. 2018; Vervliet et al. 2019a) or the wider changes of the metabolome in abusers (Boxler et al. 2018). The huge potential of these techniques for the identification of biomarkers of DOA or NPS abuse can be found in the enhanced number of metabolites that might be detected and the identification of compounds that at first do not seem to be related to the drug (Manier et al. 2019a; Vervliet et al. 2019b). However, the toxicometabolomics, which means applying metabolomics to toxicology (Manier and Meyer 2020; Milburn et al. 2013), of DOA/NPS in HepaRG cells by means of metabolomics techniques has not been investigated yet. As such lines offer a comparable standardized biological environment, a high similarity to the actual physiology of the liver, and metabolites comparable to that of the microsomal fractions (Richter et al. 2017a), this approach appears to be promising.

The aims of study were therefore to investigate the toxicometabolomics of the two NPS α-pyrrolidinobutiophenone (1-phenyl-2-(pyrrolidin-1-yl)butan-1-one, α-PBP) and

α-pyrrolidinoheptaphenone (1-phenyl-2-(pyrrolidin-1-yl) heptan-1-one, α-PEP, PV8) in HepaRG incubations. Pyrrolidinophenone-derived NPS are synthetic derivatives of the natural alkaloid cathinone. The primary amine moiety within the cathinone molecule is replaced by a pyrrolidine ring and the α-carbon is substituted with alkyl chains of different lengths. Consumption and seizure of these stimulants has been reported in Europe as well as Japan (EMCDDA 2015; Kudo et al. 2015; Odoardi et al. 2016; Swortwood et al. 2016). The general metabolism of the two NPS in, e.g., pHLM has so far been investigated (Manier et al. 2018, 2019a; Matsuta et al. 2015; Swortwood et al. 2016). The results shall be compared with those studies.

Materials and methods

Chemicals and reagents

α-PBP and α-PEP were provided by the Bavarian State Criminal Police Office (Munich, Germany). Water was purified with a Millipore filtration unit (which purifies water to a resistance of 18.2 $\Omega \times cm$). Cryopreserved, differentiated HepaRG cells, 96-well plates coated with type I collagen, fetal bovine serum, Williams' E Medium, GlutaMAX, supplement HPRG620, and supplement HPRG670 were from Life Invitrogen (Darmstadt, Germany). Penicillin and streptomycin were purchased from Sigma-Aldrich (Taufkirchen, Germany), tryptophan-d_5 was purchased from Alsachim (Illkirch Graffenstaden, France), acetonitrile (LC–MS grade), ammonium formate (analytical grade), formic acid (LC–MS grade), methanol (LC–MS grade), and all other chemicals and reagents (analytical grade) were from VWR (Darmstadt, Germany). Reaction tubes and pipette tips were obtained from Sarstedt (Nümbrecht, Germany).

Incubations using HepaRG cells

Incubations using HepaRG cells were performed according to a previous publication (Richter et al. 2019). For each experiment, cells were maintained in an incubator (Binder, Tuttlingen, Germany) at 37 °C with 95% air humidity and 5% CO_2 atmosphere. Cell handling was done under sterile conditions using a laminar flow bench class II (Thermo Scientific Schwerte, Germany). All given concentrations are final concentrations. Cryopreserved, differentiated HepaRG cells were cultivated according to the manufacturer's instructions and seeded in a density of 80,000 cells/well in collagen-coated 96-well plates using Williams' E medium supplemented with 1% GlutaMAX, HPRG670, 100 U/mL penicillin, 100 μg/mL streptomycin, and 0.5% DMSO on day 1. On day 2, this medium was replaced by the above described medium containing HPRG620 instead of ADD670

and subsequently renewed on day 5. On day 8, α-PBP and α-PEP were freshly dissolved in DMSO and subsequently diluted using the medium to the required concentration. The cell medium was finally renewed and additionally contained either 0 (group Blank), 12.5 (group Low) or 25 μM (group High) α-PBP or α-PEP, respectively. Each concentration was used in nine different wells. Medium volume was always 100 μL. After 24 h of exposure, the medium was transferred into a second 96-well plate that was not collagen coated. The cells were washed twice using 100 μL of phosphate-buffered saline (PBS buffer). Both plates were shock frosted using liquid nitrogen and subsequently stored at − 80 °C until analysis.

Metabolomics sample preparation

After 3 days at − 80 °C, the cells were extracted (extract 1) on dry ice using a modified extraction method and recommendations published previously (Barnes et al. 2016b; Van den Eede et al. 2015). For this purpose, 100 μL of a precooled (− 80 °C) extraction mixture containing methanol and purified water (8:2, v/v) and 5 μM tryptophan-d$_5$ as internal standard was added to the cells. The mixture was incubated for 15 min on dry ice until the content of each well was transferred into a reaction tube. This procedure was repeated once and both aliquots of each well were combined. All samples were shaken for 2 min at 2000 rpm and subsequently centrifuged for 30 min at 15,000 rpm and 2 °C. 150 μL of the supernatant was transferred into a new reaction tube and evaporated to dryness using a vacuum centrifuge (Concentrator plus, Eppendorf, Hamburg) at room temperature and program "V-aq" for roughly 1 h. The residue was reconstituted in 50 μL of a mixture containing methanol and acetonitrile (3:7, v/v) by shaking for 5 min at 15,000 rpm and 22 °C. Ten μL of each sample of both drugs of abuse were pooled to obtain one quality control sample (group QC) for every cell experiment.

For cell media extraction (extract 2), 70 μL of each of the cell media samples was transferred into a reaction tube and mixed with 210 μL precooled methanol (− 80 °C) containing 5 μM tryptophan-d$_5$ by shaking for 2 min at 2000 rpm. 200 μL of each supernatant was transferred into a new reaction tube and evaporated to dryness under the above described conditions for roughly 2.5 h. Again, the residues were reconstituted in 50 μL of a mixture containing methanol and acetonitrile (3:7, v/v) by shaking for 5 min at 15,000 rpm and 22 °C. Ten μL of each sample of both drugs was pooled to obtain quality control samples (group QC) for every medium experiment.

Every obtained sample was transferred into an amber glass vial and 1 μL was injected onto the HPLC–HRMS/MS as described in the corresponding paragraph.

Incubation and sample preparation for investigation of imine formation

To confirm the formation of imines by α-PBP and α-PEP when being incubated with glycine, several conditions were chosen based on previous studies (Welter et al. 2013). Glycine concentration was based on its concentration in the Williams' E medium. α-PBP and α-PEP were freshly dissolved and subsequently diluted using either purified water, Williams' E medium, or Tris buffer to obtain the required concentrations prior to the experiment. The same was done for glycine, except for the dilution in Williams' E medium. Incubations were conducted at 37 °C for 24 h using 25 μM α-PBP or α-PEP in either Tris buffer containing 0 or 666 μM glycine, Williams' E medium, or purified water containing 0 or 666 μM glycine. Additionally, all incubations were performed without α-PBP and α-PEP containing 0 or 666 μM glycine. Incubation volume was 50 μL, respectively. Each experiment was performed in triplicate. After incubation, 10 μL of 25% formic acid in purified water was added to the samples, as well as 40 μL of Eluent F as described in the following paragraph to obtain pH 3 in all samples. A 10-μL aliquot was subsequently injected onto the HPLC–HRMS/MS.

LC–HRMS/MS apparatus

The analysis was performed using a Thermo Fisher Scientific (TF, Dreieich, Germany) Dionex UltiMate 3000 RS pump consisting of a degasser, a quaternary pump, and an UltiMate Autosampler, coupled to a TF Q-Exactive Plus system equipped with a heated electrospray ionization HESI-II source. Mass calibration was done prior to analysis according to the manufacturer's recommendations using external mass calibration. Additionally before each experiment, the spray shield and capillary were cleaned. The performance of the column and the mass spectrometer was tested using a mixture as described by Maurer et al. (2016, 2018) prior to every experiment. The conditions were set according to published procedures (Helfer et al. 2015; Wagmann et al. 2017). Gradient reversed-phase elution was performed on a TF Accucore PhenylHexyl column (100 mm × 2.1 mm, 2.6 μm, TF, Dreieich, Germany) or on a hydrophilic interaction liquid chromatography (HILIC) Nucleodur column (125 × 3 mm, 3 μm, Macherey–Nagel, Düren, Germany) for normal-phase chromatography. The mobile phases for gradient elution using the PhenylHexyl column consisted of 2 mM aqueous ammonium formate containing acetonitrile (1%, v/v) and formic acid (0.1%, v/v, pH 3, eluent A), as well as 2 mM ammonium formate in acetonitrile and methanol (1:1, v/v), containing water (1%, v/v) and formic acid (0.1%, v/v, eluent B). The flow rate was set from 1–10 min to 500 μL/min and from 10–13.5 min to 800 μL/min using the following gradient: 0–1.0 min hold 99% A, 1–10 min to

1% A, 10–11.5 min hold 1% A, 11.5–13.5 min hold 99% A. Normal-phase chromatography was performed using aqueous ammonium acetate solution (200 mM, eluent C) and acetonitrile containing formic acid (0.1%, v/v, eluent D). For chromatography of imines, eluent C was replaced by aqueous ammonium formate solution (20 mM, eluent E) adjusted to pH 3 using formic acid and eluent D was replaced with a mixture of 200 mM aqueous ammonium formate and acetonitrile (1:10, v/v, eluent F). These experiments were performed on the HILIC column using the positive ionization mode. The flow rate was set to 500 µL/min using the following gradient: 0–1 min 2% C, 1–5 min to 20% C, 5–8.5 min to 60% C, 8.5–10 min hold 60% C, 10–12 min hold 2% C. For preparation and cleaning of the injection system, a mixture containing isopropanol and water (90:10, v/v) was used. The following settings were used: wash volume, 100 µL; wash speed, 4000 nL/s; loop wash factor, 2. Every analysis was performed at 40 °C column temperature, maintained by a Dionex UltiMate 3000 RS analytical column heater. The injection volume for metabolomics analyses was 1 µL and for those analyses investigating the formation of imines 10 µL. The HESI-II source conditions for every experiment were as follows: ionization mode, positive or negative; sheath gas, 60 AU; auxiliary gas, 10 AU; sweep gas, 3 AU; spray voltage, 3.50 kV in positive mode and -4.0 kV in negative mode; heater temperature, 320 °C; ion transfer capillary temperature, 320 °C; and S-lens RF level, 50.0. Mass spectrometry for untargeted metabolomics (UM) was performed according to a previously optimized workflow using full scan (FS) only (Manier et al. 2019b). The settings for FS data acquisition were as follows: resolution, 140,000 fwhm; microscans, 1; automatic gain control (AGC) target, 5×10^5; maximum injection time, 200 ms; scan range, m/z 50–750; polarity, negative or positive; spectrum data type, centroid.

The settings for parallel reaction monitoring (PRM) data acquisition were as follows: resolution, 35,000 fwhm; microscans, 1; AGC target, 5×10^5; maximum injection time, 200 ms; isolation window, 1.0 m$/z$; collision energy (CE), 10, 20, or 40 eV; spectrum data type, centroid. The inclusion list contained the monoisotopic masses of all significant features and a time window of their retention time ± 30 s. Analysis was performed using a randomized sequence order with five injections of pure methanol (reversed-phase chromatography) or eluent D (normal-phase chromatography) samples at the beginning of the sequence for apparatus equilibration, followed by five injections of the pooled QC sample. Additionally, one QC injection was performed every five samples to monitor batch effects as described by Wehrens et al. (2016).

Analysis concerning additional incubations to confirm the formation of imines was performed using full scan (FS) data and subsequent data-dependent acquisition (DDA). The settings for FS data acquisition were as follows: resolution, 35,000; microscans, 1; automatic gain control (AGC) target, 1e6; maximum injection time, 120 ms; and scan range, m/z 50–50. The settings for the DDA mode were as follows: dynamic exclusion, 0.1 s; resolution, 17,500; microscans, 1; loop count, 5; AGC target, 2e4; maximum injection time, 250 ms; isolation window, m/z 1.0; high collision dissociation (HCD) with stepped normalized collision energy (NCE), 17.5, 35, and 52.5%; spectrum data type, profile; and underfill ratio, 1%. Additionally, an inclusion list containing m/z values of the suspected adducts was used, although MS^2 experiments were not limited to these (if idle, pick others). TF Xcalibur software version 3.0.63 was used for all data handling.

Data processing

Thermo Fisher LC-HRMS/MS RAW files were converted to mzXML format using Proteo Wizard (Adusumilli and Mallick 2017). Peak picking was performed using XCMS in an R environment (Smith et al. 2006; Team R Core Team); annotation of isotopes, adducts, and artifacts was performed using the R package CAMERA (Kuhl et al. 2012). Optimization of XCMS parameters was in accordance with a previously optimized strategy (Manier et al. 2019b). Peak picking and alignment parameters are summarized in Table S1. According to Wehrens et al. (2016), feature abundances with a value of zero were replaced by the lowest measured abundance as a surrogate LOD and subsequently log10 transformed. A batch correction was performed for those features that were detected in every QC sample. The corresponding feature abundance was corrected using a linear model to extrapolate its abundance drift between QC samples (Wehrens et al. 2016). Additionally, all feature areas were normalized to the area of tryptophan-d$_5$, to remove unwanted variation, e.g., from pipetting − 80 °C extraction mixtures. Subsequently, a corresponding p value was calculated using a one-way analysis of variance (ANOVA) and insignificant features were removed from the data set. The data set was filtered keeping merely those features with a p-value of < 0.001. Patterns in the data set were subsequently investigated using principal component discriminant function analysis (PC-DFA) and hierarchical clustering. For principal component analysis, the features were centered. The subsequent discriminant analysis was performed using those principal components that fulfilled Kaisers's criterion, but at least two. The quality of the model was assessed using its accuracy of predicting group membership, as well as Cohen's κ after Monte Carlo cross-validation. Cohen's κ was interpreted as proposed by Landis and Koch (Landis and Koch 1977). Hierarchical clustering was performed after row scaling, using Euclidean distances. The names of the features were adopted from XCMS using "M" followed by the rounded mass and "T" followed

by the retention time in seconds (e.g., "M218T222" as given in Table S2 for protonated α-PBP at *m/z* 218.1538 and a retention time of 222 s by reversed-phase chromatography).

Identification of significant features

MS^2 spectra were recorded using the above-mentioned PRM method to allow identification of significant features. Individual spectra were exported after subtracting the baseline left and right of the peak. After conversion to mzXML format using Proteo Wizard, spectra were imported to NIST MSSEARCH version 2.3. A library search for identification was conducted using the following settings: spectrum search type, identity (MS/MS); precursor ion *m/z*, in spectrum; spectrum search options, none; presearch, off; other options, none. MS/MS search was conducted using the following settings: precursor tolerance, ± 5 ppm; product ion tolerance, ± 10 ppm; ignoring peaks around precursor, ± *m/z* 1. The search was conducted by using the following libraries: NIST 14 (nist_msms and nist_msms2 sublibraries) and Wiley METLIN Mass Spectral Database. Metabolites of the investigated NPS were identified by comparing and interpreting their spectra to those of the parent compounds.

Results

Data files in mzXML format and the R script files can be found at www.github.com/saskema/hepargmetabolomics. The MS^2 spectra of significant features, available as indicated in Table S2–S5 in the supplementary data, can be found as well on the above-mentioned repository in mzXML format.

Untargeted metabolomics for significant feature detection

The results of the ANOVA can be found in Figures S1 and S2, scores of the PC-DFA are displayed in Figs. 1 and 2, and the corresponding loadings in Figures S3 and S4. The results of the hierarchical clustering are displayed in heatmaps in Figures S5 and S6. Due to a technical error of the autosampler, one analysis of α-PEP (+ HepaRG) had to be excluded from statistical evaluation.

Only few features were found significant after analyses of extract 1 (Figure S1 a-d and Figure S2 a-d). For incubations with α-PBP, four significant features were found after reversed-phase chromatography and positive ionization and two significant features after normal-phase chromatography and positive ionization, as well as one after analysis using normal-phase chromatography and negative ionization (Figures S1 a-d). Analyses using reversed-phase chromatography and negative ionization did not lead to any significant

feature. Concerning extract 1 after α-PEP incubation, any analysis using positive ionization led to two significant features, while negative ionization did not lead to any significant feature. Inspection of the extracted ion chromatograms did not imply a high variance within incubation groups, but a lack of variance between them, which led to negative ANOVA results. Analyses of extract 2 revealed far more significant features. For α-PBP, analyses using positive ionization and reversed-phase chromatography resulted in seven significant features and using normal-phase chromatography six. Analyses using negative ionization did not expose any significant changes. Analyses of cell media using positive ionization after incubations with α-PEP led to the discovery of 14 significant features after either using reversed- or normal-phase chromatography. Negative ionization analyses led to four significant features after reversed-phase chromatography column and three after using normal-phase chromatography. After filtering the data set and evaluation using PC-DFA, these features showed a consistent clustering of incubation groups in each experiment (Figs. 1, 2). Throughout all score plots, those incubation groups containing the corresponding NPS are clearly separated from the group "Blank". Since pooled QC samples were obtained from mixing all three incubation groups containing equidistant concentrations of the NPS, they contained a concentration approximately corresponding to that of the incubation group "Low". This circumstance led to overlapping of both groups in most of the displayed score plots.

Concerning the analysis of extract 1, the accuracy of the PC-DFA model was 73% for incubations with α-PBP after analysis using reversed-phase chromatography and 63% after using normal-phase chromatography. Corresponding κ values were 64% and 51%, respectively. Concerning α-PEP, κ values obtained after cross-validation imply good discriminant properties for features found in cell samples with 84% after using reversed-phase chromatography and 71% after using normal-phase chromatography.

The quality of the PC-DFA models was best after analysis of extract 2 in positive mode, where at least an accuracy of 86% and Cohen's *κ* of 82% (category "almost perfect" according to Landis and Koch) were achieved. Models of cell media experiments (extract 2) of α-PEP that were analyzed in negative mode and reversed-phase chromatography led to a *κ* value of 67%, which might be categorized as "substantial" according to Landis and Koch, while corresponding experiments using normal-phase chromatography led to a rather low *κ* value of 56%. The results of hierarchical clustering corresponded to those found after PC-DFA. Almost all samples from group "Blank" were clustered and separated from all other samples containing one of the investigated NPS. The Euclidian distance of "Blank" group to other samples and the distances between
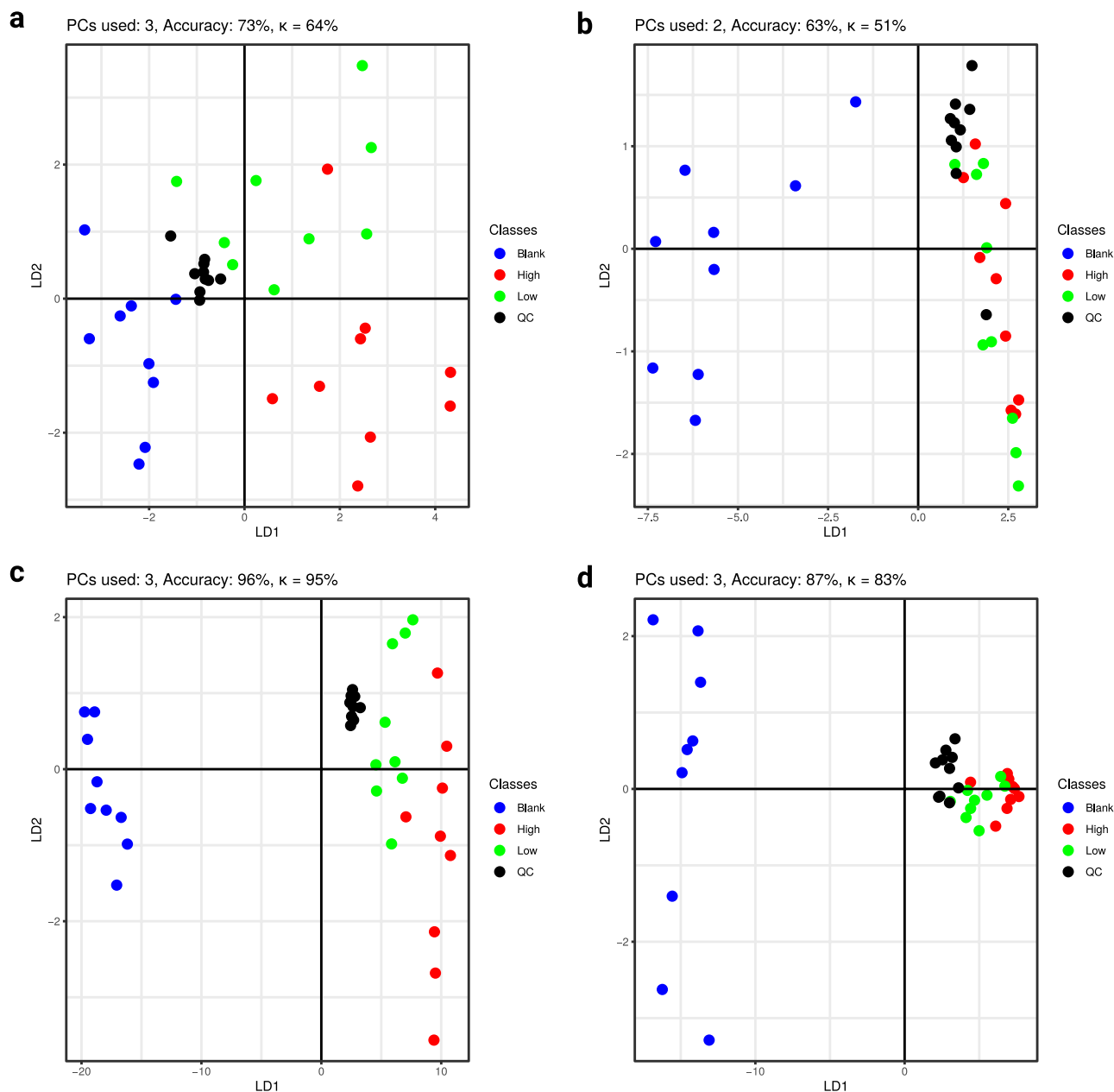
Fig. 1 Scores of PC-DFA for α-PBP with the number of principal components used for discriminant function analysis, as well as prediction accuracy and Cohen's κ. **a** Extract 1 using phenylhexyl column and positive mode; **b** Extract 1 using HILIC column and positive mode, **c** Extract 2 using phenylhexyl column and positive mode, **d** Extract 2 using HILIC and positive mode, *PC* = principal component, *LD* = linear discriminant

other incubation groups were higher in experiments investigating extract 2, than in extract 1. Furthermore, groups of extract 2 analyzed in negative ionization mode (Figure S6 e and f) were less clearly separated than in positive mode. Also, the z-scores of the peak intensities indicated discrimination of the groups corresponding to hierarchical clustering and PC-DFA scores.

Identification of significant features

The results of the identification of significant features are summarized in Tables S2-5 in the supplementary data. The given level of identification was in accordance with Sumner et al. (2007). Isotopes that were putatively identified by CAMERA were not further identified. No MS^2 spectra could be recorded for several low abundant features.

Extract 1

Mainly, the parent compounds and their ^{13}C-isotopes were found after α-PBP and α-PEP incubations. Several additional features showed significant changes in α-PBP incubations, but only the ^{13}C-isotope of *N*-methylnicotinamide and the ammonium adduct of decaethylene glycol could successfully be identified. Decaethylene glycol was identified by a partial match with hexaethylene glycol. Since the structure of polyethylene glycols is highly repetitive, the polymer length was able to be deduced from the protonated parent mass of hexaethylene glycol at m/z 282.1678 ($C_{12}H_{26}O_7$). The structure of the corresponding feature M476T250 is thus deducible by combination of components of a polyethylene glycol polymer and ammonium as $10 \times m/z$ 44.0261 (C_2H_4O, repeating unit) $+ m/z$ 18.0105 (H_2O, end group) $+ m/z$ 17.0263 (NH_4^+, adduct ion) $= m/z$ 476.3071 ($C_{20}H_{46}NO_{11}$).

Extract 2

A total of 11 out of 14 features found after α-PBP incubation were related to the parent compound. Four features were ^{13}C-isotopes of the parent compound, while two features were related to one metabolite, found after analysis using each of the chromatographic methods. Additionally, two features were identified to be most likely amino acid adducts of α-PBP with glycine and alanine, respectively (Table S3). Their MS[2] spectra and the proposed structures are displayed in Fig. 3. Since this feature was only found in incubations that contained α-PBP and absent in those of group "Blank", a formation of this feature from the NPS itself seemed very likely. The fragmentation patterns of these two features indicated a shared basic structure, since both spectra contained the same main fragment ions concerning lower masses, starting with the fragment ion at m/z 197.1073 ($C_{13}H_{13}N_2$). It is also worth noticing that both protonated parent compounds at m/z 271.1446 ($C_{16}H_{19}N_2O_2$) for α-PBP glycine adduct and at m/z 285.1603 ($C_{17}H_{21}N_2O_2$) for α-PBP alanine adduct merely differ by one methyl group in mass and deduced sum formula. Additionally, their absolute loadings implied that the contribution of these features (M271T249 and M285T265 in Figure S3 c, M271T423 in Figure S3 d) to group separation was as high as that of a metabolite (M220T217 in Figure S3 c and M220T319 in Figure S3 d). The amount of metabolites and adducts of α-PBP that were identified in cell media samples explained the higher discriminating properties of these features, as indicated by Cohen's κ which was 95% for those found after analysis using reversed-phase chromatography (Fig. 1c) and 83% for those found after analysis using normal-phase chromatography, compared to 64% and 51% for extract 1, respectively.

Analysis of samples after α-PEP incubation 2 allowed identification of the parent compound, five metabolites, as well as one glycine adduct and three more compounds not related to α-PEP. Cholesterol sulfate and 25-hydroxycholesterol were two of the identified compounds, indicating an increased cholesterol metabolism. The proposed structure and MS[2] spectra of α-PEP glycine adduct are also displayed in Fig. 3. Compared to the spectra of the other adducts, the spectrum again contained the same main fragment ions with regard to lower masses, starting with the fragment ion at m/z 197.1073 ($C_{13}H_{13}N_2$), indicating a shared basic structure of all three compounds. Additionally, if compared to the spectrum of the α-PBP glycine adduct, both spectra share the same main fragment ions starting with the second main fragment ion at m/z 255.1128 ($C_{15}H_{15}N_2O_2$). Considering these obvious similarities and the fact that both glycine adducts merely differ in their protonated parent mass by the difference as α-PBP and α-PEP do, it is very likely that these features indicate actual amino acid adducts. The feature M51T284 in Table S5 could not further be investigated due to the mass cutoff of m/z 50 of the used mass spectrometer. Nevertheless, concerning its mass and retention time, it is likely that this feature is an artifact of α-PEP and was thus annotated in Table S5. The feature M465T121 did not show any fragmentation after using 10, 20, or 40 eV. The only compound in the used mass spectra libraries for identification that had the same monoisotopic mass and did not show any fragmentation at the given collision energies was cholesterol sulfate. Since higher collision energies than 40 eV lead to not detecting any signal, it was not possible to further confirm its identity. The feature M338T87 in Table S5 was identified as oleamide.

Incubations for further investigating the formation of imines

To confirm the formation of the adducts of the investigated NPS with glycine, further incubations were performed to confirm the findings described above under simplified conditions. A lower pH in the eluent was used to be able to detect glycine. The analysis of the obtained samples revealed that both adducts were formed in each incubation containing one of the investigated compounds with glycine and Tris buffer or cell medium. In incubations with α-PBP and cell media, the alanine adduct was found as well. None of the adducts were found after incubations using purified water instead of buffer solution. Additionally, no adduct of α-PEP and alanine was found in incubations with cell medium only.
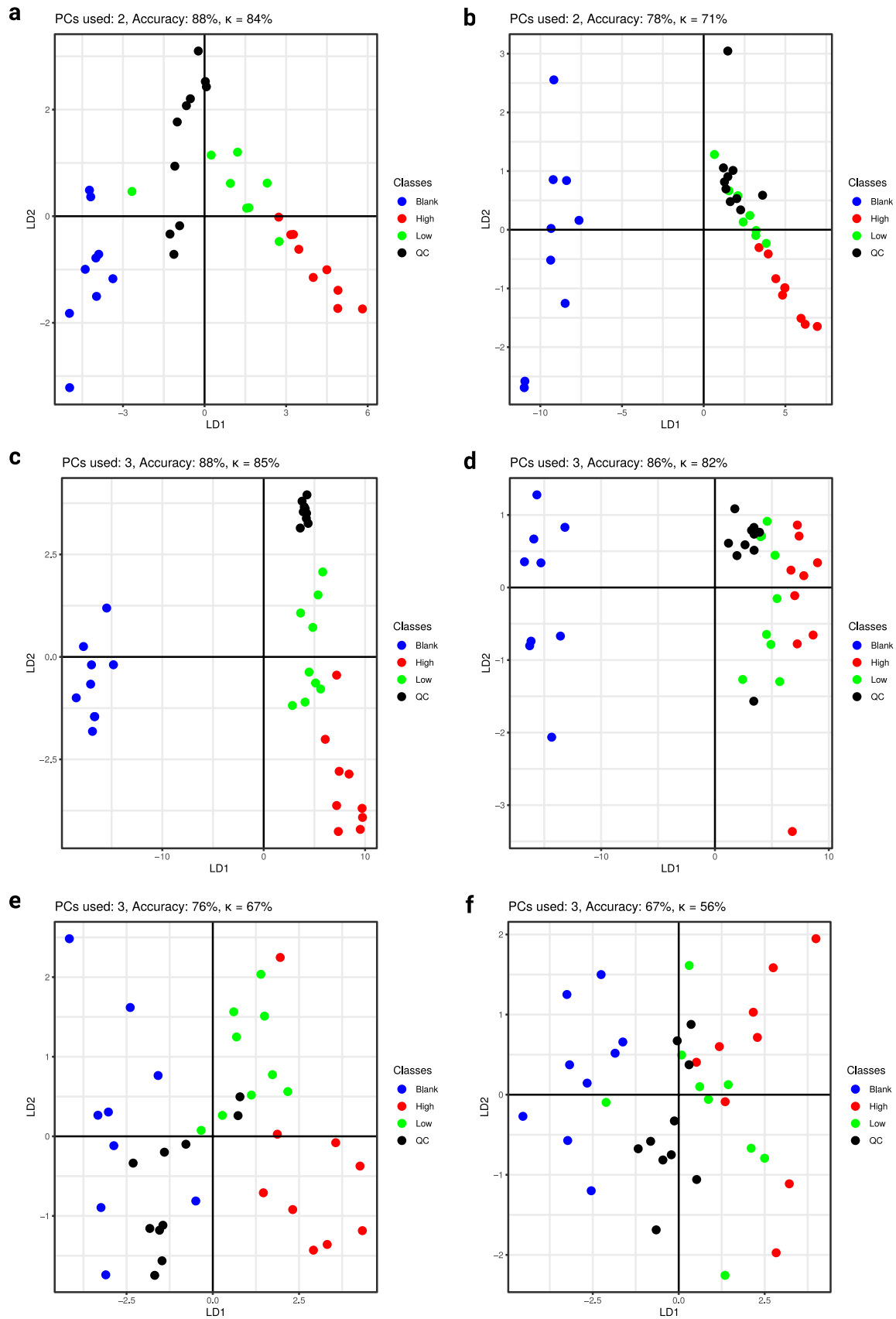
a PCs used: 2, Accuracy: 88%, κ = 84%

b PCs used: 2, Accuracy: 78%, κ = 71%

c PCs used: 3, Accuracy: 88%, κ = 85%

d PCs used: 3, Accuracy: 86%, κ = 82%

e PCs used: 3, Accuracy: 76%, κ = 67%

f PCs used: 3, Accuracy: 67%, κ = 56%

◀ **Fig. 2** Scores of PC-DFA for α-PEP with the number of principal components used for discriminant function analysis, as well as prediction accuracy and Cohen's *κ*. **a** Extract 1 using phenylhexyl column and positive mode; **b** Extract 1 using HILIC column and positive mode, **c** Extract 2 using phenylhexyl column and positive mode, **d** Extract 2 using HILIC and negative mode, **e** Extract 2 using phenylhexyl column and negative mode, **f** Extract 2 using HILIC and negative mode. *PC* = principal component, *LD* = linear discriminant

Discussion

This study revealed different discriminant properties of extract 1 and 2 after PC-DFA. Since it is a multi-class study, rather than merely investigating the classification in a blank or treatment group, the evaluation of Cohen's κ is more appropriate, due to the fact that it resembles the accuracy of the model normalized to the accuracy one would obtain by chance (Landis and Koch 1977). Nevertheless, the prediction accuracy of the models was also given for completeness.

κ values for analyses extract 1 would be classified as "moderate" according to Landis and Koch (Landis and Koch 1977), indicating that they have to be interpreted with care, while those of extract 2 can be generally classified as "almost perfect".

Those identified compounds that are not related to the investigated NPS, give a hint to their effect on physiology of the used liver cells. *N*-Methylnicotinamide is linked to liver cirrhosis and might indicate a liver toxic effect of α-PBP (Pumpo et al. 2001). The reason why merely its ^{13}C-isotope and not *N*-nicotinamide itself was found significant after ANOVA is likely due to a high within-group variance. The interpretation of the role of the two found cholesterol metabolites is not possible without speculating, since both metabolites are not directly connected to each other. The occurrence of polyethylene glycols is rather peculiar. Since they are not natural endogenous compounds of cells, it is very likely that this feature is the result of contamination by a lubricant. During experiments, no lubricant was used and it appears to be likely that this contamination happened during analysis by the used device. The origin of oleamide on the other side is not clearly determinable. Although this substance is a naturally occurring endogenous compound, McDonald et al. (2008) earlier described that several plasticware contains it as a slip agent. They also demonstrated that oleamide is detectable in the water these plasticware were rinsed with. Given the fact that the plasticware used in this study were among those tested by McDonald et al. and the ion chromatograms of oleamide showed high variability within each incubation group, it is very likely that the detected oleamide is not of endogenous origin, but a leached slip agent.

It is most likely that the investigated NPS formed imines with amino acids during incubations. This formation might be achieved after nucleophilic attack of the amine moiety of

the amino acid at the cathinone carbonyl group. Since incubations using only Tris buffer did not contain any enzymes, the ring is likely to be formed during analysis in the ion source. It is notable that not every incubation using only NPS and amino acid lead to the detection of these adducts. The absence of adducts in those incubations using purified water might indicate a pH dependency of the formation, while the absence of the alanine adduct with α-PEP might be due to the fact that it was formed with too low concentrations to be detectable in this assay. A summary of the proposed mechanism is displayed in Fig. 4. The formation of such an adduct also in vivo is likely, since the used concentrations of glycine and alanine are similar to those concentrations that can be found in human blood (Psychogios et al. 2011).

The metabolism of α-PBP and α-PEP has been thoroughly investigated in previous publications using either pHLM (Manier et al. 2018, 2019a), primary human hepatocytes (Swortwood et al. 2016), or authentic human urine (Matsuta et al. 2015). α-PBP was described to be transformed to five metabolites, one after reduction of the cathinone carbonyl group resulting in a dihydro metabolite and several others after oxidation of the pyrrolidine ring, resulting in a mono and dihydroxylated metabolite, as well as an oxo and a ring-opened hydroxy metabolite. HepaRG did only form the dihydro metabolite, one of the main metabolites of α-PBP (Manier et al. 2018). Oxidation of the pyrrolidine ring was not observed, although, for example, the metabolite found after lactam formation was also described as the second main metabolite. This is most probably due to fact that the HepaRG cell line was derived from a donor known to be a CYP2D6 poor metabolizer (Guillouzo et al. 2007). Investigations of the CYP isoforms involved in the metabolism of α-PBP revealed that lactam formation of α-PBP was only catalyzed by CYP2D6 (Manier et al. 2018). Additionally, pyrrolidine ring hydroxylation was catalyzed by CYP2B6, CYP2C19, and CYP2D6, of which CYP2D6 is expressed to a reduced extent due to the cells being derived from a poor metabolizing patient and CYP2B6 has a low contribution to the hepatic total net clearance of α-PBP. It is very likely that the number of metabolites formed after oxidation of the pyrrolidine ring was too low to be detected. This assumption is supported by the generally low amount of CYP2C19 expressed in human liver (Achour et al. 2014). The formation of amino acid adducts was not mentioned in any of the previously published studies, although the "α-PBP impurity (dehydro-) artifact (imido-)" described by Manier et al. might represent another in-source artifact of an adduct formed after the mechanism proposed in this study.

Concerning the metabolism of α-PEP, only five of the nine metabolites described by Manier et al. (2019a) were found after incubation of HepaRG cells, although its metabolism is catalyzed by a wide variety of CYP enzymes such as CYP1A2, CYP2B6, CYP2C9, CYP2C19, CYP2D6, and
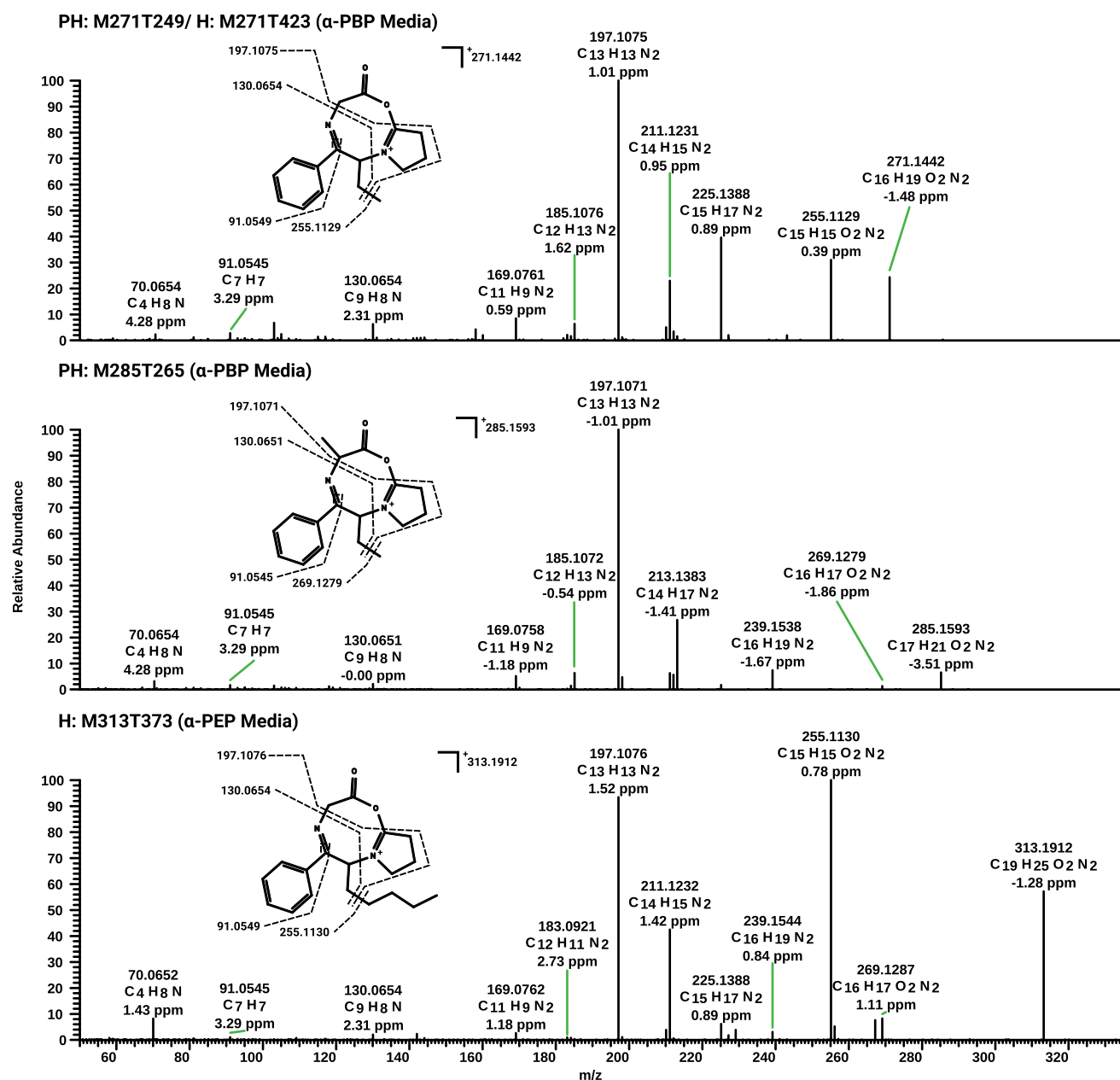
Fig. 3 LC–HRMS/MS spectra of amino acid adducts and their predominant fragmentation patterns after incubations with α-PBP or α-PEP. Fragments with accurate mass, calculated elemental formula, and mass error value in parts per million (ppm). The order corresponds to their masses

CYP3A4. Lactam formation, dihydroxylation, hydroxylation of the side chain, hydroxylation after opening of the pyrrolidine ring, and reduction of the cathinone carbonyl group were observed. Single pyrrolidine ring hydroxylation, dealkylation, and several combinations were not detected. Metabolites after *N*-oxidation, ring opening and formation of a carboxylic acid, and dehydrogenation as described by Swortwood et al. (2016) were also not detected. Nevertheless, alkyl hydroxylation, lactam formation, and reduction of the cathinone carbonyl group were described as the main

metabolic steps of α-PEP and were detected after incubation with pHS9/pHLM (Manier et al. 2018). Again, adduct formation of α-PEP with glycine was not mentioned by any of the previously published studies.

Since most metabolites were mainly found in extract 2 (cell media) and HepaRG cells were described to express functional transporter proteins, it is likely that they were actively transported (Guillouzo et al. 2007). Although metabolomics studies using pHLM led to higher amounts of metabolites of the investigated drugs of abuse, incubations
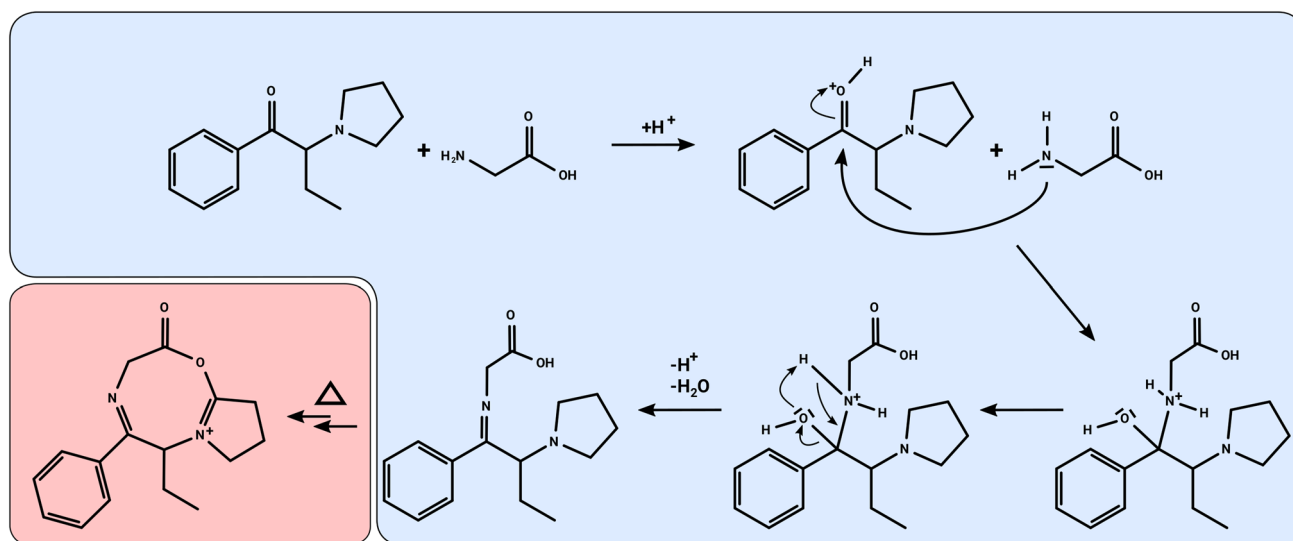
Fig. 4 Proposed mechanism of the formation of amino acid adducts exemplified for α-PBP and glycine. Blue colored part is presumably occurring during incubation. The red part presumably occurs in heated electrospray ionization source or in transfer capillary of the mass spectrometer (color figure online)

using HepaRG cells led to more significant compound changes that were not directly linked to the parent compounds. This might give a wider insight into the physiological impact on the liver cell metabolome. Depending on the aims of the study, it seems more appropriate to use pHLM for the investigation of metabolic pathways. If the aims of the study are to investigate the direct effect of compounds on the physiology of the cells such as hepatotoxicity, it seems more appropriate to use HepaRG cells.

Conclusions

Toxicometabolomics of the two NPS α-PBP and α-PEP after HepaRG cell line incubation were evaluated by analyzing the cells and the cell medium separately. The cross-validation results of the cell media lead to the conclusion that the features found in these experiments had better discriminant properties and thus are more suitable as biomarkers for the intake of the NPS investigated by this study. Significant features found in the cell extracts were mainly the parent compounds and their corresponding ^{13}C-isotopes. Significant features found in the cell media led to a considerably higher amount of significant changes in the metabolome that were identified as metabolites of both synthetic cathinones, as well as amino acid adducts but also remained unknown several features due the lack of reference spectra. They might give a wider insight into the physiological changes of the cells, since they were not able to be linked to the investigated cathinones. So far, only cholesterol sulfate and 25-hydroxy-cholesterol could be identified to have significantly changed

in concentrations after incubation of α-PEP, as well as N-methylnicotinamide in cell samples after incubation with α-PBP. These increased levels of N-methylnicotinamide may indicate a potential liver toxic effect of α-PBP. The investigation of the metabolism of the two synthetic cathinones led to fewer metabolites compared to investigations using pHLM or primary human hepatocytes, partially owing to the fact that HepaRG cells are derived from a CYP2D6-poor metabolizing patient. The number of metabolites found in α-PBP and α-PEP HepaRG incubated using metabolomics techniques may lead to two conclusions. HepaRG cells are not appropriate to investigate the metabolism of compounds mainly metabolized by CYP2D6. Metabolomics techniques are not able to extract all formed metabolites, particularly if they are very low abundant. The second conclusion could at least be excluded in the present study, as manual inspection of the data also did not allow identification of the missed metabolites.

The results of the conducted experiments, especially those of the incubations of the NPS with amino acids, revealed that both NPS formed the highly discriminating but unexpected imines with the corresponding amino acid during incubations. Their detection underlined the potential of toxicometabolomics studies.

Compliance with ethical standards

Conflict of interest The authors declare that there are no conflicts of interest.

References

Achour B, Barber J, Rostami-Hodjegan A (2014) Expression of hepatic drug-metabolizing cytochrome p450 enzymes and their intercorrelations: a meta-analysis. Drug Metab Dispos 42(8):1349–1356

Adusumilli R, Mallick P (2017) Data conversion with ProteoWizard msConvert. Methods Mol Biol 1550:339–368

Barnes S, Benton HP, Casazza K et al (2016a) Training in metabolomics research. II. Processing and statistical analysis of metabolomics data, metabolite identification, pathway analysis, applications of metabolomics and its future. J Mass Spectrom 51(8):535–548

Barnes S, Benton HP, Casazza K et al (2016b) Training in metabolomics research. I. Designing the experiment, collecting and extracting samples and generating metabolomics data. J Mass Spectrom 51(7):ii–iii

Boxler MI, Streun GL, Liechti ME, Schmid Y, Kraemer T, Steuer AE (2018) Human metabolome changes after a single dose of 3,4-methylenedioxymethamphetamine (MDMA) with special focus on steroid metabolism and inflammation processes. J Proteome Res 17(8):2900–2907

Brandon EF, Raap CD, Meijerman I, Beijnen JH, Schellens JH (2003) An update on in vitro test methods in human hepatic drug biotransformation research: pros and cons. Toxicol Appl Pharmacol 189(3):233–246

D'Elia RV, Goodchild SA, Winder CL et al (2019) Multiple metabolic pathways are predictive of ricin intoxication in a rat model. Metabolomics 15(7):102

Dang L, White DW, Gross S et al (2009) Cancer-associated IDH1 mutations produce 2-hydroxyglutarate. Nature 462(7274):739–744

EMCDDA (2015) EMCDDA–Europol Joint Report on a new psychoactive substance: 1-phenyl-2-(1-pyrrolidinyl)-1-pentanone (α-PVP) Publications Office of the European Union. http://www.emcdda.europa.eu/attachements.cfm/att_242501_EN_TDAS15001ENN.pdf. Accessed 14 April 2020

Guillouzo A, Corlu A, Aninat C, Glaise D, Morel F, Guguen-Guillouzo C (2007) The human hepatoma HepaRG cells: a highly differentiated model for studies of liver metabolism and toxicity of xenobiotics. Chem Biol Interact 168(1):66–73

Helfer AG, Michely JA, Weber AA, Meyer MR, Maurer HH (2015) Orbitrap technology for comprehensive metabolite-based liquid chromatographic-high resolution-tandem mass spectrometric urine drug screening - exemplified for cardiovascular drugs. Anal Chim Acta 891:221–233

Kudo K, Usumoto Y, Kikura-Hanajiri R, Sameshima N, Tsuji A, Ikeda N (2015) A fatal case of poisoning related to new cathinone designer drugs, 4-methoxy PV8, PV9, and 4-methoxy PV9, and a dissociative agent, diphenidine. Leg Med (Tokyo) 17(5):421–426

Kuhl C, Tautenhahn R, Bottcher C, Larson TR, Neumann S (2012) CAMERA: an integrated strategy for compound spectra extraction and annotation of liquid chromatography/mass spectrometry data sets. Anal Chem 84(1):283–289

Landis JR, Koch GG (1977) The measurement of observer agreement for categorical data. Biometrics 33(1):159–174

Lindon JC, Nicholson JK, Holmes E, Everett JR (2000) Metabonomics: metabolic processes studied by NMR spectroscopy of biofluids. Concept Magn Reson 12(5):289–320

Liu X, Locasale JW (2017) Metabolomics: a primer. Trends Biochem Sci 42(4):274–284

Manier SK, Meyer MR (2020) Current situation of the metabolomics techniques used for the metabolism studies of new psychoactive substances. Ther Drug Monit 42:93–97

Manier SK, Richter LHJ, Schaper J, Maurer HH, Meyer MR (2018) Different in vitro and in vivo tools for elucidating the human metabolism of alpha-cathinone-derived drugs of abuse. Drug Test Anal 10:1119–1130

Manier SK, Keller A, Schaper J, Meyer MR (2019a) Untargeted metabolomics by high resolution mass spectrometry coupled to normal and reversed phase liquid chromatography as a tool to study the in vitro biotransformation of new psychoactive substances. Sci Rep 9(1):2741

Manier SK, Keller A, Meyer MR (2019b) Automated optimization of XCMS parameters for improved peak picking of liquid chromatography-mass spectrometry data using the coefficient of variation and parameter sweeping for untargeted metabolomics. Drug Test Anal 11:752–761

Matsuta S, Shima N, Kamata H et al (2015) Metabolism of the designer drug alpha-pyrrolidinobutiophenone (alpha-PBP) in humans: identification and quantification of the phase I metabolites in urine. Forensic Sci Int 249:181–188

Maurer HH, Meyer MR, Helfer AG, Weber AA (2018) Maurer/Meyer/Helfer/Weber MMHW LC-HR-MS/MS library of drugs, poisons, and their metabolites. Wiley, Weinheim

Maurer HH, Pfleger K, Weber AA (2016) Mass spectral data of drugs, poisons, pesticides, pollutants and their metabolites. Wiley, Weinheim

McDonald GR, Hudson AL, Dunn SM et al (2008) Bioactive contaminants leach from disposable laboratory plasticware. Science 322(5903):917

Milburn MV, Ryals JA, Guo L (2013) Toxicometabolomics. In: Faqi AS (ed) A comprehensive guide to toxicology in nonclinical drug development. Elsevier, pp 875–891

Mortele O, Vervliet P, Gys C et al (2018) In vitro Phase I and Phase II metabolism of the new designer benzodiazepine cloniprazepam using liquid chromatography coupled to quadrupole time-of-flight mass spectrometry. J Pharm Biomed Anal 153:158–167

Odoardi S, Romolo FS, Strano-Rossi S (2016) A snapshot on NPS in Italy: distribution of drugs in seized materials analysed in an Italian forensic laboratory in the period 2013–2015. Forensic Sci Int 265:116–120

Psychogios N, Hau DD, Peng J et al (2011) The human serum metabolome. PLoS ONE 6(2):e16957

Pumpo R, Sarnelli G, Spinella A, Budillon G, Cuomo R (2001) The metabolism of nicotinamide in human liver cirrhosis: a study on *N*-methylnicotinamide and 2-pyridone-5-carboxamide production. Am J Gastroenterol 96(4):1183–1187

R Core Team (2020) R: a language and environment for statistical computing. R Foundation for Statistical Computing, Vienna, Austria. https://www.R-project.org/

Richter LHJ, Flockerzi V, Maurer HH, Meyer MR (2017) Pooled human liver preparations, HepaRG, or HepG2 cell lines for metabolism studies of new psychoactive substances? A study using MDMA, MDBD, butylone, MDPPP, MDPV, MDPB, 5-MAPB, and 5-API as examples. J Pharm Biomed Anal 143:32–42

Richter LHJ, Herrmann J, Andreas A et al (2019) Tools for studying the metabolism of new psychoactive substances for toxicological screening purposes—a comparative study using pooled human liver S9, HepaRG cells, and zebrafish larvae. Toxicol Lett 305:73–80

Richter LHJ, Maurer HH, Meyer MR (2017) New psychoactive substances: studies on the metabolism of XLR-11, AB-PINACA, FUB-PB-22, 4-methoxy-alpha-PVP, 25-I-NBOMe, and meclonazepam using human liver preparations in comparison to primary human hepatocytes, and human urine. Toxicol Lett 280:142–150

Sinz MA (2012) In VitroandIn VivoModels of drug metabolism encyclopedia of drug metabolism and interaction. Wiley, Amsterdam

Sinz MW, Kim S (2006) Stem cells, immortalized cells and primary cells in ADMET assays. Drug Discov Today Technol 3(1):79–85

Sinz MA, Lyubimov AV (2011) In vitro and in vivo models of drug metabolism encyclopedia of drug metabolism and interactions. Wiley, Amsterdam

Smith CA, Want EJ, O'Maille G, Abagyan R, Siuzdak G (2006) XCMS: processing mass spectrometry data for metabolite profiling using nonlinear peak alignment, matching, and identification. Anal Chem 78(3):779–787

Sumner LW, Amberg A, Barrett D et al (2007) Proposed minimum reporting standards for chemical analysis Chemical Analysis Working Group (CAWG) Metabolomics Standards Initiative (MSI). Metabolomics 3(3):211–221

Swortwood MJ, Ellefsen KN, Wohlfarth A et al (2016) First metabolic profile of PV8, a novel synthetic cathinone, in human hepatocytes and urine by high-resolution mass spectrometry. Anal Bioanal Chem 408(18):4845–4856

Van den Eede N, Cuykx M, Rodrigues RM et al (2015) Metabolomics analysis of the toxicity pathways of triphenyl phosphate in HepaRG cells and comparison to oxidative stress mechanisms caused by acetaminophen. Toxicol In Vitro 29(8):2045–2054

Vervliet P, Mortele O, Gys C et al (2019) Suspect and non-target screening workflows to investigate the in vitro and in vivo metabolism of the synthetic cannabinoid 5Cl-THJ-018. Drug Test Anal 11(3):479–491

Vervliet P, Mortelé O, Gys C et al (2019) Suspect and non-target screening workflows to investigate the in vitro and in vivo metabolism of the synthetic cannabinoid 5Cl-THJ-018. Drug Test Anal 11(3):479–491

Wagmann L, Maurer HH, Meyer MR (2017) An easy and fast adenosine 5'-diphosphate quantification procedure based on hydrophilic interaction liquid chromatography-high resolution tandem mass spectrometry for determination of the in vitro adenosine 5'-triphosphatase activity of the human breast cancer resistance protein ABCG2. J Chromatogr A 1521:123–130

Wehrens R, Hageman JA, van Eeuwijk F et al (2016) Improved batch correction in untargeted MS-based metabolomics. Metabolomics 12:88

Welter J, Meyer MR, Wolf EU, Weinmann W, Kavanagh P, Maurer HH (2013) 2-methiopropamine, a thiophene analogue of methamphetamine: studies on its metabolism and detectability in the rat and human using GC-MS and LC-(HR)-MS techniques. Anal Bioanal Chem 405(10):3125–3135

Wild J, Shanmuganathan M, Hayashi M, Potter M, Britz-McKibbin P (2019) Metabolomics for improved treatment monitoring of phenylketonuria: urinary biomarkers for non-invasive assessment of dietary adherence and nutritional deficiencies. Analyst 144(22):6595–6608

Worley B, Powers R (2013) Multivariate analysis in metabolomics. Curr Metabolomics 1(1):92–107

Zhang D, Luo G, Ding X, Lu C (2012) Preclinical experimental models of drug metabolism and disposition in drug discovery and development. Acta Pharm Sin B 2(6):549–561

4 Discussion and conclusions

The here presented work studied the metabolism of the five synthetic cathinones alpha-PBP, alpha-PVT, alpha-PHP, alpha-PEP, and alpha-POP. The metabolism of the given drugs of abuse was studied using pHLM and pHS9 and compared to already published metabolism studies using pHLM, PHH, and authentic human urine. Additionally kinetic studies were performed after identification of the CYP enzymes involved in the metabolism. Subsequently a UM workflow was developed and applied to metabolism studies using pHLM. After optimization of the solvent mixture for reconstitution of evaporated samples, the UM workflow was additionally applied to HepaRG cells.

Fragmentation after LC-HRMS/MS followed the same pattern for each of the investigated cathinones. The first step was the elimination of the pyrrolidine ring resulting in the fragment ion of the pyrrolidine ring and the corresponding phenylalkylone. Additionally, an alpha-cleavage was observed either before or after the elimination of the pyrrolidine ring. It is notable that the typically observed initial elimination of the cathinone oxo group was not observed. This might be due to the fact, that the elimination is performed forming an azirine structure[99]. The formation of such an ion is ruled out by tertiary amines and thus not observable in the investigated compounds. Compared to other drugs of abuse the investigated cathinones were mainly metabolized to a lower extend[42,47,48]. The main metabolic steps observed in vitro were the hydroxylation of the pyrrolidine ring, as well as the lactam formation for each of the synthetic cathinones. With an increasing length of the alkyl chain, the additional hydroxylation and formation of an oxo group at the alkyl chain was additionally observed. The reduction of the cathinone oxo group was only observed in PHH and human urine, while the formation of glucuronides was observed exclusively in human urine. PHH seemed to reflect the human metabolism the best among the included metabolism models. Kinetic studies indicated that the metabolism of the investigated cathinones was mainly catalyzed by polymorphically expressed CYP enzymes such as CYP2D6, CYP2C9, and CYP2C19, which leads to in increased risk of interindividual variability in the formation of the metabolites. Since only alpha-PEP and alpha-POP were extensively metabolized and

the parent compound was always detectable in the considered studies, this circumstance might only affect the confirmation of an intake by metabolites.

The development and optimization of a UM workflow revealed the high impact of peak-picking parameters and the resolution of the mass spectrometer to the recovery of analytes. The optimization of the preprocessing parameters was conducted by evaluation of the variability of the obtained features using the coefficient of variation (CV). Compared to a universal set of parameters proposed by XCMS Online[100], the number of detected parent compounds after analysis of a neat standard solution mixture increased, while the total number of features was reduced by at least half. These results indicated an increased accuracy and precision of the optimized conditions. The chosen parameter sweeping approach, meaning a one by one optimization of each parameter within a given range, was computing-intensive leading to a time span of roughly 15 hours for the algorithm to finish. Other approaches such as AutoTuner[101] or IPO[102] estimate peak-picking parameters from raw data or evaluate the obtained isotopic patterns concerning naturally occurring ^{13}C isotopologues. Pang et al. recently compared the computing time and evaluated the results of different optimization approaches including the ones mentioned above using different data sets such as large scale clinical studies[103]. The results were comparable throughout each of the data sets. While AutoTuner completed the optimization the fastest, IPO performed comparably slower and the parameter sweeping approach using the features's CV was by far the slowest. Unfortunately, the authors decided not to evaluate all obtained optimized parameters but merely focused on the fastest approaches. This leaves the comparison of the parameter sweeping approach in terms of suitability of the obtained parameters to the faster approaches, as suspect of further investigations. Due to the fact that the variability of the features' areas is an endpoint that directly reflects the quality of the peak-picking and other approaches merely use surrogate characteristics for their optimization, there is reason to assume that the parameter sweeping approach using CVs is more appropriate for at least smaller scaled metabolomics studies such as in vitro studies. The decision on which approach is suitable for a given type of study is likely to be made by weighing up the necessary computing time, as well as the obtained accuracy and precision.

Applying metabolomics techniques for the evaluation of the metabolism of alpha-PBP and alpha-PEP using pHLM led to the detection of several new metabolites compared to the conventional approach. In addition to the previously detected metabolites, one of the main metabolites detectable in human urine, the dihydro metabolites of the investigated cathinones formed after reduction of the cathinone oxo group was detected

as well. In general, the method was more sensitive and let to the detection of several more metabolites. At least for alpha-PEP, the result was comparable to that of the previously reported metabolism using PHH, except for the missing *N*-oxides and dehydro metabolites that were detected in PHH[104]. Concerning alpha-PBP, the results were comparable to those found in human urine, merely missing the metabolite formed after hydroxylation of the alkyl chain[105]. The evaluation using metabolomics techniques did not only lead to the detection of metabolites but also of several artifacts such as a cyano and an imido artifact of alpha-PBP. These artifacts gave a first hint to the potential of metabolomics techniques to reveal not only metabolism-specific biomarkers for the detection of drugs of abuse but also those from unexpected reactions. The variability of the replicates within incubation groups was very low leading to a high significance of the detected metabolites' areas between groups. This fact lead to the conclusion that pHLM incubations are well suited for metabolism studies, even with as few as five replicates for each incubation group.

Quality assurance is an important aspect of metabolomics studies[88]. This includes monitoring and optimization of several experimental parameters. One aspect that has not been focused on in previous publications is the evaluation of the reconstitution solvent that is used to dissolve evaporated samples. The reconstitution solvent is a critical experiment parameter, especially when applying several chromatographical columns since not every solvent is tolerated. The evaluation of several reconstitution solvent mixtures after evaporation of plasma samples resulted in a significant impact on the area of several features as well as the overall feature count. The overall feature count is a parameter that needs to be evaluated with care. Since features are not solely metabolites or endogenous compounds but also artifacts that can be the result of thermic decomposition or adducts, an increase of the overall feature count does not necessarily mean a better suitability of the chosen conditions. Since several mixtures of reconstitution solvents do not facilitate the formation of artifacts or other additional features, this parameter was a suitable parameter to evaluate concerning this study. The study showed that a reconstitution solvent mixture consisting of 30% methanol and 70% acetonitrile was suited best to result in high feature areas while avoiding damage of the applied chromatographical columns. This result stresses the impact of the experimental conditions on results of metabolomics experiments.

Since HepaRG cells are a living system, the formation of more complex metabolites such as Phase II metabolites were expected after using them to study the metabolism of alpha-PBP and alpha-PEP. Concerning the analysis of cells extracts, mainly the parent

compounds of alpha-PBP and alpha-PEP were detectable. Several features that were additionally detected allowed an estimation of the cells response to the incubated synthetic cathinones. N-Methylnicotinamine of which the ^{13}C-isotope was increased after incubations using alpha-PBP, is associated with hepatotoxic effects. Metabolites of the investigated synthetic cathinones were detected in extracts of the surrounding cell media. It is likely that the formed metabolites were transported out of the cell after their metabolism. In general, fewer metabolites were detected in HepaRG cells than in incubations using pHLM. This might be due to the fact that HepaRG cells have lower enzyme activities than pHLM. Additionally the lactam formation of alpha-PBP was not observed due to the fact, that HepaRG cells were derived from a CYP2D6 poor metabolizer. The characterization of the CYP enzymes involved in the metabolism of alpha-PBP showed that the formation of the lactam is only catalyzed by CYP2D6. The detection of a significant increase in oleamide was ambiguous and the cause was not clearly determinable. Since McDonald et al. previously described the detection of oleamide which is used as a slip agent after rinsing plasticware with water and the variability within incubation groups was relatively high, it appeared likely that this analyte was not an endogenous compound[106]. The detection of adducts of the investigated cathinones with glycine and alanine was not explainable with metabolic reactions. Additional experiments investigating the formation of the glycine adduct in Tris buffer containing merely one of the synthetic cathinones and glycine, revealed the detection of the feature itself including the ring closure. These findings led to the conclusion that the adduct is likely to form spontaneously starting with the formation of a Schiff base and subsequent thermally induced ring closure in the mass spectrometer. Since the concentration of the amino acids in the incubation medium was comparable to that in human blood, it is likely that these adducts are also detectable in authentic cases. It is worth mentioning that these adduct have not been reported before in any studies investigating the metabolism of these cathinones, underlining the efficiency of metabolomics techniques.

For the detection of drugs of abuse in human biomatrix the toxicokinetic properties of the given substance needs to be known in prior. This necessity results from metabolites being important biomarkers that can be the only detectable analytes. The application of toxicometabolomics techniques, meaning metabolomics techniques in the context of toxicology, facilitates the investigation of biomarkers due to the fact that the applied statistical methods enable an evaluation of metabolism studies without depending on the investigator to be well-educated in potential metabolic reactions. Additionally, metabolomics techniques are well suited to provide knowledge about novel biomark-

ers that are not necessarily related to metabolic reactions or provide knowledge of the organism's response to the substance revealing hepatotoxic or other effects after their consumption. One of the main disadvantages of metabolomics studies is the high amount of analyses that needs to be performed. In addition to the application of several chromatographic columns and ionization modes for the comprehensive characterization of the samples, each substance needs to be analyzed in several replicates to provide the possibility for a statistical evaluation. This leads to a huge amount of time and effort, especially if the analytes of interest need to be identified by separate MS/MS experiments. A notable challenge of toxicometabolomics in particular is the elucidation of the chemical structures of novel biomarkers. Since the chemical structure of novel biomarkers such as amino acid adducts of alpha-PBP and alpha-PEP are neither obtainable as a standard nor necessarily deducible from the MS/MS spectrum of the parent compound, an additional amount of attention must be paid to avoid filing features as "unknown" that are actually derived from the parent compound. A potential pitfall of toxicometabolomics might be the investigation of the metabolism of a given substance in a non-human metabolism model. Concerning the often applied rat model for the investigation of the metabolism of drugs of abuse, every low abundant metabolite might be the main metabolite in humans. Since toxicometabolomics techniques evaluate significant changes in the metabolome, the danger of missing low abundant metabolites due to adverse variability is given.

Toxicometabolomics is a promising new technique that is at least an important support of conventional metabolism studies. The application of toxicometabolomics techniques might be especially suited for the investigation of substances that are difficult to detect in standard screening approaches. This might be either due to the fact that the substance has a very short half-life, is pharmacologically very potent or can not be sufficiently ionized.

References

[1] Howe G. A., Jander G.. Plant immunity to insect herbivores. *Annual Review of Plant Biology.* 2008;59:41–66.

[2] Musto D. F.. Opium, cocaine and marijuana in american history. *Scientific American.* 1991;265:40–47.

[3] Gaujac A., Navickiene S., Collins M. I., Brandt S. D., Andrade J. B.. Analytical techniques for the determination of tryptamines and β-carbolines in plant matrices and in psychoactive beverages consumed during religious ceremonies and neo-shamanic urban practices. *Drug Testing and Analysis.* 2012;4:636–648.

[4] Al-Motarreb A., Al-Habori M., Broadley K. J.. Khat chewing, cardiovascular diseases and other internal medical problems: the current situation and directions for future research. *Journal of Ethnopharmacology.* 2010;132:540–548.

[5] Wright C. R. A.. XLIX.—On the action of organic acids and their anhydrides on the natural alkaloïds. Part I. *Journal of the Chemical Society.* 1874;27:1031–1043.

[6] Sneader W.. The discovery of heroin. *The Lancet.* 1998;352:1697–1699.

[7] Tyers G. F. O.. Heroin history. *Canadian Medical Association Journal.* 2018;190:E144–E144.

[8] Edeleano L.. Ueber einige derivate der phenylmethacrylsäure und der phenylisobuttersäure. *Berichte der deutschen chemischen Gesellschaft.* 1887;20:616–622.

[9] Nagai N.. Kanyaku maou seibun kenkyuu seiseki (zoku). *Yakugaku Zashi.* 1893;13:901-933.

[10] Kaddoumi A., Kikura-Hanajiri R., Nakashima K.. High-performance liquid chromatography with fluorescence detection for the simultaneous determination

of 3,4-methylenedioxymethamphetamine, methamphetamine and their metabolites in human hair using DIB-Cl as a label. *Biomedical Chromatography.* 2004;18:202–204.

[11] Freudenmann R. W., Öxler F., Bernschneider-Reif S.. The origin of MDMA (ecstasy) revisited: the true story reconstructed from the original documents. *Addiction.* 2006;101:1241–1245.

[12] EMCDDA . European drug report 2019: Trends and developments. European Monitoring Centre for Drugs and Drug Addiction 2019.

[13] UNODC . World drug report 2019. United Nations Office on Drugs and Crime 2019.

[14] UNODC . A century of international drug control. United Nations Office on Drugs and Crime 2008.

[15] UN . Single convention on narcotic drugs. United Nations 1961.

[16] UN . Convention on psychotropic substances. United Nations 1971.

[17] UN . Protocol amending the single convention on narcotic drugs. United Nations 1972.

[18] UN . United nations convention against illicit traffic in narcotic drugs and psychotropic substances. United Nations 1988.

[19] Helander A., Bäckberg M.. New psychoactive substances (NPS) – the hydra monster of recreational drugs. *Clinical Toxicology.* 2016;55:1–3.

[20] Rech M. A., Donahey E., Cappiello Dziedzic J. M., Oh L., Greenhalgh E.. New drugs of abuse. *Pharmacotherapy: The Journal of Human Pharmacology and Drug Therapy.* 2015;35:189-197.

[21] Reuter P., Pardo B.. Can new psychoactive substances be regulated effectively? An assessment of the British Psychoactive Substances Bill. *Addiction.* 2016;112:25–31.

[22] Wang R., Yin Y., Zhu Z.-J.. Advancing untargeted metabolomics using data-independent acquisition mass spectrometry technology. *Analytical and Bioanalytical Chemistry.* 2019;411:4349–4357.

[23] Huffman J. W., Dai D., Martin B. R., Compton D. R.. Design, synthesis and pharmacology of cannabimimetic indoles. *Bioorganic & Medicinal Chemistry Letters.* 1994;4:563–566.

[24] Karila L., Benyamina A., Blecha L., Cottencin O., Billieux J.. The synthetic cannabinoids phenomenon. *Current Pharmaceutical Design.* 2017;22:6420–6425.

[25] Katz D., Deruiter J., Bhattacharya D., et al. Benzylpiperazine: "a messy drug". *Drug and Alcohol Dependence.* 2016;164:1–7.

[26] Feng L.-Y., Battulga A., Han E., Chung H., Li J.-H.. New psychoactive substances of natural origin: A brief review. *Journal of Food and Drug Analysis.* 2017;25:461–471.

[27] EMCDDA . Germany country drug report 2019. European Monitoring Centre for Drugs and Drug Addiction 2019.

[28] Bundesministerium für Gesundheit . Drogen- und Suchtbericht 2019. Die Drogenbeauftragte der Bundesregierung beim Bundesministerium für Gesundheit 2019.

[29] Bundestag . Gesetz zur Bekämpfung der Verbreitung neuer psychoaktiver Stoffe. *Bundesgesetzblatt.* 2016;55.

[30] Bundestag . Gesetz über den Verkehr mit Betäubungsmitteln. *Bundesgesetzblatt.* 1994;13.

[31] Reichstag . Gesetz über den Verkehr mit Betäubungsmitteln. *Reichsgesetzblatt.* 1929;43.

[32] Valente M. J., Pinho P., Lourdes Bastos M., Carvalho F., Carvalho M.. Khat and synthetic cathinones: a review. *Archives of Toxicology.* 2013;88:15–45.

[33] Simmler L. D., Buser T. A., Donzelli M., et al. Pharmacological characterization of designer cathinones in vitro. *British Journal of Pharmacoloygy.* 2013;168:458–470.

[34] Mas-Morey P., Visser M. H. M., Winkelmolen L., Touw D. J.. Clinical toxicology and management of intoxications with synthetic cathinones ("bath salts"). *Journal of Pharmacy Practice.* 2012;26:353–357.

[35] Coppola M., Mondola R.. Synthetic cathinones: chemistry, pharmacology and toxicology of a new class of designer drugs of abuse marketed as "bath salts" or "plant food". *Toxicology Letters.* 2012;211:144–149.

References

[36] Graddy R., Buresh M. E., Rastegar D. A.. New and emerging illicit psychoactive substances. *Medical Clinics of North America.* 2018;102:697–714.

[37] Lusthof K. J., Oosting R., Maes A., Verschraagen M., Dijkhuizen A., Sprong A. G.. A case of extreme agitation and death after the use of mephedrone in the Netherlands. *Forensic Science International.* 2011;206:e93–e95.

[38] Al-Habori M.. The potential adverse effects of habitual use of catha edulis (khat). *Expert Opinion on Drug Safety.* 2005;4:1145–1154.

[39] Brunt T. M., Atkinson A. M., Nefau T., et al. Online test purchased new psychoactive substances in 5 different european countries: A snapshot study of chemical composition and price. *International Journal of Drug Policy.* 2017;44:105–114.

[40] Maurer H. H.. *Analytical toxicology.* Basel: Birkhäuser Basel 2010.

[41] Meyer M. R., Maurer H. H.. Current status of hyphenated mass spectrometry in studies of the metabolism of drugs of abuse, including doping agents. *Analytical and Bioanalytical Chemistry.* 2011;402:195–208.

[42] Michely J., Manier S., Caspar A., Brandt S., Wallach J., Maurer H.. New psychoactive substances 3-methoxyphencyclidine (3-MeO-PCP) and 3-methoxyrolicyclidine (3-MeO-PCPy): metabolic fate elucidated with rat urine and human liver preparations and their detectability in urine by GC-MS, "LC-(High Resolution)-MSn", and "LC-High Resolution-MS/MS". *Current Neuropharmacology.* 2016.

[43] Caspar A. T., Helfer A. G., Michely J. A., et al. Studies on the metabolism and toxicological detection of the new psychoactive designer drug 2-(4-iodo-2,5-dimethoxyphenyl)-*N*-[(2-methoxyphenyl)methyl]ethanamine (25I-NBOMe) in human and rat urine using GC-MS, LC-MSn, and LC-HR-MS/MS. *Anal Bioanal Chem.* 2015;407:6697–6719.

[44] Caspar A. T., Gaab J. B., Michely J. A., Brandt S. D., Meyer M. R., Maurer H. H.. Metabolism of the tryptamine-derived new psychoactive substances 5-MeO-2-Me-DALT, 5-MeO-2-Me-ALCHT, and 5-MeO-2-Me-DIPT and their detectability in urine studied by GC-MS, LC-MSn, and LC-HR-MS/MS. *Drug Testing and Analysis.* 2017;10:184–195.

[45] Musshoff F.. Ilegal or legitimate use? Precursor compounds to amphetamine and methamphetamine. *Drug Metabolism Reviews.* 2000;32:15–44.

80

[46] Manier S. K., Felske C., Eckstein N., Meyer M. R.. The metabolic fate of two new psychoactive substances - 2-aminoindane and *N*-methyl-2-aminoindane - studied in vitro and in vivo to support drug testing. *Drug Testing and Analysis.* 2019;12:145–151.

[47] Caspar A. T., Westphal F., Meyer M. R., Maurer H. H.. LC-high resolution-MS/MS for identification of 69 metabolites of the new psychoactive substance 1-(4-ethylphenyl-)-*N*-[(2-methoxyphenyl)methyl] propane-2-amine (4-EA-NBOMe) in rat urine and human liver S9 incubates and comparison of its screening power with further MS techniques. *Analytical and Bioanalytical Chemistry.* 2017;410:897–912.

[48] Wagmann L., Richter L. H. J., Kehl T., et al. In vitro metabolic fate of nine LSD-based new psychoactive substances and their analytical detectability in different urinary screening procedures. *Analytical and Bioanalytical Chemistry.* 2019;411:4751–4763.

[49] Staeheli S. N., Poetzsch M., Veloso V. P., et al. In vitro metabolism of the synthetic cannabinoids CUMYL-PINACA, 5F-CUMYL-PINACA, CUMYL-4CN-BINACA, 5F-CUMYL-P7AICA and CUMYL-4CN-B7AICA. *Drug Testing and Analysis.* 2017;10:148–157.

[50] Wagmann L., Manier S. K., Eckstein N., Maurer H. H., Meyer M. R.. Toxicokinetic studies of the four new psychoactive substances 4-chloroethcathinone, *N*-ethylnorpentylone, *N*-ethylhexedrone, and 4-fluoro-alpha-pyrrolidinohexiophenone. *Forensic Toxicology.* 2019;38:59–69.

[51] Peters F. T., Meyer M. R.. In vitro approaches to studying the metabolism of new psychoactive compounds. *Drug Testing and Analysis.* 2011;3:483–495.

[52] Sinz M. A.. In vitro and in vivo models of drug metabolism. *Encyclopedia of Drug Metabolism and Interactions.* 2012.

[53] Richter L. H., Herrmann J., Andreas A., et al. Tools for studying the metabolism of new psychoactive substances for toxicological screening purposes – a comparative study using pooled human liver S9, HepaRG cells, and zebrafish larvae. *Toxicology Letters.* 2019;305:73–80.

[54] Sharma V., McNeill J. H.. To scale or not to scale: the principles of dose extrapolation. *British Journal of Pharmacology.* 2009;157:907–921.

References

[55] Liu X., Jia L.. The conduct of drug metabolism studies considered good practice (I): analytical systems and in vivo studies. *Current Drug Metabolism.* 2007;8:815–821.

[56] Jia L., Liu X.. The conduct of drug metabolism studies considered good practice (II): In vitro experiments. *Current Drug Metabolism.* 2007;8:822–829.

[57] Brandon E. F. A., Raap C. D., Meijerman I., Beijnen J. H., Schellens J. H. M.. An update on in vitro test methods in human hepatic drug biotransformation research: pros and cons. *Toxicology and Applied Pharmacology.* 2003;189:233–246.

[58] Zhang D., Luo G., Ding X., Lu C.. Preclinical experimental models of drug metabolism and disposition in drug discovery and development. *Acta Pharmaceutica Sinica B.* 2012;2:549–561.

[59] Sinz M. W., Kim S.. Stem cells, immortalized cells and primary cells in ADMET assays. *Drug Discovery Today.* 2006;3:79–85.

[60] Guillouzo A., Corlu A., Aninat C., Glaise D., Morel F., Guguen-Guillouzo C.. The human hepatoma HepaRG cells: A highly differentiated model for studies of liver metabolism and toxicity of xenobiotics. *Chemico-Biological Interactions.* 2007;168:66–73.

[61] Gerets H. H. J., Tilmant K., Gerin B., et al. Characterization of primary human hepatocytes, HepG2 cells, and HepaRG cells at the mRNA level and CYP activity in response to inducers and their predictivity for the detection of human hepatotoxins. *Cell Biology and Toxicology.* 2012;28:69–87.

[62] Li A. P., Maurel P., Gomez-Lechon M. J., Cheng L. C., Jurima-Romet M.. Preclinical evaluation of drug—drug interaction potential: present status of the application of primary human hepatocytes in the evaluation of cytochrome P450 induction. *Chemico-Biological Interactions.* 1997;107:5–16.

[63] Kanebratt K. P., Andersson T. B.. HepaRG cells as an in vitro model for evaluation of cytochrome P450 induction in humans. *Drug Metabolism and Disposition.* 2007;36:137–145.

[64] Clarke S. E.. In vitro assessment of human cytochrome P450. *Xenobiotica.* 1998;28:1167–1202.

82

[65] Bozina N., Bradamante V., Lovrić M.. Genetic polymorphism of metabolic enzymes P450 (CYP) as a susceptibility factor for drug response, toxicity, and cancer risk. *Archives of Industrial Hygiene and Toxicology.* 2009;60:217–242.

[66] Crespi C. L., Miller V. P.. The use of heterologously expressed drug metabolizing enzymes–state of the art and prospects for the future. *Pharmacology & therapeutics.* 1999;84:121–131.

[67] Meyer G. M. J., Meyer M. R., Wink C. S. D., Zapp J., Maurer H. H.. Studies on the in vivo contribution of human cytochrome P450s to the hepatic metabolism of glaucine, a new drug of abuse. *Biochemical Pharmacology.* 2013;86:1497–1506.

[68] Sauer C., Peters F. T., Schwaninger A. E., Meyer M. R., Maurer H. H.. Investigations on the cytochrome P450 (CYP) isoenzymes involved in the metabolism of the designer drugs *N*-(1-phenyl cyclohexyl)-2-ethoxyethanamine and *N*-(1-phenylcyclohexyl)-2-methoxyethanamine. *Biochemical Pharmacology.* 2009;77:444–450.

[69] Venkatakrishnan K., Moltke L. L., Court M. H., Harmatz J. S., Crespi C. L., Greenblatt D. J.. Comparison between cytochrome P450 (CYP) content and relative activity approaches to scaling from cDNA-expressed CYPs to human liver microsomes: ratios of accessory proteins as sources of discrepancies between the approaches. *Drug metabolism and disposition: the biological fate of chemicals.* 2000;28:1493–1504.

[70] Barnes S., Benton H. P., Casazza K., et al. Training in metabolomics research. I. designing the experiment, collecting and extracting samples and generating metabolomics data. *Journal of Mass Spectrometry.* 2016;51.

[71] Worley B., Powers R.. Multivariate analysis in metabolomics. *Current Metabolomics.* 2013;1:92–107.

[72] Liu X., Locasale J. W.. Metabolomics: A primer. *Trends in Biochemical Sciences.* 2017;42:274–284.

[73] Lindon J. C., Nicholson J. K., Holmes E., Everett J. R.. Metabonomics: Metabolic processes studied by NMR spectroscopy of biofluids. *Concepts in Magnetic Resonance.* 2000;12:289–320.

References

[74] Wild J., Shanmuganathan M., Hayashi M., Potter M., Britz-McKibbin P.. Metabolomics for improved treatment monitoring of phenylketonuria: urinary biomarkers for non-invasive assessment of dietary adherence and nutritional deficiencies. *The Analyst.* 2019;144:6595–6608.

[75] D'Elia R. V., Goodchild S. A., Winder C. L., et al. Multiple metabolic pathways are predictive of ricin intoxication in a rat model. *Metabolomics.* 2019;15.

[76] Smith C. A., Want E. J., O'Maille G., Abagyan R., Siuzdak G.. XCMS: processing mass spectrometry data for metabolite profiling using nonlinear peak alignment, matching, and identification. *Analytical Chemistry.* 2006;78:779–787.

[77] Lommen A.. Metalign: Interface-driven, versatile metabolomics tool for hyphenated full-scan mass spectrometry data preprocessing. *Analytical Chemistry.* 2009;81:3079–3086.

[78] Pluskal T., Castillo S., Villar-Briones A., Orešič M.. MZmine 2: modular framework for processing, visualizing, and analyzing mass spectrometry-based molecular profile data. *BMC Bioinformatics.* 2010;11:395.

[79] Worley B., Powers R.. Mvapack: A complete data handling package for NMR metabolomics. *ACS Chemical Biology.* 2014;9:1138–1144.

[80] Tautenhahn R., Böttcher C., Neumann S.. Highly sensitive feature detection for high resolution LC/MS. *BMC Bioinformatics.* 2008;9:504.

[81] Mahieu N. G., Spalding J. L., Patti G. J.. Warpgroup: increased precision of metabolomic data processing by consensus integration bound analysis. *Bioinformatics.* 2015;32:268–275.

[82] Smith R., Mathis A. D., Ventura D., Prince J. T.. Proteomics, lipidomics, metabolomics: a mass spectrometry tutorial from a computer scientist's point of view. *BMC Bioinformatics.* 2014;15.

[83] Coble J. B., Fraga C. G.. Comparative evaluation of preprocessing freeware on chromatography/mass spectrometry data for signature discovery. *Journal of Chromatography A.* 2014;1358:155–164.

[84] Myers O. D., Sumner S. J., Li S., Barnes S., Du X.. Detailed investigation and comparison of the XCMS and MZmine 2 chromatogram construction and

chromatographic peak detection methods for preprocessing mass spectrometry metabolomics data. *Analytical Chemistry.* 2017;89:8689–8695.

[85] Lange E., Tautenhahn R., Neumann S., Gröpl C.. Critical assessment of alignment procedures for LC-MS proteomics and metabolomics measurements. *BMC Bioinformatics.* 2008;9:375.

[86] Jin W., Riley R. M., Wolfinger R. D., White K. P., Passador-Gurgel G., Gibson G.. The contributions of sex, genotype and age to transcriptional variance in drosophila melanogaster. *Nature Genetics.* 2001;29:389–395.

[87] Hotelling H.. Analysis of a complex of statistical variables into principal components. *Journal of Educational Psychology.* 1933;24:498–520.

[88] Dudzik D., Barbas-Bernardos C., García A., Barbas C.. Quality assurance procedures for mass spectrometry untargeted metabolomics. a review. *Journal of Pharmaceutical and Biomedical Analysis.* 2017.

[89] Brereton R. G., Lloyd G. R.. Partial least squares discriminant analysis: taking the magic away. *Journal of Chemometrics.* 2014;28:213–225.

[90] Gromski P. S., Muhamadali H., Ellis D. I., et al. A tutorial review: Metabolomics and partial least squares-discriminant analysis – a marriage of convenience or a shotgun wedding. *Analytica Chimica Acta.* 2015;879:10–23.

[91] Picard R. R., Cook R. D.. Cross-validation of regression models. *Journal of the American Statistical Association.* 1984;79:575–583.

[92] Milburn M. V., Ryals J. A., Guo L.. Toxicometabolomics. *A Comprehensive Guide to Toxicology in Preclinical Drug Development.* 2013:807–825.

[93] Richter L. H. J., Kaminski Y. R., Noor F., Meyer M. R., Maurer H. H.. Metabolic fate of desomorphine elucidated using rat urine, pooled human liver preparations, and human hepatocyte cultures as well as its detectability using standard urine screening approaches. *Analytical and Bioanalytical Chemistry.* 2016;408:6283–6294.

[94] Manier S. K., Richter L. H., Schäper J., Maurer H. H., Meyer M. R.. Different in vitro and in vivo tools for elucidating the human metabolism of alpha-cathinone-derived drugs of abuse. *Drug Testing and Analysis.* 2018;10:1119–1130.

References

[95] Manier S. K., Keller A., Meyer M. R.. Automated optimization of XCMS parameters for improved peak picking of liquid chromatography–mass spectrometry data using the coefficient of variation and parameter sweeping for untargeted metabolomics. *Drug Testing and Analysis.* 2018;11:752–761.

[96] Manier S. K., Keller A., Schäper J., Meyer M. R.. Untargeted metabolomics by high resolution mass spectrometry coupled to normal and reversed phase liquid chromatography as a tool to study the in vitro biotransformation of new psychoactive substances. *Scientific Reports.* 2019;9.

[97] Manier S. K., Meyer M. R.. Impact of the used solvent on the reconstitution efficiency of evaporated biosamples for untargeted metabolomics studies. *Metabolomics.* 2020;16.

[98] Manier S. K., Wagmann L., Flockerzi V., Meyer M. R.. Toxicometabolomics of the new psychoactive substances α-PBP and α-PEP studied in HepaRG cell incubates by means of untargeted metabolomics revealed unexpected amino acid adducts. *Archives of Toxicology.* 2020.

[99] Frański R., Gierczyk B., Kasperkowiak M., Jankowski W., Hoffmann M.. The mechanism of water loss from protonated cathinones. *Rapid Communications in Mass Spectrometry.* 2020;34.

[100] Tautenhahn R., Patti G. J., Rinehart D., Siuzdak G.. XCMS online: a web-based platform to process untargeted metabolomic data. *Analytical Chemistry.* 2012;84:5035–5039.

[101] McLean C., Kujawinski E. B.. AutoTuner: High fidelity and robust parameter selection for metabolomics data processing. *Analytical Chemistry.* 2020;92:5724–5732.

[102] Libiseller G., Dvorzak M., Kleb U., et al. IPO: a tool for automated optimization of XCMS parameters. *BMC Bioinformatics.* 2015;16:118.

[103] Pang Z., Chong J., Li S., Xia J.. MetaboAnalystR 3.0: Toward an optimized workflow for global metabolomics. *Metabolites.* 2020;10:186.

[104] Swortwood M. J., Ellefsen K. N., Wohlfarth A., et al. First metabolic profile of PV8, a novel synthetic cathinone, in human hepatocytes and urine

by high-resolution mass spectrometry. *Analytical and Bioanalytical Chemistry.* 2016;408:4845–4856.

[105] Matsuta S., Shima N., Kamata H., et al. Metabolism of the designer drug α-pyrrolidinobutiophenone (α-PBP) in humans: identification and quantification of the phase I metabolites in urine. *Forensic Science International.* 2015;249:181–188.

[106] McDonald G. R., Hudson A. L., Dunn S. M. J., et al. Bioactive contaminants leach from disposable laboratory plasticware. *Science.* 2008;322:917–917.